The in vitro plasticity of hair follicle dermal and mesenchymal stem cells

Robert Emmerson

Durham University

Robert Emmerson

The *in vitro* plasticity of hair follicle dermal and mesenchymal stem cells

MSc Thesis

Supervisor

Dr. S. A. Przyborski

Researched and written

October 2006 – March 2008

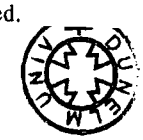

Abstract

Stem cells from the hair follicle are an easily accessible population of cells that have a broad *in vitro* developmental capabilities and potential for autologous replacement of damaged adult tissue. The bulge region and follicle dermis play key roles in hair follicle development. Stem cells of the bulge region are of epithelial origin, whereas dermal components of the hair follicle are of mesenchymal origin. Here we have compared the characteristics of rat clonal stem cell lines derived from both the hair follicle dermal sheath and dermal papilla with rat bone marrow-derived primary mesenchymal stem cells. The cell types were compared in terms of their morphology, proliferation, expression of intracellular and cell surface antigens and differentiation potential into bone and fat. The evidence presented here suggests that clonally derived stem cells from the follicle dermis posses some homologies with mesenchymal stem cells derived from bone marrow. Hence the hair follicle represents a potential niche for a mesenchymal-like population of stem cells. Both mesenchymal stem cells from bone marrow and stem cells from the follicle under specific *in vitro* conditions produce neural-like phenotypes. Here the two cell types were grown under conditions used in the culture of neural stem cells and formed aggregates that expressed the neural stem cell marker nestin. The effect of soluble factors produced by these aggregates on the development of neural progenitor cell populations was determined using aggregate conditioned media. The conditioned media induced process elaboration and differentiation towards the astrocytic lineage in a subpopulation of neural progenitors. Differential expression of antigens, loss of fat differentiation potential and extended proliferation capabilities were observed in the dermal clones. This aberrant behaviour could be attributable to transformation after extensive expansion *in vitro*, which has been demonstrated by their abnormal karyotype.

Acknowledgements

Many people have been of great help to me throughout the production of this thesis, and I would not have been able to complete it without their unwavering support. I would like to thank my supervisor Dr Stefan Przyborksi for the opportunity he has given me to do the project in the first place. I am greatly indebted to Professor Colin Jahoda and his research group, who supplied me with the two dermal clones, and collected their karyotype data. I am also eternally grateful to all the help and support given to me by the people in lab 9. Special thanks go to Vikki Christie for her technical help with the flow cytometry, to Dr Ross Carnachan for the use of his house and '24' DVDs and to Mike Cooke for being a general hero. I would also like to thank my brother, Brian, who always went out of his way to help me whenever I needed it. Finally I would like to thank my parents for supporting me throughout and especially over the final few months writing up at home.

Contents

Abbreviations

AHPCs	adult hippocampal progenitor cells
AIM-GFS	The control aggregate induction media without growth factors.
BDNF	brain derived neurotrophic factor
bFGF	basic fibroblast growth factor
BHA	butylated hydroxyanisole
BMP	bone morphogenic protein
BrdU	Bromodeoxyuridine
BSA	albumin from bovine serum
cAMP	cyclic adenosine monophosphate
CCM	complete culture medium
CFU-F	fibroblast colony forming units
CNS	central nervous system
DAPI	4'-6-Diamidino-2-phenylindole
DMEM	Dulbecco's modified eagle's medium
DMSO	dimethyl sulfoxide
DP9	dermal clone dermal papilla 9
DP9-CM	DP9 conditioned medium
DS7	dermal clone dermal sheath 7
DS7-CM	DS7 conditioned medium
EDA	ectodysplasin-A
EDAR	ectodysplasin-A receptor
EGF	epidermal growth factor
ES cells	embryonic stem cells
FABP4	fatty acid binding protein 4
FCS	foetal calf serum
FITC	fluorescein isothiocyanate
GFAP	glial fibrillary acidic protein
GFP	green fluorescent protein
^{3}H thymidine	tritiated thymidine
HFSCs	hair follicle stem cells
hLIF	human leukaemia inhibitory factor
IBMX	3-isobutyl-1-methylxanthine
IBZ	ischemic boundary zone
Lef-1	lymphoid enhancer factor-1

MBP	myelin basic protein
MCAO	middle cerebral artery occlusion
MEK/Erk1/2	mitogen-activated protein kinase kinase/extracellular signal-regulated kinase
MEM	minimum essential medium
MSC-CM	MSC conditioned medium
MSCs	mesenchymal stem cells
NGF	nerve growth factor
NICD	notch intracellular domain
NPCs	neural progenitor cells
NSCs	neural stem cells
NSE	neuron-specific enolase
NSS	neurological severity score
P	passage when suffixed by any number (e.g. P0)
PBS	phosphate buffered saline
PFA	Paraformaldehyde
PI	propidium iodide
PI3k/Akt	phosphoinositide 3-kinase/threonine protein kinase
PROLIF	The control AHPC expansion medium.
RA	retinoic acid
rMSCs	rat mesenchymal stem cells
RT-PCR	real time polymerase chain reaction
Shh	sonic hedgehog
SKPs	skin-derived precursors
α-SMA	α-Smooth Muscle actin
TA	transit amplifying
Tcf	T cell factor
TGF-β1	transforming growth factor-beta1
TH	tyrosine hydroxylase
TTX	Tetrodotoxin
TuJ-1	neuron-specific class III β-tubulin
YFP^+	yellow fluorescent protein positive

CHAPTER 1: LITERATURE REVIEW

1.1 Introduction

1.1.1 Definition of a stem cell

Stem cells can be defined as clonogenic, self-renewing progenitor cells, that are able to generate progeny capable of producing one or more specialised cell types. Commitment of stem cells to specialised cell types (or differentiation) is produced by number of steps. The nature of these steps and the identities of the mature cell types formed depend on signals from the environment. In vertebrates stem cells can be divided into two groups; embryonic stem (ES) cells and adult stem cells (also referred to as organ- or tissue- specific stem cells). ES cells are derived from the inner cell mass of the early blastocyst and are pluripotent because they capable of producing all differentiated cell types in the body [1, 2]. Adult stem cells are derived from ES cells after gastrulation and persist into adult life. The most well characterised example of adult stem cells is the haematopoietic stem cell, which is multipotent and generates all the blood and immune system cell types. Other populations of adult stem cells that have been enriched but not in all cases definitively isolated include; mesenchymal stem cells, hair follicle stem cells, skin stem cells, corneal stem cells, neural stem cells (NSCs), and muscle (satellite) stem cells.

1.1.2 Basic biology of adult stem cells

Monitoring adult stem cell movement and division has shown that they normally divide slowly and that transit amplifying (TA) cells constitute to the vast majority of dividing cells in a tissue [3]. TA cells are not stem cells because they are committed to differentiate after a limited number of divisions and they often have a lower level of plasticity. TA cells in the brain, for example, only differentiate into one cell type whereas NSCs are bipotent, differentiating into both neurons and glia [4]. TA cells increase the efficiency that adult stem cells can maintain tissues, because they allow replacement of a large number of differentiated cells, whilst utilising only a limited stock of stem cells [5]. However, alternative paradigms to TA cells that maintain epidermal homeostasis have recently been suggested [6].

Adult stem cells are the source cells that enable cellular renewal to take place and maintain adult tissues and organs as dynamic entities in a constant state of flux. The speed of renewal is highly variable between different adult stem cell populations. Stem cell populations in the brain turn over very slowly, whereas stem cells in the skin have a very rapid turn over. For example it is estimated that NSCs in adult mouse and rat brains produced only one neuron per day for every 2000 existing neurons in the brain [7]. Whereas keratinocytes, in samples of mouse epithelium, whose turnover was accurately estimated using "heavy" keratin (synthesized with ^2H_2O), showed a much more rapid turnover. The epithelia reached full replacement after around three weeks in normal mice and four days in flaky skin mice [8]. It is speculated that different populations of adult stem cells are being activated to fulfil the reparative and maintenance functions of adult stem cells. Activation of dormant populations of multipotent adult stem cells may occur following tissue damage and unipotent stem cells for routine tissue renewal [5]. Adult stem cells serve to support and repair tissues and they have highly variable characteristics in terms of their proliferative and differentiation potential.

Adult stem cells exist in a protected environment termed the niche that protects the stem cells from damage and maintains them in an undifferentiated state. Mammalian NSCs are maintained in their niche by the close proximity of blood vessels to the basal lamina. This close proximity enables the basal lamina to sequester the growth factors epidermal growth factor (EGF) and basic fibroblast growth factor (bFGF) from the blood vessels, which maintains the NSC population [4]. When needed adult stem cells proliferate and migrate from the niche and differentiate to form the cell type of the tissue in which they reside. The process of differentiation is very complex and controlled by a cocktail of molecules that activate molecular switches at specific times during development. Understanding what the molecules are, and the roles they play in controlling stem cell differentiation is a key question in stem biology.

1.1.3 Adult stem cells: lineage-restricted or a greater differentiation repertoire?

In the past decade an avalanche of work has been published that challenges the concept of lineage-restriction in adult stem cells [9]. These studies have proposed transitions form bone marrow to brain, skin to brain, bone marrow to liver, brain to heart and many more such unexpected feats of differentiation [10]. It was originally thought that adult stem cells produce a limited number of cell types, and have irreversibly lost the ability to produce cells that are developmentally unrelated in the

adult body. However, if the recent findings are entirely accurate then they would mean adult stem cells can reverse their lineage restrictions – perhaps by reprogramming gene expression – upon exposure to new environments (referred to as transdifferentiation). A second possibility is the notion of lineage restriction in adult stem cells is false, and there is little difference between adult stem cells and their embryonic counterparts [9, 11, 12].

Reprogramming of adult cell nuclei has been demonstrated in the past, with the ultimate example of this being the formation of ES cells from fully differentiated adult stem cells [13]. Reprogramming of nuclei resets the biological clock of a cell to its most primitive form. In doing so the adult cell – termed the "embryonic" adult stem cell is able to develop as if it were an ES cell. "Embryonic" adult stem cells are produced by transplanting the nucleus of an adult cell into an enucleated unfertilised egg. It has been demonstrated that reprogramming the nucleus of an adult cell is achieved by remodelling chromatin orgranisation using a cocktail of molecules. The first instance of nuclear reprogramming using nuclear transfer dates back to the late 1950s using the model organism *Xenopus laevis* [14]. Here viable cloned embyos were created from nuclei taken from adult cells. More recently this was extended to the mammalian system when an adult ewe was cloned in the mid-1990s [13]. The event of nuclear reprogramming alone is not proof that adult stem cells are able to undergo transdifferentiation, because the cytoplasm that significantly defines the developmental status of the cell is artificially removed [9].

1.1.4 The focus of this review

This review will focus on the basic biology, distribution and plasticity of two types of adult stem cells; hair follicle stem cells (HFSCs) and mesenchymal stem cells (MSCs). HFSCs principally reside in the bulge region of the hair follicle and contribute to the cyclical development of hair follicles [15]. Hair follicle development is initiated by the unique inductive properties of the hair follicle dermal papilla [16]. MSCs are multipotent stem cells showing adipocytic, chondrocytic and osteocytic differentiation potential [17]. MSCs are typically derived from bone marrow but have also been isolated from a number of other source tissues including the hair follicle [18, 19], which suggests a proportion of HFSCs could be represented by MSCs. MSCs and HFSCs are no exception to the emerging idea that adult stem cells may display surprising plasticity in their differentiation range. The notion of MSCs differentiating into cell types beyond their mesodermal germ layer is well established, through their

formation of cell types known to originate from ectoderm and endoderm germ layers [12, 20-24]. There is also growing evidence that the hair follicle is a potential source of stem cells capable of extraordinary differentiation potential beyond the confines of the hair follicle [11, 25-29]. This review will focus on the relationship between HFSCs and MSCs and the capabilities of these cells to produce neural lineages. Some researchers have been more sceptical about the notion of enhanced plasticity of adult stem cells and they have questioned the rigor of experimental methods used to demonstrate adult stem cell plasticity [30]. These findings will be reviewed with respect to MSCs and neural differentiation.

1.2 Hair follicle Stem Cells

1.2.1 Basic Biology of the hair follicle

The hair follicle is a highly dynamic structure that forms during a process called morphogenesis and is subsequently cyclically renewed into post natal life by adult stem cells. In post natal life its development passes through three phases during one hair cycle; growth (anagen), regression (catagen) and rest (telogen). Hair follicles are formed by unique epithelial-mesenchymal signalling, which persists into adulthood [31]. A number of organisms have been used to study the adult hair follicle, which include mouse, rat, chicken and human. The rodent whisker (vibrissae) represents a good model for studying the hair follicle, because it is easily accessible and amenable to microdissection [28]. The post natal hair follicle is composed of a number of interconnected structures. These include the epithelial components and dermal components. Epithelial components consist of the bulge region, the bulb region, the shaft, the outer root sheath and the inner root sheath, whereas dermal components are the dermal papilla and dermal sheath. The dermal components and the bulge are the permanent structures of the hair follicle, while the other epithelial components appear at varying degrees of development depending on the stage of the hair cycle.

1.2.2 Contribution of stem cells to post natal hair follicle development

Populations of stem cells that contribute to hair follicle renewal are present in the bulge component of the hair follicle. Stem cells in the bulge region were originally suggested when it was noted that label retaining cells were restricted to the bulge region [15]. Early studies showed the differentiation potential and motility rate of

bulge stem cells was high as they were found in many areas of the hair follicle including the bulb region after transplantation [32].

A number of studies have attempted to label bulge stem cells, using several different techniques, to monitor their subsequent development and characteristics. The contribution of bulge stem cells to structures within the hair follicle has been monitored using β-galactosidase labelling of transplanted LacZ positive bulge derived cells into athymic mice [32]. Bulge cells were labelled using green fluorescent protein (GFP) based on their slow cycling properties [33]. Other studies were able to express GFP in the bulge regions of transgenic mice by utilising the regulatory control element of the intermediate filament protein nestin [29, 34, 35]. Finally a double label consisting of bromodeoxyuridine (BrdU) and tritiated thymidine (^{3}H-thymidine) was used by [25] to track the movement and proliferation of stem cells originating from the upper follicle.

An early study that monitored the progeny of transplanted bulge stem cells implanted bulge stem cells from transgenic mice constitutively expressing the reporter gene lacZ (Rosa26) into the bulge regions of whiskers (vibrassa) of athymic mice [32]. The lacZ positive bulge stem cells were tracked in the chimeric follicles using X-gal. Eight weeks after transplant intense blue X-gal positive bulge cells were located in all regions of the hair follicle including the bulb region, indicating bulge cells had migrated throughout the hair follicle and contributed to development of all but one of its structures. The only structure not positive for X-gal was the dermal papilla – this indicated it was not formed by stem cells from the bulge region and suggests a mesenchymal origin. Together these findings strongly indicate that the bulge region contains a highly motile and proliferative population of stem cells that are capable of differentiating into all structures of the hair follicle [32].

Bulge stem cells remained multipotent during migration to the end bulb. When keratinocytes reach the bulb region they stopped migrating and began to accumulate along the length of the follicle – shown by keratinocyte colony formation in all regions of the follicle. Once cells covered the length of the hair follicle and stopped migrating they differentiated into structures of the hair follicle depending on their position [32]. Hence, the length of anagen is dependent on the cessation of migration of bulge derived cells rather than an exhaustion of proliferative capacity and consequent shortage of progenitor cells, which has been suggested by others [36].

The intermediate filament protein nestin was originally thought to label NSCs within the central nervous system (CNS). However, more recent findings have shown nestin is also expressed by progenitors within the hair follicle. Several studies were able to demonstrate nestin expression in follicle sections. Nestin expression has been reported in the inner root sheath, outer root sheath and bulge region of hair follicles isolated from human scalp tissue [37]. Importantly, nestin expression was not found in more mature structures such as the sebaceous gland and the hair shaft, indicating nestin exclusively marks progenitor cells. Based on these findings it could be hypothesized that nestin is downregulated in immature progenitor cells as they differentiate. Another study of human scalp tissue by showed nestin was expressed at the periphery of sebaceous glands, perhaps suggesting incomplete differentiation in these areas or variation between samples [38].

Nestin expression in hair follicle bulge regions has been used to label bulge derived stem cells by coupling its expression to GFP to create nestin-GFP cells in transgenic mice [34]. When the hair follicle progressed from telogen to anagen nestin-GFP cells proliferated and migrated out the bulge region to the outer root sheath. These cells occupied the upper portion of the hair follicle and were not present in the bulb region, which underwent terminal differentiation. In the catagen phase nestin-GFP cells declined in the outer root sheath until they could only be seen in the bulge region. Hence, nestin-GFP cells are direct progenitors of the inner root sheath, which may contribute to other structures within the hair follicle after nestin expression declines [34]. Bulge stem cells can also be marked with both ^{3}H thymidine and BrdU using pulse chase, whereby after a long eight week chase period these labels are lost from faster cycling TAcells and retained by slow cycling bulge cells. BrdU labelled bulge stem cells have been tracked and found to migrate into the hair follicle similar to nestin expressing cells [25].

1.2.3 The signalling events leading to hair follicle morphogenesis in the embryo

The hair follicle represents a unique model of reiterative epithielial-mesenchymal signalling events that lead to stem cell proliferation and differentiation. Early tissue recombination experiments elucidated the order of these signalling events [39]. The first signal in hair follicle morphogenesis arises from the dermis during embryogenesis, and causes regularly spaced thickenings in the epidermis referred to as placodes, which induce the formation of cellular clusters in the dermis called

dermal condensates [39]. Subsequent sequential signalling between the epidermis and the mesenchyme leads to the formation the dermal papilla from the dermal condensates and root sheaths and hair shafts from the placodes [40]. Hair follicle morphogenesis is regulated by a number of intercellular signalling molecules that activate signalling pathways, including Wnt and sonic hedgehog (Shh).

Wnt is a strong candidate for the signalling pathway that initially conveys information regarding size and spacing of dermal appendages to the epidermis from the dermis during embryogenesis. The role of Wnts in hair follicle morphogenesis was confirmed through the expression of Dickkopf1 – a diffusible inhibitor of Wnt signalling – which caused a complete block on the formation of all dermal appendages including hair follicles. This indicated the Wnt pathway is at least required for the initiation of hair follicle morphogenesis [41]. Wnts are a family of extracellular ligands that signal by binding to frizzled receptors in a wide range of developmental situations. There are 19 genes encoding Wnts and 10 encoding the frizzled receptor, which implies a wide variety of responses Wnts can elicit [42]. One response to a Wnt ligand binding to the frizzled receptor is a chain of downstream signalling events that result in the accumulation of nuclear β-catenin (See [42] for a full explanation of the mechanism). β-catenin forms transcription inducing complexes with DNA binding factors from the lymphoid enhancer factor-1 (Lef-1) and T cell factor (Tcf) families, which induces the expression of many different target genes [40]. It is important to note that Wnt signalling is not simply an 'on' or 'off' switch for hair follicle morphogenesis, instead relative levels of interacting factors at specific times during development of the recipient cell dictates the effects of the signal [43].

The first dermal signal initiates a response in the epidermis that produces changes in gene expression, which result in placode and ultimately hair follicle formation. These changes are elicited by signalling molecules that both promote and repress hair follicle formation [40]. Wnt signalling is also induced in the epidermis by the dermis and promotes placode formation [44]. Fibroblast growth factors have a role alongside Wnt signalling in assisting placode formation, which has been demonstrated in developing chick placodes. [45]. The molecule ectodysplasin-A (EDA) and its receptor ectodysplasin-A receptor (EDAR) have been identified as essential for placode development based on mutant phenotypes observed in humans and mice [46]. However, variability in the hierarchy between Wnt and EDA/EDAR signalling in the epidermis in response to the first dermal signal has been reported in different organisms [41]. Bone morphogenic proteins (BMPs) and secreted BMP inhibitors

including Noggin, Follistatin, and Gremlin have a great influence on the epithelial response to the first dermal signal. BMPs are secreted signalling molecules that repress hair follicle formation and when they are themselves inhibited the formation of follicles is permitted. BMPs are expressed throughout the epithelium. Hence, the distribution of hair follicle placodes reflects the pattern of BMP inhibitor expression as they are present in developing hair follicles to nullify the effect of BMPs, and absent in interfollicular regions [40].

Hair follicle morphogenesis progresses through several other key signalling events between the dermis and epidermis after the formation of the epidermal placode. The first epidermal signal to the dermis is governed by Wnt and Shh signals, which initiates dermal condensate formation. Subsequently the second dermal signal is likely to be activated by Shh and causes epithelial proliferation and downgrowth. Finally formation of the hair shaft and inner root sheath are controlled by Notch and BMP signalling. For a detailed review of signalling events that lead to hair follicle morphogenesis see [40].

1.2.4 Post natal signalling in hair follicle development

Molecular analysis has revealed that the progression of post natal hair follicles through anagen, catagen and telogen, is thought to be governed by similar signalling pathways to those outlined for hair follicle morphogenesis. The first suggestion of homologies came when the new anagen phase was shown to be governed by signalling between dermal and epithelial follicular cells [47]. Some examples of characterised homologous signalling events in post natal hair follicles – between the dermis papilla and bulge region – that contribute to hair follicle development are outlined here. Wnt signalling is thought to play a pivotal role throughout hair follicle morphogenesis and is also prominent in post natal hair follicle development. Active Wnt signalling has been demonstrated in the bulge and dermal papilla of post natal hair follicles at the onset of anagen [33, 43, 48]. Further Wnt3a and Wnt7a have been shown to maintain the hair inducing properties of cultured dermal papilla cells, indicating the importance of Wnt signalling from the overlying epidermis in maintaining hair follicles in the anagen state [49]. The progression of slow cycling bulge stem cells to rapidly cycling TAcells in post natal hair follicles is influenced by Wnt signalling, because the activation of transcription in cell cycle genes c-Myc and cyclin D1 is induced Lef-1 expression [42]. Like in morphogenesis the expression of secreted BMP inhibitors can activate epithelial stem cells in the bulge region and

induce anagen. The BMP inhibitor noggin overrides inhibition of the Wnt/β-catenin pathway by BMPs and enables hair follicle to progress into anagen [50]. These are just a small number of the numerous examples of homologies in signalling between morphogenesis and post natal hair follicle development.

1.2.5 The extraordinary plasticity of HFSCs

Bulge cells of the hair follicle have shown differentiation potential beyond hair follicle specific lineages. Experiments by Oshima *et al.* (2001) indicated that bulge stem cells were able to differentiate into epithelial structures other than the hair follicle such as the interfollicular epidermis and the sebaceous gland. Nestin-GFP follicular bulge cells have been shown to migrate beyond the hair follicle and contribute to structures in its immediate vicinity. Indeed after transplantation nestin expressing bulge cells can form blood vessels which anastamose with existing blood vessels in both wounded and non-wounded skin [35]. Bulge cells have also been dual labelled with BrdU and periodic pulses of ^{3}H thymidine to track their movement. Using this technique epidermal cells were found to proliferate much more slowly than follicular cells [25]. Intriguingly overtime the number of rapidly proliferating dual labelled cells in the follicle declined at a similar rate to an increase in rapidly proliferating cells in the epidermis. This demonstrated an emigration of progenitor cells from the hair follicle to the epidermis. Furthermore, in response to wounding a very similar emigration pattern was observed. These labelling studies strongly suggests that bulge derived stem cells produce proliferating progenitors that migrate and terminally differentiate into components of the hair follicle, blood vessels and cornified epithelial cells [25]. Finally potential neural differentiation has also been reported in the bulge region by a population of cells thought to be closely related to the neural crest [11, 51].

We have alluded to the notion of the hair follicle dermal papilla and the neighbouring dermal region the dermal sheath being a vital signalling centre that controls hair follicle cycling with its powerful inductive properties [49, 52]. However, until recently the dermal component of the hair follicle was not recognised as a source of adult stem cells with a differentiation repertoire beyond the confines of hair follicle specific lineages. Dermal stem cells that have shown mesenchymal potential have been isolated from the dermal papilla and dermal sheath components of the hair follicle [18, 19]. Intriguing plasticity has been demonstrated by the reconstitution of the haematopoietic system of lethally irradiated recipient mice by transgenically marked

hair follicle dermal sheath and dermal papilla cells [26]. Hair follicle dermal cells have also been implicated in would healing [27] and neural differentiation [28, 53].

The precursor or precursors within the hair follicle dermis and bulge regions responsible for their unprecedented differentiation repertoire are largely uncharacterised. The only exception being the likely presence of a neural crest related progenitor to explain the neural cell differentiation, which will be reviewed more closely in the section '*In vitro* neural differentiation of hair follicle stem cells'. Plasticity could be attributed to transdifferentiation of committed progenitors, dormant precursors of specific lineages or multipotent stem cells residing in the hair follicle.

1.2.6 The mesenchymal properties of HFSCs

Numerous locations have been suggested for MSCs – for a full review of these locations see the section 'Sources of MSCs'. The hair follicle represents a possible location for MSCs. A cloning strategy has been used to determine the *in vitro* fat and bone differentiation capabilities – already shown in primary explants – of progenitor cells derived from two hair follicle dermal cell populations [18]. A total of four dermal sheath clones (DS2, DS4, DS5 and DS7), and four dermal papilla clones (DP4, DP5, DP11 and DP12) were selected for potency testing based on their ability to efflux the dye Rhodamine 123, which had previously been used to identify stem cell populations in the pancreas [54]. Two of the clones tested (DP4 and DS5) were able to differentiate into fat and bone, four clones formed fat only (DS7, DP5, DP11 and DP12), one clone (DS2) formed bone only and one clone formed neither fat nor bone (DS4). Therefore it is clear from the potency analysis that cells residing in the dermal component of the hair follicle show a degree of mesenchymal potential. However, their relationship to MSCs is brought into question because the two clones that showed both bone and fat differentiation (DP4 and DS5) showed very low α-Smooth muscle actin (α-SMA) expression (a marker of MSCs), whereas another clone (DS7) showed α-SMA expression and differentiated towards the fat lineage only. These conflicting data show a lack of correlation between marker expression and differentiation potential of the clones. Interestingly cultured primary populations of follicle dermal papilla and dermal sheath show high levels of α-SMA expression [55], which suggests MSCs could be associated with these niches and that the cloning procedure may have caused a reduction in α-SMA expression. A second study also attempted cloning serial dilution from a heterogeneous population of human scalp-derived adherent cells, which was isolated from hair follicle and interfollicular dermal

cells [56]. Both the cloned and primary cells showed the cell surface antigen profile of MSCs and differentiated into fat, cartilage and bone (see section 'Isolation and characterisation of MSCs'). It was noted that only 0.5 – 2% of isolated scalp cells adhered in the initial isolation, which indicated a low frequency of MSC-like cells in scalp tissue. In addition, unlike MSCs from other tissue sources these cells were dependent on EGF and bFGF for *in vitro* expansion [56]. Taken together these studies have used cloning techniques to reveal a potential niche for MSC-like cells in the hair follicle. The mesenchymal potential of primary cells isolated from the hair follicle dermis has been demonstrated by their differentiation towards fat, bone, cartilage and muscle lineages [19]. This reinforces the data from the dermal clones. Primary stem cell populations were also isolated from discrete sections of the hair follicle – including the bulge and dermal regions – and were differentiated towards both the bone and fat lineages, which indicates mesenchymal potential throughout the hair follicle [19].

1.2.7 In vitro neural differentiation of hair follicle stem cells

The seminal paper which identified the skin dermis as a potential source of stem cells capable of differentiating into neural cell types was published by Toma and colleagues in 2001. Nestin positive spheres – termed skin-derived precursors (SKPs) – were isolated from both adult and juvenile mouse abdomen and back skin after mechanical dissociation, and cultured in conditions known to obtain NSCs from the brain. Serum free medium supplemented with EGF and bFGF induced the formation of SKPs in a small proportion of primary skin cells. After expansion the SKPs could be dissociated and plated on coated slides. Culture for seven days on these slides in the absence of growth factors induced a small proportion (less than 10%) of SKPs to differentiate towards neuronal, astrocytic and oligodendrocytic lineages [57]. Isolation of SKPs that differentiated towards neural lineages in a very similar fashion to mouse SKPs was also demonstrated in both adult and neonatal human dermis [57, 58]. Differentiation towards neural lineages of SKPs from all tissue types was demonstrated in clonally derived cultures, which illustrated plasticity of SKPs at a single cell level. A peripheral neuronal phenotype, in SKPs derived from neonatal human dermis, was confirmed using a larger panel of markers after differentiation in neurotrophin supplemented medium. Further the ability to expand these SKPs *ex vivo* for prolonged periods (greater than 15 months) whilst maintaining a normal karyotype was demonstrated [58]. More rigorous functional analysis of neuronal differentiation in SKPs was provided, when both fresh and culture expanded SKPs, were shown to

undergo changes in protein expression at time points that were indicative of a peripheral neuronal phenotype [59]. The peripheral neuronal phenotype was maintained in the CNS microenvironment, indicating a high degree of commitment. However, the differentiated SKPs did not form electrophysiologically active peripheral neurons as the cells did not posses voltage gated inward sodium currents [59]. Sphere forming dermal derived cells with similar properties to SKPs have been isolated from adult human skin by other investigators [60]. However, unlike SKPs these spheres were only expandable *in vitro* as an adherent monolayer in serum containing mitogen free medium. After expansion the cells could be induced to form spheres again that expressed nestin and were differentiated in hippocampal-astrocyte-conditioned medium over a much shorter two day time course. Despite this shorter time neuronal proteins such as neuron-specific class III β-tubulin (TuJ-1) were expressed in around 11% of cells, and perhaps more importantly the cells displayed some electrophysiological activity [60]. We have seen that dermal cells capable of rudimentary neural differentiation can be isolated from both rodent and human dermal tissues at different stages of development. The cells mimicked a time course of neuronal development based on protein expression patterns, but showed little evidence of producing fully functional neurons, which is a necessary property for these cells to be used in autologous transplantation.

The identity of SKPs within the dermis has been determined by Fernandes and colleagues through further characterisation [28, 53]. They showed SKPs expressed the transcription factors slug, snail, twist, Pax3 and Sox9, which is an expression profile indicative of neural crest stem cells. SKPs also follow a migratory path of neural crest cells *in ovo*, as demonstrated by transplantation of yellow fluorescent protein positive (YFP^+) SKP single spheres into a chick neural crest migratory system. Finally SKPs were found not to be derived from transdifferentiation of cell types formed from neural crest stem cells, namely melanocytes and Schwann cells. These pieces of evidence strongly support an undifferentiated neural crest identity of the precursor that has remained in the dermis since embryogenesis [28].

The markers that identified SKPs were used to single out a possible niche within the dermis for SKPs [28]. The key findings and conclusions from these data will be summarised here. Firstly *in situ* hybridisation on mouse back skin at various developmental stages, revealed expression of the neural crest markers expressed by SKPs, in the hair follicle dermal papilla. The dermal papilla location was confirmed by co-expression alongside neural crest markers of the dermal papilla markers versican

and nexin but not keratin 17 (a marker of the hair follicle bulge and outer root sheath). Further characterisation of embryonic and post natal whisker follicles provided additional evidence for a dermal papilla location of SKPs. Both embryonic and post natal vibrissae dermal papilla expressed neural crest markers *in vivo*, which are associated with cultured SKPs. SKP spheres derived directly from whisker dermal papilla also showed an expression and differentiation profile indicative of SKPs isolated from whole dermis. Importantly the presence of SKPs in the whisker dermal papilla was independent of other neural crest derivatives. A genetic method was used to permanently label cells with β-galactosidase that expressed the neural crest marker Wnt-1 *in vivo*. Visualisation of labelled neural crest cells in mouse dermal papilla was achieved using the X-gal reaction, and provided further confirmation of the dermal papilla as a potential niche in the dermis for SKPs [28]. The same labelling technique has since been repeated on rat facial skin by others and neural crest derivatives were also found in the dermal papilla. Furthermore 25% of cells microdissected from the dermal papilla were able to form free floating spheres with a similar phenotype to SKPs after seeding single cells out, which represented a much higher conversion of cells to spheres compared to the whole hair follicle and dermis [53]. Taken together these data strongly suggest SKPs are of neural crest origin and reside in the dermal papilla of hair follicles of the rodent facial dermis.

SKPs have also been isolated from the microdissected dermal papilla of human adult facial skin [53]. Successful isolation of these SKPs – referred to as papillaspheres – was intriguing since a rapid decline in the frequency of SKPs isolated was shown in rats with aging. The neural crest origin of these papillaspheres was confirmed by the expression of the neural crest marker Sox10. These papillaspheres were nestin positive like SKPs, and formed neuronal and Schwann cell phenotypes, as shown by their morphology and protein expression profiles after differentiation. SKPs have also been isolated form the dermis of neonatal human foreskins [58], which do not have hair follicles, and therefore the niche for these SKPs cannot have been the dermal papilla. Isolation difficulties were encountered – in studies that used a similar protocol to SKPs – on whole human adult dermis from different hairless tissues, which either suggests that the extra-follicular neonatal SKP niche is restricted to the foreskin, or the niche becomes very rare in adult tissues [53]. Overall these findings are encouraging because they support data gathered from rodent facial skin and in doing so they further confirm the dermal papilla as a niche for SKPs.

Neural crest derived cells have been isolated from the bulge region of mouse facial skin [11]. Similar to neural crest derived cells from the dermal papilla these cells could be visualised based on their expression of the marker Wnt1. Sections of Wnt1-cre/R26R compound transgenic mice skin showed neural crest derived cells located along the length of the follicle, indicating migration of these progenitors from the bulge region. The labelled cells could be explanted and differentiated towards neural crest derivatives both after cloning and at the population level. These lineages included glial fibrillary acidic protein (GFAP) positive Schwann cells and TuJ-1 positive neurons [11]. These neural crest derived cells were later shown to express a transcriptome that was distinct from other stem cell types in the bulge region [61]. However, neural crest derived cells could be related to nestin expressing cells from the bulge [29, 62]. Nestin expressing cells were isolated from the bulge region of previously discussed nestin-GFP mice and grown as spheres or colonies. The spheres showed differentiation potential of neural crest cells, migrated along pathways similar to neural crest cells after transplantation and expressed the neural crest transcription factors snail and twist. After *in vitro* differentiation the sphere derived cells expressed the neural lineage markers TuJ-1 and GFAP [62]. A second study, explanted cells from the bulge region and grew them for four weeks as colonies in serum free medium. After differentiation in serum containing medium for a further four weeks, the cells showed sequential differentiation towards the keratinocyte, astrocytic, neuronal, and smooth muscle lineages [29]. These data also strongly suggest that bulge stem cells show neural crest like characteristics. However, the expression of the epidermal stem cell marker CD34 and the marker K15 shows these bulge derived cells were not identical to cells of neural crest origin.

Cells expressing nestin have been isolated from human scalp tissue, expanded as an adherent monolayer and differentiated towards neural lineages. However, these cells were not isolated specifically from the bulge region; instead they were isolated from samples of tissue that included whole hair follicles and interfollicular epidermis [38]. After expansion in culture nestin expression remained in 10-20% of adherent cells and they also acquired neuronal markers without the addition of differentiation factors to the medium. These neuronal phenotypes could be an artefact of the *in vitro* expansion conditions as they formed spontaneously in culture [38]. Another group isolated and expanded cells with neurogenic potential from whole human scalp tissue. These cells were specifically differentiated toward neuron-specific enolase (NSE) positive neuronal lineages in the majority of cases [56]. Together these two studies suggest there are cells within the human scalp that differentiate towards neuronal

lineages but they do not suggest a specific niche or cell identity like previous studies from facial skin.

These data strongly suggest that cells isolated from the dermis of the rodent and human facial dermis are of neural crest origin and reside in the hair follicle dermal papilla. Neural differentiation was also found in cultured cells from within bulge region expressing the early neural stem cell marker nestin and the neural crest marker Wnt-1. These data suggest that the bulge and dermal papilla stem cell populations in the hair follicle could be related through their homologies with neural crest cells and their propensity to differentiate towards neural lineages.

1.2.8 In vivo neural differentiation of HFSCs

There is a limited amount of *in vivo* evidence showing the capability of HFSCs to produce differentiated neural derivatives after transplant into the injured nervous system. However, the most prominent example of neural differentiation *in vivo* is SKPs, for which there is strong evidence of a hair follicle dermal papilla niche for these cells [28, 53]. Consistent with their relationship to neural crest cells, SKPs were shown to produce fully functional myelinating Schwann cells after transplant into the shiverer mouse mutant; a mouse unable to produce Schwann cell derived myelin basic protein (MBP) [63]. A purified population of YFP^+ SKPs, which expressed the Schwann cell markers GFAP and p75 neurotrophin receptor in over 95% of cells after differentiation in neuroregulin-1 and forskolin, was produced *in vitro*. YFP^+ purified Schwann cell differentiated SKPs and YFP^+ undifferentiated SKPs were then transplanted into an injured peripheral sciatic nerve site in a shiverer mouse mutant and left for between six and eight weeks. SKPs at both developmental stages were able to form cells expressing the MBP antigen along the length of the injured sciatic nerve. Immunoelectron microscopy revealed these MBP expressing cells represented genuine myelin architecture, indistinguishable from mature Schwann cells. MBP expression indicative of fully functional Schwann cells was also evident when SKPs were transplanted into the CNS of the shiverer mouse. These findings were also recapitulated in an *in vitro* coculture model. Together these data suggest that both peripheral damaged axons and CNS axons produce cues that cause naïve and *in vitro* differentiated SKPs to differentiate into fully functional Schwann cells capable of producing myelin [63]. Cell fusion may be occurring and causing these phenotypes, but the frequency of occurrence would not be high enough to explain the number of Schwann cells observed.

Nestin-GFP cells isolated from the bulge region as previously described, showed neuronal potential after they were transplanted into the subcutis of a nude mouse and expressed TuJ-1 after two weeks [29]. Schwann cell differentiation was also observed in cells expressing GFP that were isolated from the bulge region [64]. These cells were also cultured *in vitro* as colonies prior to transplantation, and their similarity to nestin-GFP bulge cells was confirmed by their expression of nestin and absence of CD34 expression. Schwann cell differentiation was produced when – like SKPs – the bulge derived cells were transplanted into a peripheral nervous system site close to a severed sciatic nerve. After two months live images showed GFP cells had localised around the repaired axon. Sections revealed GFAP expressing bulge cells had also closely surrounded the host axons with myelin sheath. Behavioural improvements were also apparent, with gastrocnemious contraction evident after electrical stimulation in injured mice that had bulge derived cells transplanted, but no contraction in those mice that were not administered a transplant [64]. These data strongly suggest that bulge derived stem cells are capable of enabling functional recovery by promoting and guiding axon development. A second study characterised the development of bulge derived cells that had been transplanted into a damaged mouse CNS site (the spinal cord) [51]. These bulge cells were marked by enhance enhanced GFP and their previously established neural crest phenotype was confirmed *in vitro* prior to transplant [11]. Enhanced GFP labelled cells were present around the injured spinal cord up to three months after transplant. Approximately half of the transplanted cells expressed the neuronal marker TuJ-1 and one third of cells expressed oligodendrocyte marker MBP. Host neurites were closely associated with bulge derived cells, suggesting the transplanted cells provided a microenvironment for regeneration. However, expression of GFAP was not reported in bulge cells transplanted into the spinal cord, unlike the sciatic nerve peripheral site, where GFAP was expressed [51]. Although neural differentiation was reported in the spinal cord, functional recovery after transplantation was not tested. From these data it is clear that bulge derived stem cells are capable of forming neural cell types *in vivo*, however, their fate is determined by the central and peripheral nervous system microenvironments into which they are administered.

1.3 MSCs

1.3.1 Isolation and characterisation of MSCs

MSCs are a multipotent adult stem cells population that can be induced to differentiate into adipocytic, chondrocytic, or osteocytic lineages [17]. MSCs were first isolated from mouse bone marrow, spleen, thymus and lymph node cells by Friedenstein *et al.* in 1974. The cells were distinct from haematopoietic stem cells through their adherence to tissue culture ware and ability to form colonies 'capable of protracted self maintenance', hence they were initially referred to as fibroblast colony forming units (CFU-F) [65, 66]. In these early stages it was recognised that CFU-F were capable of contributing to the bone marrow and spleen microenvironment, and providing functional support for haematopoietic stem cells [67], but their differentiation ability had yet to be fully recognised. Since their isolation the developmental boundaries of MSCs is still a hotly debated topic being actively researched in stem cell Biology today.

MSCs represent a scarce population in adult human bone marrow, typically contributing between 0.001% and 0.01% of the total cell number [17]. The most widely used technique to isolate the small proportion of MSCs from bone marrow utilises their adherence to tissue culture ware and subsequent *ex vivo* proliferative capabilities [65]. MSCs are isolated by aspiration of bone marrow onto tissue culture ware. The MSCs adhere whereas the contaminating non-adherent haematopoietic stem cells are removed by medium changes and passage. The resulting culture should consist of a heterogeneous population of MSCs at various stages of development. During *ex vivo* expansion the cells are constantly changing morphology. For example, it has been noted that there is a conversion – between early, small, spindle shaped, rapidly cycling progenitors and later, larger, mature progenitors that proliferate more slowly – as MSCs are expanded *ex vivo* [68].

Unlike haematopoietic stem cells there are no definitive phenotypic markers of MSCs. Instead a battery of cell surface adhesion and receptor markers and intracellular markers – not exclusive to MSCs – are used to illustrate the phenotype of the plastic adherent population. Common markers expressed by MSCs are the intracellular proteins α-SMA and vimentin alongside the extracellular matrix component fibronectin [69]. MSCs express cell surface markers known to interfere with haematopoietic stem cell proliferation and differentiation; these include CD9, CD29, CD44 and CD106 [70].

Other cell adhesion and receptor molecules expressed by MSCs are CD54, CD55, CD73 (SH3 and SH4), CD90 (Thy-1), CD105 (SH2 or endoglin) and CD166 (ALCAM). MSCs coexist alongside haematopoietic stem cells in the bone marrow, and therefore their successful isolation is determined by the absence of haematopoietic stem cells. Hence they must be tested for the absence of haematopoietic stem cell markers CD11b, CD34 and CD45 [17]. There are limitations with using these cell surface proteins to define MSCs as some groups report different expression patterns of specific proteins. Pittenger *et al.* (1999) reported CD106 expression in human MSCs whereas others did not [71]. Variability in the proliferative stages of the MSCs could be responsible for the differences in expression patterns of antigens. For example CD34 negative MSCs have been shown to develop from a CD34 positive bone marrow fraction after prolonged *ex vivo* expansion [72]. Analysis of cell surface marker expression is a useful tool in characterisation of MSCs, but it is not definitive as none of the markers are specific to MSCs, and there are variations in their expression between studies.

Attempts have been made to isolate a more homogeneous population of MSCs from bone marrow by fluorescent activated cell sorting, using a single phenotypic marker called STRO-1, which identified clonogenic bone marrow derived progenitors able to form adipocytes, osteocytes and smooth muscle cells [73]. However it should be noted that STRO-1$^+$ cells only represent 3 – 5% of the MSC population [70]. Furthermore, a method based on immunodepletion has been utilised in an attempt to fractionate haematopoietic cells from MSCs prior to culture. However these cells were compromised by the immunodepletion process as they proliferated very slowly [74]. Therefore without a definitive marker for MSCs the most effective way to isolate MSCs remains their ability to adhere to tissue culture ware.

Marker analysis is a useful tool to characterise stem cell populations, however, it has limitations, including a lack of specificity to the stem cell population concerned. The gold standard used to define a multipotent adult stem cell is their capability to differentiate down several lineages. Hence, what defines MSCs as a multipotent stem cell is their ability to differentiate towards mesenchymal lineages. An *in vivo* example of mesenchymal differentiation, was when MSCs demonstrated their potential clinical application, through ostoegenic differentiation and the consequent repair of rat femurs after in vitro expansion [75]. Mesenchymal differentiation can also be achieved *in vitro* by adding inductive factors to the culture medium. The most prominent examples of this include: a) adipogenic (fat) differentiation where MSCs are treated

with dexamethasone, 3-isobutyl-1-methylxanthine (IBMX), indomethacin and insulin; b) chondrogenic (cartilage) differentiation during which MSCs are induced with transforming growth factor-beta1 (TGF-β1); c) osteogenic (bone) differentiation where MSCs are induced using a combination of dexamethasone, β-glycerophosphate and ascorbic acid; d) Myogenic (muscle) differentiation where MSCs are induced using 5-azacytidine, hydrocortisone and bFGF. There are numerous examples of these differentiation techniques in the literature and some degree of variability can be seen in the concentration of these factors and the time periods used for differentiation. It has also been noted in the case of fat differentiation that pharmacological stimuli such as IBMX and indomethacin may induce adipogenic phenotypes in cells non-reactive to physiological stimuli, and therefore interpretation of positive *in vitro* differentiation results should be treated with a degree of caution [17]. Histological assays are used to monitor differentiation into fat, cartilage and bone. The most common assays include; oil red O which monitors accumulation of intracellular lipid droplets after fat differentiation, Alcian blue stain which detects mucopolysaccharides after cartilage differentiation and Alizarin red or Von Kossa staining that detects a calcium rich mineralised matrix after bone differentiation. Further confirmation is provided in using immunological techniques for example detection of fatty acid binding protein 4 (FABP4), aggrecan and ostoecalcin expression after fat, cartilage and bone differentiation.

1.3.2 Sources of MSCs

For the vast majority of studies MSCs have been isolated from the bone marrow of adult long bones such as femurs and tibias by aspiration. The condition called Osseous heteroplasia suggests MSCs could reside in tissues beyond bone marrow, because bone formation occurs within subcutaneous adipose tissues. This plasticity towards a mesenchymal lineage additional to fat suggests the existence of MSCs within adipose tissue [70]. It is now widely accepted that MSCs can be isolated from a variety of foetal and adult tissues. Adult tissues containing MSCs include peripheral blood [76], synovial membranes [77], pancreas [78], vibrissae follicles [19], exfoliated deciduous teeth [79], scalp [56] and adipose tissue [70]. Examples of foetal tissues containing MSCs include placenta [80], umbilical cord blood [81, 82], amniotic fluid [83], bone marrow, liver, lung and spleen [84]. Perhaps the most striking of findings was the residence of MSCs in most major organs of postnatal mice [85]. MSCs form these tissue have been comprehensively characterised in terms of their morphology, cell surface markers and mesenchymal differentiation potential. In doing so MSCs

from these tissue sources have been shown to have a high degree of homology to those isolated from bone marrow. Isolation of MSCs from tissues other than bone marrow again exploits their ability to adhere to tissue culture plastic. However, MSCs in the majority of other tissues are more difficult to isolate from their niche. Surrounding tissue must therefore be removed by mechanical mincing [19, 70, 80, 84] and by using enzymes such as collagenases [70, 77, 79, 85, 86] and trypsin [19, 80] to release the MSCs prior to *ex vivo* expansion. MSCs isolated from human pancreatic ducts were initially grown as free floating aggregates in medium supplemented with EGF and bFGF and adherent cells were able to grow out of these aggregates [78]. As discussed previously all MSCs isolated from tissues other then bone marrow were able to differentiate into at least two of the mesenchymal lineages previously discussed, with fat and bone being the most common lineages. Differentiation into lineages representing their tissue of origin as well as mesenchymal lineages was observed in pancreatic ductal epithelial cells, when they differentiated into beta cells expressing glucagon [78].

MSCs residing in a common perivascular niche throughout a wide range of adult tissues, would explain the paradox of the same cell type being isolated from a number of very different tissue sources. A perivascular niche for MSCs was alluded to in explanted dental pulp cells that showed mesenchymal potential through their differentiation into fat and bone. *In vivo* immunohistochemical staining showed dental pulp cells expressing the *in vitro* mesenchymal marker STRO-1 around blood vessels, which suggested a perivascular niche for this source of MSCs [79]. In addition a second study utilised STRO-1 to immunoselect dental pulp derived MSCs that showed a perivacular phenotype [87]. However, the marker STRO-1 is only specific to MSCs in an *in vitro* context and therefore could bind to non-mesenchymal cells *in vivo*, making it unreliable for analysing MSC distribution [85]. The contribution of MSCs to different tissue types has been monitored by marking cells and delivering them systemically [88]. Using this experimental approach would be limited in determining the niche of MSCs because the cells could engraft non-specifically to different tissues. The most successful approach so far that determined a perivascular niche for MSCs cantered around the successful isolation of MSCs from post natal vasculature and all major organs tested [85]. Their identity was verified by differentiating the cells into fat and bone and showing they expressed α-SMA. One of the blood vessels from which MSCs could be isolated was the kidney glomerulus, which compromised capillaries only. Hence MSCs could be isolated from the simplest of blood vessels. Taken together these results suggest MSCs reside in all post natal

organs by virtue of their perivascular location. However, variability existed between the cells form different locations in terms of their developmental capabilities. For example MSCs from the vena cava blood vessel showed significant bone formation and rudimentary fat differentiation, whereas muscle MSCs showed little bone formation and strong fat differentiation capabilities [85]. These developmental variations could be explained by MSCs being subjected to different environmental cues within their perivascular niche.

1.3.3 Cloning as a tool to characterise bone marrow derived MSCs

Cloning is a strategy which has been used assess the differentiation of MSCs – isolated from a variety of tissues – into fat, cartilage and bone at a single cell level. Therefore cloning is a strategy which can be used to determine whether *in vitro* cultured MSC populations consist of a variety of progenitors committed to specific mesenchymal lineages or multipotent stem cells [85, 89, 90]. For example, cloning of MSCs was used as a strategy to determine if progenitors with proliferative and multipotent capacities were at least in part responsible for the phenotypes observed in explants from a number of adult tissues, including kidney, lung and muscle [85]. The successful isolation of these clones indicated a proportion of cells were committed to self renewal. Like their parent cultures the clones were able to differentiate into fat and bone. The proliferation and plasticity of these clones indicates a multipotent stem cell could be responsible for mesenchymal differentiation seen in a range of adult tissues [85]. Clones are generated using a technique called limiting or serial dilution, which involves seeding cells out at a density of one cell per well and expanding these cells to confluence. Hence the cloning process selects for cells from within a primary explant that have considerable proliferative capabilities, which is usually only a small proportion of the original population. This is highlighted by the vast majority of cloning attempts being unsuccessful with most single cells failing to divide sufficiently. For example, the successful isolation of hair follicle dermal sheath and dermal papilla clones in one study occurred in only 12-15% of cases [18].

In a study by Muraglia *et al.* (2000) human bone marrow MSC clones were successfully isolated both with and without bFGF, and hierarchical model of differentiation of a single multipotent progenitor into fat, cartilage and bone was proposed. The model is based on data showing multipotent clones capable of differentiation into fat, cartilage and bone that progressively lost plasticity as the number of progenitor population doublings increased. These data suggested that the

fat lineage diverges and becomes independent at lower population doublings, whereas cartilage and finally bone lineages gain independence at higher population doublings. This evidence is supported by the fact all but one of the clones fell into just three potency categories; those showing fat-cartilage-bone differentiation, those capable of cartilage-bone differentiation and those capable of bone differentiation only, which indicates an ordered loss of plasticity symptomatic of the hierarchical differentiation model [89]. Furthermore, MSCs isolated from pancreatic ductal epithelium showed a similar divergence of the fat lineage before cartilage and bone as the cells were expanded *ex vivo* [78]. A study by Okamoto *et al.* (2002) found plasticity in human MSC clones additional to the Muraglia group as clones were able to differentiate towards fat-bone, pure fat and pure cartilage lineages. Furthermore, the majority of clones were unable to differentiate down any of the three lineages. These data provided evidence against a hierarchical model for lineage commitment from a single multipotent progenitor, and suggested a random assortment of committed progenitors with variable degrees of plasticity within bone marrow. The apparent heterogeneity could, however, have resulted from the genetic manipulations required to immortalise the human MSC population from which the clones were isolated [90].

1.3.4 MSCs and HFSCs in the treatment of neurological diseases

There are currently very few useful therapies for the treatment of neurological diseases. Difficulties have arisen in the treatment of these diseases through variations in pathologies between the different conditions. The administration of adult stem cells such as MSCs and HFSCs to treat neurological disorders represents a very exciting and genuine opportunity. HFSCs and MSCs have number of characteristics, which give them a lot of promise for the treatment of neurological disorders. The apparently high plasticity of HFSCs and MSCs, their ease of isolation and expansion, their potential for use in autologous transplantation and the circumvention of the ethical issues associated with the use of ES cells, all mean these adult stem cells have potential therapeutic applications in the treatment of neurodegenerative diseases.

We have already seen the promise of HFSCs through their ability to differentiate towards neural lineages *in vitro* and produce functional Schwann cells after transplant into damaged nervous tissue. A wider ranging and far greater amount of research has investigated the potential use of MSCs in the treatment of neurodegenerative

diseases, which has produced much conflict and discussion. MSCs have been reported to induce varying degrees of functional recovery in many animal models of neurological disorders such as Huntington's disease, multiple sclerosis, Parkinson's disease and spinal cord injury [91-94]. Recovery of nervous system function was assessed using a range of techniques including behavioural tests and assessment of nerve regeneration. However, there are a number of questions which need to be addressed before MSCs and HFSCs can be used in the clinic for treatment of human neurological diseases. For example, should any attempt be made to purify populations of bone marrow or hair follicle primary explants prior to implantation? How should MSCs and HFSCs be administered, directly into the nervous system or systemically? At what time and at what frequency should MSCs and HFSCs be administered [95]?

A much bigger issue for the use of MSCs in the treatment of neurological disorders, which must be overcome first, is the mechanism by which they elicit functional recovery after injury, which is a subject of great dispute. Three theories for contribution of MSCs to neural lineages have developed. It has been proposed that MSCs can form neural cells through direct differentiation stimulated by the extracellular environmental cues produced by cells already committed to the neural lineage or by a wide range of induction protocols. Another theory suggests MSCs can adopt neural lineage characteristics by fusing with existing neural progenitors. Finally it has been hypothesised that MSCs do not undergo differentiation themselves to elicit functional recovery; instead they manufacture soluble factors which mediate differentiation and repair of existing neural cells.

1.3.5 Chemical induction of MSCs towards a neural lineage in vitro

One of the seminal papers that induced MSCs toward neural lineages *in vitro* used neurotrophic factors that had been identified for NSC differentiation [22]. Differentiation conditions for NSCs were replicated by culturing MSCs for 7-14 days with medium containing 0.5μM retinoic acid (RA), 10% foetal calf serum (FCS) and brain derived neurotrophic factor (BDNF). Morphological transformations from flat fusiform to spindle shaped cells, and the up regulation of the neural markers lead to conclusions of neural differentiation in MSCs. However, the neural differentiation of MSCs was only evident in a small proportion (0.2%) of cells, which suggested the heterogeneous MSC population either contained a very low frequency of multipotent

progenitors or contained a small proportion of cells capable of being reprogrammed towards neural lineages upon culture *in vitro*.

A considerably larger frequency of MSCs developed neural progenitor phenotypes based on morphological and protein expression profile, after induction for 6 days with the phosphodiesterase inhibitor IBMX and the a cyclic adenosine monophosphate (cAMP) analogue dbcAMP [23]. It was proposed that the increase in intracellular cAMP concentration caused by this treatment, decreased proliferation and increased process extension, which induced a neural-like phenotype. This differentiation was not reversible because removal of IBMX and dbcAMP caused neural-like cells to die within a number of days. A second chemical treatment, which caused differentiation of MSCs into progenitors resembling neural cells was caused by culture of high passage MSCs in serum free medium containing dimethyl sulfoxide (DMSO) and butylated hydroxyanisole (BHA) [21]. This protocol produced the most neural-like cells with 75% of induced cells showing neuronal morphologies. These chemical induction protocols produced very high yields of cells displaying neuronal-like phenotypes compared to neurotrophic factor driven induction.

Several neuronal markers were also used after chemical induction to confirm the neural phenotypes. Western blot data have shown the neural markers TuJ-1 and NeuN were expressed both before and after MSCs were induced, which suggests MSCs already have some characteristics of the neural lineage. Furthermore, GFAP expression has been shown to be completely absent, indicating changes to growth medium do not induce expression of some neural proteins [21, 23]. This is perhaps due to MSCs being driven away from the glial lineage and towards a neuronal lineage under certain induction conditions [96]. Commitment to the neuronal lineage was confirmed by the early neuronal marker NSE, which had seemingly dramatically increased its expression levels after treatment with the chemicals IBMX and dbcAMP [23]. These NSE data verify the findings of a previous study, where an increase NSE expression was observed alongside the acquisition of morphological neuronal phenotypes under DMSO/BHA chemical induction conditions [21]. This marker analysis indicates commitment towards a neural lineage by MSCs upon chemical induction.

1.3.6 Summary of early neural induction protocols in MSCs

We have seen that chemical induction protocols such as treatment with IBMX/dbcAMP and DMSO/BHA are able to induce a very large number of neural-like phenotypes, whereas treatment with neurotrophic factors induce similar phenotypes in a much smaller proportion of cells. Furthermore cocultures of MSCs with neural cell types can also be used to effectively induce neural-like phenotypes. Finally, gene transfection with notch intracellular domain (NICD) or noggin has also been used to specifically produce neuronal-like phenotypes in MSCs [97, 98]. There are many other very similar examples of *in vitro* MSC neural induction in the literature, which use simple induction protocols that have slight variations on those outlined here.

1.3.7 Re-evaluation of early in vitro neural differentiation protocols

Recently pioneering work by Woodbury and co-workers that showed *in vitro* MSC differentiation into neural-like phenotypes has been more thoroughly examined [21]. The analyses from several independent studies present strong evidence that neural differentiation is a potential artefact of the *in vitro* culture conditions, and not true neural differentiation, which was originally suggested. Serum withdrawal and treatment with the chemicals BHA and DMSO demonstrated the appearance of neural-like MSCs in a very short time period of just five hours [21], whereas NSCs usually take several weeks to differentiate [99]. The rapidity of neural phenotype development casts serious doubts on the validity of this early study, and was the premise for further investigation. Time-lapse video revealed the morphological changes that produced pseudo neuronal and glial phenotypes actually resulted in a reduction of cell area, after treatment with serum free medium supplemented with the chemicals DMSO/BHA [100-102]. Cytoplasm retraction was caused by disassembly of focal adhesion sites, and filopodium-like extensions appeared as a result of strong paxillin positive focal adhesion sites that remained along thin transects of the cytoplasm [102]. These morphological changes are atypical of neural development, which is produced by active neurite outgrowth after induction, rather than the differential rates of cytoplasm retraction observed here. Further investigations into changes to the cytoskeletal architecture involved in neuron-like differentiation, revealed disruption of the actin cytoskeleton was the primary mechanism through which neuron-like morphologies were acquired *in vitro* by MSCs [100-102]. Selective disruption of the F-Actin cytoskeleton using the drug cytochalasin B, caused morphological and protein expression profile changes very similar to those produced

when MSCs were cultured in response to serum withdrawal and DMSO/BHA chemical treatment. These changes were also reversible, which is not thought to be typical of cells undergoing lineage commitment. The ability to very closely mimic neural-like development induced by DMSO/BHA treatment using a technique that induces cytoskeletal changes completely unrelated to neural development, questions the validity of chemical induction.

A reduction in cell area following induction lead to the suggestion that a concomitant increase in NSE and neural morphological change, was due to an increase in antigen expression per unit area rather than a true increase in protein expression. As previously described MSCs express a number of neural antigens including NSE at low levels prior to induction; therefore a concentrating effect due to a reduced cell area after induction, which mimics an increase in antigen expression, seems conceivable. Also, the non-neural marker αSMA showed a similar increase in expression after DMSO/BHA induction, which was likely to have been caused by a similar mechanism. The pseudo increase in NSE expression was demonstrated elegantly when the same 'increases' in expression after chemical induction were shown in MSCs that had protein expression completely abolished prior to treatment. Therefore observed expression could not have been due to increases in transcription and translation of the NSE protein after induction, which would be required for true differentiation [103]. Furthermore, microarray analysis of the whole transcriptome of MSCs after treatment with DMSO/BHA revealed very little change in gene expression, whereas huge differences in gene expression between untreated MSCs and NSCs were observed. These data confirm that large scale changes in gene expression are required for neural differentiation, which do not occur after DMSO/BHA chemical induction [100]. Treatment of MSCs with DMSO has caused an increase in expression at the protein level of the neural stem cell marker nestin and the neuronal antigen NeuroD1, which indicates these antigens are up regulated at the transcriptional and translational level. The increases were shown by Western blot and therefore could not have been due to the concentration of existing proteins. However, the increased expression of nestin and NeuroD1 proved to be linked to signalling pathways activated as a result of cytoskeleton disruption associated with DMSO treatment, and were therefore independent of neural differentiation [101]. Together these data show phenotypic changes caused by DMSO/BHA chemical induction are a result of mechanisms not associated with neural development.

There are some uncertainties regarding the specificity and correct applications of some of the markers that have been used to indicate neural differentiation after chemical induction. For example, nestin is used to show neural progenitor commitment but is also expressed in skeletal muscle development [104]. Expression of the early neuronal marker TuJ-1 has been shown in many human tissues, therefore its use in studying human MSC neural development is limited [100]. The antigens NeuN and Tau have been used to demonstrate neural development but their distribution was not typical of neurites. After chemical differentiation both NeuN and Tau were distributed throughout the cytoplasm but NeuN expression should have been concentrated around the nucleus and Tau should have localised along the pseudo neurites. Therefore the distribution of NeuN and Tau actually provides evidence against true neural differentiation [100]. These observations show caution should be taken when analysing data based upon expression of a limited number of neural protein markers.

The reviewed studies provide a very comprehensive argument against claims that phenotypic changes observed *in vitro* after chemical treatment with DMSO/BHA represent commitment to the neural lineage. However, they do not completely rule out the possibility that MSCs differentiate towards neural lineages using different protocols. Another theory suggests the plasticity of MSCs can be accounted for by a rare pluripotent population of cells that exists within the bone marrow [12]. These cells were termed multipotent adult progenitor cells (MAPCs). The existence of MAPCs could explain why a very low proportion of MSCs were able to differentiate into neural lineages after treatment with BDNF and RA [22]. Also an increase in Nesitn positive MSCs capable of forming neural lineages [105] could be explained by an increase in the proportion of MAPCs in the culture after extensive passage. The pluipotency of MAPCs was demonstrated when they were differentiated into cells of the visceral mesoderm, neuroectoderm and endoderm at the single cell level. Human mesodermal progenitor cells have been isolated using the same low density culture technique that was used for the isolation of MAPCs [106]. MAPCs could be expanded in culture without differentiation. A high proliferation potential was demonstrated in MAPCs because telomere length remained stable for 40 population doublings. Furthermore, MAPCs differentiated into all three germ layers both *in vitro* and *in vivo*, which illustrated similarities with ES cells. However, some dissimilarity with ES cells does exist. For example, proliferation non-purified cultured MSCs is induced by EGF, whereas ES cells require human leukaemia inhibitory factor (hLIF) to induce proliferation. Propensity of MAPCs towards a mature neuronal lineage was

demonstrated by expression of the neuronal marker MAP-2 as well as the absence of the astrocytic marker S100 and the oligodendrocyte marker MBP.

It must still be cautioned that up regulation of neural markers in response to simple changes to growth medium *in vitro* does not provide enough evidence that sub-populations of MSCs are capable of forming mature fully functional neurons, displaying electrophysiological activity indicative of the neural lineage. Furthermore, the variation in stimuli used to induce neural morphologies, the diversity of starting populations and discrepancies in passage number prior to induction complicates comparison of *in vitro* neural differentiation studies. These additional factors lead to further uncertainties surrounding the *in vitro* neural differentiation capabilities of MSCs.

1.3.8 Production of neural phenotypes by MSCs in vivo

A number of early *in vivo* studies imply transplanted MSCs have differentiation capabilities beyond the mesenchymal lineage and also form cells from the neural lineage [107-109]. The majority of studies made some attempt to purify MSCs from bone marrow and expanded them *ex vivo* prior to transplantation. An exception was the transplantation of a mixed population of bone marrow into mice. The haemaotpoetic contingent either differentiated into other cells types or died because the hematopoetic antigen CD45+ was downregulated post transplantation [110]. There are other significant variations in experimental approach across *in vivo* studies showing neural phenotypes. MSCs have been marked using a variety of methods including GFP and the nuclear labels BrdU and bis-bezimide [108, 109, 111]. Implantation of MSCs uses a variety of techniques. A systemic approach, involves introducing MSCs into the circulatory system and allowing them to migrate and engraft into the brain [112], whereas other groups have directly injected MSCs into specific areas of the brain [107]. The condition and age of the recipient's nervous system has great variation. Some studies involve neonatal recipients, whereas others use adult recipients [107, 109]. There are examples of transplantation of MSCs into fully functioning nervous tissue [107, 109], whereas in other studies the nervous tissue was damaged [108]. Early studies reveal there are significant variations in the experimental approach used to analyse the activity of transplanted MSCs *in vivo*, which makes interpreting and analysing the data difficult. However, a variety of experimental approaches will ultimately allow determination of the best ways to implant MSCs into the nervous system.

Commitment of MSCs towards a neural-like lineage *in vivo* was often based on the coexpression of neural markers in labelled MSCs. For example, the differentiation of MSCs after transplantation into cerebral infarct mice was validated through the expression of neuronal markers NeuN and MAP2 [108]. However, after transplantation of MSCs into the injured spinal cord GFAP was expressed, which indicated glial differentiation. Furthermore, glial-like differentiation was also shown by GFAP positive MSCs that had engrafted into the hippocampus of non-infarct mice [109]. From this it can be concluded that differentiation of MSCs into glial and neuronal phenotypes was determined by the specific microenvironment the nervous tissue provided. Others alluded to the loss of mesodermal identity in MSCs as an indicator of neural differentiation when MSCs were implanted into rat brains [107]. The investigators in these studies deem that MSCs are beginning differentiation into functional neuronal and glial cells upon implantation into the nervous system using a number of different approaches. However, the simple expression of a limited array of markers *in vivo* is not sufficient evidence to validate this theory and more vigorous analysis needs to be considered. For example it needs to be assessed if MSCs are differentiating into functional neurons that express a number of mature neural markers, and have electrophysological activity similar too mature neural cells.

1.3.9 Cell fusion is a possible explanation for neural phenotypes

Cell fusion was predicted in MSCs when spontaneous fusion events involving other stem cell types were observed *in vitro* [113, 114]. Cell fusion events were first detected between cocultured R26R MSCs expressing a Cre dependent LacZ reporter gene and Cre^+ brain multipotent progenitor cells [115]. A fusion event caused activation of the Cre dependent LacZ reporter gene in MSCs by the Cre^+ brain progenitors. LacZ activation and therefore fusion events between MSCs and brain progenitors were visualised using X-gal. After four days a small proportion of cells – one to two per 80 0000 cells – were positive for X-gal. Dual nuclei were confirmed in the stained MSCs by electron microscopy. The supernumeracy of nuclei was lost through mitosis, which was illustrated using BrdU. Fusion of MSCs with neurons and other cell types was also detected *in vivo*, which resulted in the formation of multinucleated cells in some cases. This was demonstrated in the mouse cerebellum using electron microscopy, which showed fused cells displaying purkinje neuron morphologies that had two distinct nuclei. The frequency of cell fusion events showed great variability between recipient mice, indicating fusion is likely to be controlled by a

number of variables. This study indicates cell fusion with existing progenitors is a possible mechanism controlling reprogramming of nuclei in MSCs. However, the low frequency of fusion is unable to account for every neural like cell derived from transplanted MSCs, therefore other mechanisms – such as reprogramming without fusion – must be at large to account for these phenotypes.

Additonal studies have also advocated cell fusion between MSCs labelled with GFP and purkinje neurons [116, 117]. The GFP^+ cells had undergone cell fusion in lethally irradiated mice, and had comparable morphological features to purkinje neurons, such as complex dendritic trees and axons. In addition to previous studies the fusion event here was shown to reprogram the nuclei of MSCs. The initially compact nuclei of MSCs became increasingly dispersed with time. To investigate whether these distinct changes to chromatin morphology lead to reprogramming of the MSC nucleus, a purkinje specific promoter termed L7 was linked to GFP expression in the bone marrow derived cells. The L7-GFP construct was activated after bone marrow was transplanted into the host, which was shown by GFP^+ purkinje neurons. GFP expression definitively proved that host prukinje neurons were causing expression of a pukinje specific gene in MSCs after a fusion event. These data demonstrate a mechanism by which cell fusion between MSCs and host neural cells can lead to changes in the protein expression profile that accompany morphological alterations. However, no attempt to purify MSCs was made before implantation, which means contaminating haematopoietic stem cells may have contributed to some of the fusion events in this study. Administering MSCs after lethal irradiation could have altered cell membrane properties through genomic modifications, which would favour fusion events. Therefore it is possible the experimental set up was increasing the frequency of fusion events above what would normally be seen [105]. Even with the possibility of enhanced cell fusion, the frequency of fusion events was still very low after monitoring for more than a year. Hence it is clearly possible that populations of MSCs can undergo cell fusion and produce neural phenotypes. However other experimental techniques are needed to verify cell fusion is in fact occurring because there are some doubts surrounding the use of irradiated cells.

It is possible that neural differentiation of MSCs *in vivo* could be dictated by signals provided by microenvironments within the brain and not cell fusion. A large number of MSCs were found to be participating in neural differentiation *in vivo*, which cannot be all be accounted for by the low frequency of cell fusion. However, it may be possible for MSCs that have undergone phenotypic changes resulting from cell fusion to

appear as non fused cells with neural phenotypes, by continuing to divide after reprogramming from a fusion event has occurred [115]. Division after fusion could therefore explain the discrepancy between the frequencies of fusion events and the appearance of neural phenotypes *in vivo*. However, a group has demonstrated the appearance of a high proportion of neural-like cells upon *in vitro* coculture in the absence of cell fusion.

Cell to cell interactions – perhaps mediated by soluble factors – between nestin positive MSCs and mature neural cells are thought to be influential in causing neural differentiation in MSCs independent of cell fusion events [105]. Nestin expression was induced in high passage MSCs after transfer to serum free medium. The coculture of these rat nestin positive MSCs with GFP^+ mouse NSCs produced a high proportion of MSCs showing neural differentiation. GFP^- cells coexpressed the neural antigens GFAP and TuJ-1 indicating neural differentiation of MSCs in the absence of cell fusion with GFP^+ NSCs. Cell fusion was definitively ruled out by the mouse astrocytic antibody (M2) as well as and mouse neuronal antibody (M6) exclusively binding to GFP^+ NSCs. These antibodies exclusively binding to GFP^+ cells also ruled out downregulation of GFP causing NSCs to appear as MSCs. Furthermore, this study demonstrated that neuronal MSCs were capable of firing action potentials and responding to the glutamate neurotransmitters. Importantly the currents were abolished by tetrodotoxin (TTX), which indicates these action potentials were caused by voltage-activated sodium channels, which is symptomatic of neuronal cells. The expression of nestin prior to coculture was also shown to be essential for the formation of neurons. Nestin positive MSCs were thought to have heightened sensitivity to neuronal cues from NSCs through expression of intracellular factors important in nervous system development [105].

The imposed coculture conditions do not show that MSCs have all the electrical characteristics of fully mature neurons. This either means there is something missing in the experimental set up preventing MSCs forming mature neural derivatives, or that the phenotypic characteristics are an artefact and MSCs are incapable of forming neural derivatives. An explanation of the primitive neuronal phenotype seen could be that undifferentiated MSCs harbour some electrophysiological properties and ion channel expression [118]. These data indicate MSC plasticity without cell fusion could be responsible for the differentiation of MSCs into neural-like cells. However, the characterisation of differentiated progeny based on surface marker expression and inconclusive electrophysiological data, is not satisfactory to fully justify direct

differentiation of MSCs into fully functional neural phenotypes in the absence of cell fusion.

1.3.10 MSCs provided trophic support to existing NSCs

Repair of infarct areas of the brain can be measured using the neurological severity score (NSS) behavioural test. One explanation for the improvements in NSS is that the expression of neural markers by MSCs illustrates their differentiation into functional neural cells, which are entirely responsible for the recovery seen. However, coexpression evidence alone is insufficient to suggest MSCs were causing improvements by differentiating directly into neural cell types themselves. The time taken for large scale neural functional recovery to occur is far too short for MSCs to differentiate into fully functional neural cells with all their associated connections. Furthermore we have seen that early claims of MSCs differentiating toward neural lineages *in vitro* must be treated with great caution and that some of the neural phenotypes *in vivo* could be accounted for by rare cell fusion events. Therefore it has been hypothesised that MSCs provide support through secretion of soluble factors to existing NSC populations.

It has been proposed that the production of trophic factors and cytokines by MSCs after transplantation could be responsible for recovery after damage to nervous tissue resulting from a middle cerebral artery occlusion (MCAO) [119]. A supporting function for MSCs in renewal of neural tissues was suggested because MSCs were able to respond to different ionic microenvironments by adjusting growth factor production. It is therefore possible that the degree of tissue injury and corresponding alteration of the ionic environment determines secretion of trophic factors by MSCs, which in turn ameliorate existing nervous tissue [119]. Convincing evidence has been put forward, which shows MSCs contribute to functional recovery through production of soluble factors. After intravenous administration, MSCs initially migrated to the ischemic boundary zone (IBZ) in rats and apoptosis detection revealed they subsequently decreased levels of apoptosis in the existing neural cells within the IBZ compared to controls animals [120]. *In vitro* findings demonstrated MSCs are able to secrete factors such as BDNF and nerve growth factor (NGF), which could account for the reduction in apoptosis seen *in vivo* as well as proliferation and differentiation of endogenous neural stem and progenitor cells. Furthermore, signalling pathways contributing to increased survival of existing neural cells are upregulated following treatment of neural cells that have undergone anaerobic insult with MSCs [121]. Two

signalling pathways known to strongly influence cell survival called phosphoinositide 3-kinase/threonine protein kinase (PI3k/Akt) and mitogen-activated protein kinase kinase/extracellular signal-regulated kinase (MEK/Erk1/2) were examined. MSCs were cocultured *in vitro* with post-ischemic astrocytes and found to enhance both survival pathways in post-ischemic astrocytes after 18 hours. Real time polymerase chain reaction (RT-PCR) also showed growth factors such as BDNF and bFGF showed a considerable expression increases in ischemic astrocytes after coculture with MSCs [121]. Hence after coculture MSCs have been shown to have both protective and possibly inductive effects on post-ischemic astrocyte populations.

Amelioration of existing neural tissue was later demonstrated *in vivo* when MSCs were transplanted 24 hours after MCAO using a number of methods [122]. There are several phenotypic effects which demonstrated amelioration of damaged neural tissue after administration of MSCs. These included angiogenesis, synaptogenesis and differentiation of existing neural progenitors. Angiogenesis was shown by an increase in vascular perimeter and density in the cortical penumbra. Synaptogenesis was demonstrated post stroke by a significant increase in synaptophysin expression, 28 days after MSCs were transplanted. Increased synaptogenesis suggests MSCs induce axon remodelling in the cortex and therefore improve functional outcome in the damage brain. Lastly MSCs significantly increased the frequency and optical density of NG2 positive cells in the brain cortex. NG2 signifies the presence of oligodendrocyte progenitor cells, which enable neuroprotection by stimulating repair mechanisms in response to brain injury. Hence these data highlight the mechanisms by which MSCs can contribute to functional recovery of damaged neural tissue *in vivo* after MCAO by affecting the development of existing neural cell populations. Similar results have been produced by treatment of other models of neurodegenerative diseases with MSCs, such as the intravenous treatment of mice suffering from an animal model of multiple sclerosis [94]. Together these findings show how MSCs enable improvements after loss of neurological function *in vivo*, by inducing repair mechanisms in the host nervous system through the production of a variety of molecules.

1.4 Conclusions & perspective for future work

1.4.1 Potential niches for MSCs and cloning

In this review we have seen that there are potentially many sources of MSCs. A common perivascular niche could explain the widespread distribution of MSCs [85]. One of the common strategies used to characterise adult stem cells, which has been used in many situations is using clones. Cloning strategies have been used to propose the opposing hierarchical and committed progenitor models for bone marrow MSC development towards mesenchymal lineages [89, 90]. Mesenchymal differentiation reflective of parent cultures has been demonstrated using a cloning strategy in MSCs from tissue sources other than bone marrow [77, 80, 85]. Cloning has also been used to demonstrate neural and mesenchymal developmental potential representative of parent cultures in the hair follicle [18, 28].

1.4.2 Is the hair follicle dermis a niche for bone marrow derived MSCs?

The cloning strategy used to characterise the dermal niche for MSCs will be continued here in this study [18]. A sample of two clones (termed DS7 and DP9) from the hair follicle dermis will be further characterised and compared to bone marrow MSCs, which are a more established source of MSCs. This first part of the study will determine any similarities between the two cell types and help suggest if the hair follicle dermis could be a potential niche for bone marrow MSCs. By comparing a cloned population of adult stem cells with a primary population the analysis may also reveal disadvantages of using an *in vitro* cloning strategy to compare phenotypes.

1.4.3 Potential contributions of MSCs and HFSCs to neural development

The discoveries showing MSCs and HFSCs are capable of forming neural lineages and contributing to recovery upon implantation into the mammalian nervous system, has huge implications for the application of these two cell types in stem cell biology and in the treatment of neurological disorders. However, before these two cell types can be used safely in the treatment of neurodegenerative disorders such as Parkinson's disease and strokes the mechanisms for differentiation and amelioration of existing neural cells must be more comprehensively evaluated.

Plasticity of MSCs and HFSCs cannot be ruled out because a huge number of studies have demonstrated neural like differentiation. In the case of MSCs the importance of rigorous characterisation has been demonstrated by recent studies showing that pioneering *in vitro* neural differentiation observations were in fact produced by the removal of MSCs from their physiological environment and subsequent exposure to chemical stress rather than authentic neural differentiation. Hence, *in vitro* neural differentiation protocols may have unexpected, misleading effects and must be treated with caution. Perhaps the most likely explanation for adult stem cell plasticity is the presence of multipotent precursors that have remained in the two tissues from embryogenesis into adulthood. These are referred to as MAPCs [12] from bone marrow and neural crest related cells from the hair follicle dermal papilla and bulge region [11, 28]. We have seen that these neural crest related cells can elicit recovery *in vivo* after sciatic nerve injury and in mouse Shiverer mutants. These findings are due to differentiation of hair derived cells into Schwann cells, which are neural crest derivatives. However, both cell types do not show full neural differentiation capabilities *in vitro.* For example neither of the two cell types showed the electrophysiological activity of mature neurons after differentiation into neuronal cell types *in vitro.* This illustrates aberrant expression of neural proteins and morphologies *in vitro* is either an artifact of cell culture or that induction protocols towards neural lineages are not sophisticated enough to induce fully functional neural cell types. Therefore, a more thorough examination of the molecular signalling events leading to differentiation is necessary to verify the ability of MSCs and HFSCs to form neural lineages.

Cell fusion is a possible explanation for the *in vivo* plasticity of MSCs and HFSCs after transplantation into the peripheral and CNS. However, in the case of HFSCs the frequency of cell fusion is too low to explain the quantity of cells showing a Schwann cell phenotype [63, 64]. For MSCs also cell fusion is unlikely to be the only mechanism to explain the neural phenotypes observed because its frequency is too low. A more likely explanation for the role of MSCs in causing neural recovery is by promoting endogenous repair of the CNS by secreting cytokines and growth factors. To date promotion of endogenous repair by the secretion of soluble factors is the most convincing explanation, because it provides a link between MSC implantation and gain of neural function, which cell fusion and plasticity fail to demonstrate. The production of soluble factors that stimulate endogenous repair is a phenomenon which is likely to extend beyond MSCs to other adult stem cell types including HFSCs

1.4.4 Using conditioned media to investigate the effects of MSC secreted factors on neural development

A useful *in vitro* tool, which helps understand soluble factor mediated signalling between populations of adult stem cells and NSCs, uses MSC conditioned medium (MSC-CM). MSC-CM has been generated *in vitro* by culturing MSCs at different stages of development in defined media and then removing the media from the cells after one to three days. During this time defined media will have been 'conditioned' with secreted soluble factors from the MSCs. The effect of these soluble factors in MSC-CM has been tested on NSC populations to ascertain if it has any effects on their development.

MSC-CM has been shown to promote survival of neuronal cell types after induction of neuronal injury. Dopamine neurons from the ventral mesencepalon of rat embryos were subjected to injury using both serum deprivation and treatment with a neurotoxin [123]. MSC-CM was generated by culturing an undifferentiated confluent monolayer of MSCs for 24 hours with serum free N2 medium. The medium was found to both reduce loss of tyrosine hydroxylase (TH) positive neurons after exposure to 6-hydroxydopamine neurotoxin, and enhance expression of TuJ-1 and TH in the neurons compared to serum free medium controls [123]. Another study by Isele and co-workers (2007) found MSC-CM – harvested from confluent undifferentiated MSCs after 18-20 hours – attenuated apoptosis, which was induced in embryonic rat neurons five hours after MSC-CM was added [124]. The concentration of conditioned media was found to be very important, with 40% conditioned medium protecting stressed cells the most successfully and 100% solutions causing adverse effects. This result highlights the concentration of secreted factors produced by MSCs is vital in the effectiveness of treatment and great caution needs to be used if MSCs are to have therapeutic applications for neurological disorders. The MSC-CM was found to stimulate pathways involved in neuronal survival, because by blocking these pathways the beneficial effect of MSCs was lost. Double MSC-CM was also created by conditioning medium with MSC soluble factors that had already been conditioned with factors secreted by stressed neurons. Interestingly the double conditioned medium had a more potent protective effect, indicating a cross talk between MSCs and stressed neurons that causes an enhanced neurotrophic effect [124]. This evidence supports previous work, which indicates MSCs secrete neurotrophic factors such as bFGF and NGF after exposure to extracts of injured brain tissue.

A study by Rivera *et al.* (2006) identified that MSC-CM was able to instruct adult NSCs to form GalC$^+$ oligodendrocytes at the expense of GFAP$^+$ astrocytic differentiation [125]. Standard serum containing expansion medium was cultured with undifferentiated MSCs for three days to create MSC-CM, which was used to culture adult NSCs for seven days. Once it was established that significantly more GalC$^+$ and significantly less GFAP$^+$ NSCs were present in samples treated with MSC-CM compared to the control, it was determined if the oligodendrocyte phenotype was due to selection or induction by MSC-CM. Selection of GalC$^+$ NSCs by MSC-CM could have been either through an increase in proliferation (determined by BrdU incorporation) or a decrease in the death (determined by propidium iodide – PI – incorporation) of subpopulations of cells expressing a specific antigen. There were no significant differences in BrdU or PI incorporation in subpopulations of NSCs labelling for specific antigens when MSC-CM was compared to the control. Therefore through this analysis it was found the oligodendrocyte fate of NSCs was independent of selective mechanisms, and was likely to be an instructive effect on an uncommitted precursor by MSC-CM. Instruction was confirmed by a significant increase in expression of the oligodendrocyte transcription factors and down regulation of oligodendrocyte inhibitors compared to controls of NSCs treated with MSC-CM [125].

The developmental status of MSCs has a profound influence on the composition of MSC-CM, which has been shown to select an astrocytic phenotype in mouse embryonic NSCs [126]. In the previously outlined studies MSC-CM has been derived from undifferentiated MSCs, whereas Wislet-Gendebien and co-workers took conditioned medium from MSCs induced to express nestin. Nestin positive MSCs conditioned serum free medium for three days. For comparison MSC-CM was collected from MSCs not induced to express nestin by serum removal. A significant increase in astrocytic (GFAP$^+$) and concomitant decrease in oligodendrocytic (O4$^+$) and neuronal (TuJ-1$^+$) differentiation was found in NSCs treated with conditioned medium from nestin positive MSCs, compared to nestin negative MSCs and the control. BrdU incorporation showed MSC-CM – from nestin positive MSCs – was not causing a significant change in the proliferation of any specific NSC subpopulations. However PI incorporation showed that after two days culture, nestin positive MSC-CM significantly reduced cell death in the GFAP positive subpopulation, compared to the control and nestin negative MSC-CM. No such reductions in cell death were found in any other subpopulation. The investigators next found using Western blot that nestin positive MSC-CM had high levels of the active BMP4, whereas nestin negative MSC-

CM contained the inactive form. Further, the protective effect of nestin positive MSC-CM on the $GFAP^+$ subpopulation was negated when the conditioned medium was treated with an anti-BMP4 antibody [126]. These data strongly suggest that MSCs induced to express nestin secrete an active form of BMP4, which selectively protects astrocyte populations of NSCs, and does not instruct the astrocytic phenotype.

The four reviewed studies have shown that MSC-CM can be used to characterise the protective, inductive and selective effects MSC-derived soluble factors can have on various NSC populations, which supports previous data suggesting MSCs are able to secrete factors that mediate endogenous repair.

1.4.5 What effect do soluble factors in conditioned media from adult stem cells have on NSC *development?*

In vivo studies have shown neural antigen positive MSCs are capable of causing significant recovery after systemic injection into brain-lesioned mice. These improvements cannot be attributed to MSCs directly differentiating into neural cell types, because the proportion of cells expressing neural antigens is not high enough to cause such significant recovery [127]. An alternative explanation could be the upregulation of neural antigens in transplanted MSCs causes them to secrete soluble factors that mobilise large numbers of endogenous NSCs, which facilitate recovery from injury. We have already seen using MSC-CM that the secretion of soluble factors by MSCs induced to express the neural stem cell antigen nestin facilitates survival of NSC subpopulations [126]. This *in vitro* study supports the theory that neural antigen expression in MSCs is a prerequisite for their influence on NSC development. However, there is a paucity of information on the effect of soluble factors produced from adult stem cell populations induced to express neural antigens *in vitro*, using techniques that more closely replicate the development of NSCs *in vivo*. It is established that adult hair follicle dermal cells and MSCs can be induced to form neurosphere-like aggregates that express neural antigens [53, 128]. Therefore the second aim of this study is to induce hair follicle dermal stem cells and MSCs to form neurosphere-like aggregates, and see what effect the soluble factors these aggregates produce have on the development of NSCs using aggregate conditioned media.

CHAPTER 2: Materials and Methods

2.1 Isolation and maintenance of cells

2.1.1 The isolation MSCs from rat postnatal bone marrow

To isolate rat MSCs (rMSCs) an established procedure was used with adaptation [129]. The rMSCs were extracted from the bone marrow of 6-8 month old Wistar rats that had been euthanised using CO_2. The femurs and tibias were removed from the rat, cleaned of all muscle and connective tissue, sprayed with ethanol and placed in collection medium, which consisted of RPMI-1640 (Invitrogen) supplemented with 10% FCS (Invitrogen), 20 units/ml Penicillin-Streptomycin (Invitrogen), 1x non-essential amino acids (Invitrogen) and 2mM L-Glutamine (Cambrex). Under sterile conditions the bones were removed from the collection medium and one of the ends was clipped, exposing the medullary canal containing the bone marrow. Using a 21-gauge needle filled with 10ml of fresh collection medium the marrow was aspirated out of the bone into a 60mm Petri dish (Nunc). The flushing process was repeated using the same medium to maximise the yield of bone marrow from each bone. The aspirate was then transferred from the Petri dish to a 75cm^2 culture flask (Nunc) with an additional 10ml of fresh collection medium. Subsequently the cells were cultured in the collection medium at 37°C and 5% CO_2 for two days to allow the stromal cells to adhere to the tissue culture plastic. After this time the non-adherent contaminating haematopoietic cells were removed and the adherent cells were washed using complete culture medium (CCM) – consisting of Dulbecco's modified eagle's medium (DMEM; Sigma-Aldrich) supplemented with 10% FCS, 20 units/ml Penicillin-Streptomycin, 1x non-essential amino acids and 2mM L-Glutamine. Fresh CCM was added to the washed adherent cells. Every three days the medium was replaced with fresh CCM until the cells were 90% confluent, which usually took one week depending on the initial yield. A 90% confluent 75cm^2 flask of adherent cells was defined as passage zero (P0).

2.1.2 Passage of MSCs

To passage rMSC the CCM was removed, the cells were washed with phosphate buffered saline (PBS; Cambrex) without Mg^{2+} and Ca^{2+} and then detached by incubation with 2.5ml of 0.25% trypsin and 0.1% versene at 36°C for two minutes. The trypsin was inactivated by adding 7.5ml of CCM and the cells were spun at 250 X g for 5 minutes. The trypsin and medium were removed and the pellet was resuspended by gentle trituration in 1ml of CCM. For optimum expansion the cells were seeded at 10 000 cells/cm^2 into 20ml of fresh CCM in 75cm^2 tissue culture flasks. Using this procedure a single P0 75cm^2 flask produced three 75cm^2 tissue culture flasks of P1 MSCs. For subsequent routine expansion to higher passages the same procedure was used.

2.1.3 The preparation of hair follicle dermal clones

Both the hair follicle dermal cell clones DS7 and DP9 were kindly provided by Professor Colin Jahoda. The procedure used to isolate these cells has been previously described [18]. Briefly, primary dermal papilla and dermal sheath cells were mircrodissected from 3-month-old female Wistar rat vibrissae follicles. Dermal papilla and dermal sheath primary explants were maintained in 24 well plates using culture medium consisting of minimum essential medium (MEM; Sigma-Aldrich) containing 10% FCS and Gentamycin (50 mg/ml; Invitrogen) plus 20% dermal papilla or dermal sheath primary culture conditioned medium. Primary cultures were incubated at 37°C and 5% CO_2 for five days. In this time cell growth from the explants was evident with limited cell division. Cells were collected from each individual explant by detachment using 0.25% trypsin and 0.1% versene incubated for five minutes at 37°C. The primary cells were cloned by limiting dilution in 96 well plates (Nunc) at a density of one cell per well. After 24 hours wells with single cells were identified using a phase contrast microscope. These wells were cultured in the medium used for primary explants for 28 days with a medium replacement every seven days. The two clones were transferred to 35mm wells (Nunc) and medium was changed every three to four days over a period of 16 – 35 additional days at 37°C and 5% CO_2. Once confluency was reached, the clones were transferred into larger 12.5 cm^2 tissue culture flasks (Nunc) and expanded for 10 – 14 more days in MEM supplemented with 10% FCS.

2.1.4 Routine maintenance of clones

The two dermal clones (DS7 and DP9) were routinely maintained in 75cm^2 tissue culture flasks at 37°C and 5% CO_2, in the CCM used for the expansion of primary rMSCs with a medium change every three days. Each clone was passaged when confluent every three to six days. To passage the CCM was removed and the same trypsinisation procedure was followed as that used for the primary rMSCs. The clones were seeded in 75cm^2 tissue culture flasks containing 20ml of CCM at a density of 36 000 cells/cm^2 for the DS7 clone and 29 000 cells/cm^2 for the DP9 clone respectively. For all experiments the passage number of the clones ranged from P20 to (P41).

2.2 Characterisation of cells

2.2.1 Chromosome counting and karyotype analysis

Karyotype data for the two dermal clones DS7 and DP9 was kindly provided by Professor Colin Jahoda. The chromosome counting and karyotype analysis for the rMSCs was performed by Chrombios GmbH following the same procedures used for the dermal clones. Prior to the analysis the chromosomes had to be prepared. To ensure the rMSCs were growing exponentially they were routinely passaged into 75cm^2 tissue culture flasks at a density of 10 000 cells/cm^2 and cultured for two days. After this time colcemid (Invitrogen) was added to the culture medium at a concentration of 0.2µg/ml and incubated at 36°C for two hours. The rMSCs were trypsinised, spun at 200 X g in a 15ml tube for ten minutes and all but 0.5ml of the resulting supernatant was removed. The pellet was resuspended by gently flicking the tube and 10ml of hypotonic solution – comprising 75mM KCl (Fisher) in water – was added drop wise with continual agitation of the tube. The cells were left for ten minutes in the hypotonic solution, subsequently spun at 200 X g for 10 minutes and all but 0.5ml of the resulting supernatant was removed. The pellet was then resuspended by gentle flicking and 3ml of fixative – comprising a 3:1 mixture of methanol (Fisher) and acetic acid (Fisher) stored at -20°C – was added drop wise whilst gently flicking the tube. The tube was then filled up with a further 12ml of fixative and left for 30 minutes at -20°C. The fixed cells were spun at 270 X g for ten minutes and they were resuspended by gentle flicking in 0.5ml of supernatant. The tube was filled drop wise with 15ml of fixative and the cells were transported in a chilled box.

All work done after the fixing process was completed by Chrombios GmbH. The cells were analysed by chromosome counting and karyotype analysis. Approximately 30 rMSC metaphases were imaged, three metaphases were karyotyped in detail, and chromosomes were counted for 15 metaphases. To give good chromosome spreading 40µl of the fixed cell suspension was dropped onto a slide, incubated at 60°C for one hour, stained with 4'-6-Diamidino-2-phenylindole (DAPI) and mounted in an antifade solution. The slides were processed using a Zeiss Axioplan II fluorescence microscope attached to a b/w CCD camera and images were taken using SmartCapture VP software. Metaphase cells were imaged, printed and 15 sets of metaphase chromosomes were counted. To karyotype the cells Quips image processing software for reverse DAPI banding was utilised.

2.2.2 Immunocytochemistry: Intracellular antigens

The rMSCs and the dermal clones DS7 and DP9 were seeded at a density of 20 000 cells/cm^2 on sterilised glass cover slips in 12 well plates (nunc) and incubated for 24 hours in DMEM supplemented with 10% FCS. The medium was removed and the cells were washed for five minutes in PBS. The cells were then fixed for 15 – 20 minutes in cold 4% paraformaldehyde (PFA; Sigma-Aldrich) dissolved in PBS. To make the 4% PFA PBS was heated, PFA was dissolved in it, and the solution was filtered on ice immediately. Cells were then blocked for one hour in blocking solution consisting of 1% goat serum (Invitrogen), 1% Albumin from bovine serum (BSA; Sigma-Aldrich), 0.5% Triton-X-100 (Fisher), 0.1% sodium azide (Sigma-Aldrich) dissolved in PBS. The cells were incubated with the primary antibodies in staining solution – consisting of 1% goat serum, 1% BSA, 0.2% Triton-X-100, 0.1% sodium azide dissolved in PBS at pH 7 – for one hour at room temperature. The following intracellular antigens were tested; nestin (Chemicon; 1:200), GFAP (Sigma-Aldrich; 1:200), TuJ-1 (Covance; 1:600), fibronectin (Sigma-Aldrich; 1:200), α-SMA (Sigma-Aldrich; 1:400) and vimentin (Sigma-Aldrich 1:400). Cells were then washed three times for five minutes in blocking solution to remove any unbound primary antibody. The cells were incubated protected from light for 45 minutes in the appropriate anti-mouse (Sigma-Aldrich; 1:100) or anti-rabbit (Sigma-Aldrich; 1:100) IgG (secondary antibodies) conjugated to fluorescein isothiocyanate (FITC). A control for each cell type using secondary antibody only was tested alongside those wells initially incubated with primary antibodies. Any unbound secondary antibody was removed by washing the cells three times for five minutes in PBS. The cover slips were then

removed from the 12 well plates, mounted on microscope slides using Hoechst 33342 (Invitrogen; 1:1000) in vectorshield (Invitrogen) ready for imaging.

2.2.3 Versican immunohistochemistry and immunocytochemistry

Early anagen rat vibrissae follicles were used as a positive control for veriscan expression. The follicles were embedded in OCT embedding medium (RA Lamb) and cut in to several 7µm sections using a cryostat. The sections were mounted on histobond slides (RA Lamb) and stored at -20°C. The rMSCs and the dermal clones DS7 and DP9 were seeded at a density of 20 000 cells/cm^2 on sterilised glass cover slips in 12 well plates and incubated for 24 hours in CCM. The sectioned vibrissae follicles were dried for 30 minutes and all three cell types growing on glass cover slips were removed from the CCM and washed in PBS prior to fixing. The samples were fixed in 100% methanol at -20°C for 10 minutes followed immediately by 100% acetone (Fisher) for five minutes at -20°. The fixative was removed using three five minute washes of PBS. Versican antibody (Developmental Studies Hybridoma Bank) was applied undiluted to the samples for one hour at room temperature and was removed. Following three five minute washes of PBS, the samples were incubated for 1 hour in anti-mouse secondary antibody conjugated to FITC. The secondary antibody was taken off and unbound antibody was removed by washing three times for five minutes in PBS. The vibrissae follicles were mounted ready for imaging using Hoechst 33342 (1:1000) in PBS, whereas the three cell types on the glass cover slips were mounted on microscope slides using Hoechst 33342 (1:1000) in vectorshield.

2.2.4 Analysis of cell surface antigen expression using flow cytometry

Flow cytometry was used to analyse the expression of haematopoietic and mesenchymal cell surface antigens on both rMSCs and the dermal clones DS7 and DP9. All cell types were cultured in 75cm^2 tissue culture flasks in CCM and at confluency the medium was removed, the cells were washed with PBS and then trypsinised. A single cell suspension was produced by triturating the cells in PBS; the cells were washed with a further 9ml of PBS and spun at 250 X g for five minutes. The cells were fixed overnight at 4°C by resuspension in 0.25% PFA. The fixative was removed, the pellet was resuspended in wash buffer – consisting of 0.1% BSA and 0.1% sodium azide dissolved in PBS at pH 7 – and cell number was determined using a haemocytometer. For each antigen tested a 200µl volume of wash buffer containing 800 000 cells as a single cell suspension was dispensed into a 15ml tube

(VWR). All tubes were spun at 250 X g, the supernatant was removed, and the cells were resuspended with 50µl of primary antibody at the appropriate working dilution. Cell suspensions were incubated for one hour on ice. The following primary antibodies and primary antibody working dilutions were used: CD34 (Chemicon; 1:15), CD45 (Becton Dickinson; 1:15), CD90 (Becton Dickinson; 1:15), CD44 (abcam; 1:50), CD105 (santa cruz biotechnology; 1:50) and a negative control P3X (Professor Peter Andrews, University of Sheffield; 1:50). All antibodies had reactivity to rat and the working dilutions were created using wash buffer. After incubation the primary antibody was removed with three washes in 150µl of wash buffer. The cells were incubated protected from light on ice for 45 minutes in 50µl of the appropriate anti-mouse (1:100) or anti-goat (Sigma-Aldrich; 1:100) secondary antibodies conjugated to FITC. Secondary antibodies were subsequently removed with three washes of 150µl of wash buffer and the cells were transferred to FACS tubes (BD Biosciences). 10 000 cells from each sample were passed through a FACS Calibur flow cytometer (BD Biosciences) with fluorescence measured on a logarithmic scale. Cytometric traces were analysed for each of the antigens using CellQuest Pro software. Thresholds that determined the frequency of positive cells were set using the P3X negative control (with the appropriate secondary antibody), before levels of tested cell surface antigens were analysed.

2.2.5 Proliferation assay

Proliferation of rMSCs was compared to proliferation of the dermal clones DS7 and DP9 using an established procedure with adaptation [18]. The three cell types were plated at an initially density of 30 000 cells per well in 24 well plates (Nunc) and counted at days one, two, three, five, seven, nine and 11. At each time point the medium was removed from three wells, they were washed with PBS and trypsinised for one to three minutes – using 200µl of 0.25% trypsin and 0.1% versene at 36°C – and counted using a haemocytometer. At selected time points the cells were photographed after counting had been completed. A mean cell count at each time point was plotted and the population doubling time was determined for each cell type using the following formulae:

$$Population\ doubling\ time = \frac{Hours\ of\ growth}{Number\ of\ divisions}$$

$$Where, number\ of\ divisions = \frac{LogN1 - LogN0}{Log2}$$

N0 is the initial cell count and N1 is the subsequent cell count

2.2.6 Osteogenic assay and bone detection

To determine whether rMSCs and dermal clones DP9 and DS7 were capable of bone differentiation an osteogenic assay was performed. All cells were seeded out at a density of 3 000 cells/cm^2 in six well plates (Nunc) in CCM and were allowed to become confluent. At confluence osteogenic differentiation was initiated in four of the six wells by switching the cells into osteogenic medium. The other two control wells were cultured in control medium consisting of CCM. Osteogenic medium was made up of control medium supplemented with 100nM dexamethasone (Sigma-Aldrich), 50µM ascorbic acid 2-phosphate (Sigma-Aldrich) and 10nM β-glycerophosphate (Sigma-Aldrich). The medium was changed every three days and the cultures were maintained for three weeks.

After three weeks the medium was removed, the cells were washed twice using PBS and fixed using 4% PFA for 15 minutes. The presence of bone nodules was detected using Von Kossa staining. For Von Kossa staining the cells were incubated in 5% silver nitrate (Sigma-Aldrich) solution protected form light, washed with two changes of distilled water and subjected to intense light for 15 minutes. Mineralised areas identified by Von Kossa staining were visualised using a phase contrast microscope.

2.2.7 Adipogenic assay and lipid detection I

Prior to differentiation rMSCs and the dermal clones DS7 and DP9 were seeded in 35mm diameter six well plates (Nunc) at a density of 2 x 10^4 cells/cm^2 per well and left to adhere in CCM at 37°C and 5% CO_2. When the cells were confluent adipogenic differentiation was initiated using an induction/maintenance cycle, which was repeated until the cells had been cultured for three weeks. In detail each cycle consisted of three days in induction medium (CCM supplemented with 1µM dexamethasone, 0.2mM indomethacin (Sigma-Aldrich), 10µg/ml insulin (Sigma-Aldrich), and 0.5mM

IBMX (Sigma-Aldrich) and two days in maintenance medium (CCM supplemented with 10µg/ml insulin).

After three weeks the cells were fixed and intracellular lipid production was detected using the oil red-O assay. For fixation the cells were washed three times for five minutes in PBS, fixed with 4% PFA for 15 minutes at room temperature and washed again using PBS. The cells were then stained for 15 minutes with a filtered working solution of oil red-O, which contained 60% saturated oil red-O (RA Lamb) in isopropanol (Fisher) and 40% distilled water. Excess oil red-O was removed with three five minute washes of PBS and nuclei were stained for five minutes using hematoxylin solution (RA Lamb). The cells were washed three times in PBS and their nuclei were blued in water using 3% ammonia blueing solution. Lipids vacuoles were imaged using a microscope.

2.2.8 Adipogenic assay and lipid detection II

Differentiation of DS7 clone and MSCs was achieved using a second protocol previously outlined for the dermal clones [18]. In addition adipogenic potential of DS7 was assessed at high passage (P31) and low passage (P22) number. Briefly, prior to differentiation cells were seeded in 35mm diameter six well plates at a density of 100 000 cells per well and left to adhere overnight under proliferative conditions (10% FCS and MEM at 37˚C and 5% CO_2. Four of the wells were then switched into adipogenic medium for one week whereas the other two remained in proliferative conditions for the same length of time. Adipogenic medium consisted of MEM supplemented with 15% rabbit serum (Sigma-Aldrich), 100nM dexamethasone, 0.45mM of IBMX and 2.07mM insulin. The medium was changed every three days and the cultures were maintained for one week. Control conditions consisted of MEM supplemented with 10% FCS.

After culture cells were fixed and stained to detect lipid formation using the oil red-O assay. Firstly the cells were washed using PBS and fixed in calcium formol (4% PFA and 1% calcium chloride (Fischer)) for 15 minutes at room temperature. Subsequently the cells were incubated in 60% isopropanol for 15 minutes and then stained for a further 15 minutes with a filtered working solution of oil red-O. After staining the cells were washed with 60% isopropanol for one minute and washed again three times for five minutes with distilled water. Lipids vacuoles were visualised using a microscope.

2.3 Aggregate and conditioned media studies

2.3.1 Aggregate formation

Induction of rMSCs and the two dermal clones DS7 and DP9 to form aggregates was achieved using established methods with adaptation [128]. Prior to induction cells were cultured in CCM. For induction CCM flasks for all cell types were trypsinised and resuspended to form a single cell suspension in aggregate induction medium. Aggregate induction medium consisted of DMEM:F12 (Invitrogen) medium supplemented with 1 x N-2 supplement (Invitrogen), 2mM L-Glutamine, 20 units/ml Penicillin-Streptomycin, 40ng/ml heparin (Sigma-Aldrich), 10ng/ml of EGF (Sigma-Aldrich) and 10ng/ml bFGF (Invitrogen) at 37°C, 5% CO_2 and 4.9% O_2. The cells were induced at a range of densities; 100 000 cells/cm^2 for rMSCs, 160 000 – 320 000 cells/cm^2 for the DS7 clone and 128 000 – 256 000 cells/cm^2 for DP9 clone in 25cm^2 adherent tissue culture flasks (Nunc) and 12 well plates. For rMSCs the medium was changed every three days and for the dermal clones the medium was changed after one day of culture and every three days subsequently.

2.3.2 Aggregate expression profile

For immunocytochemistry induced cells were fixed using 4% PFA as adherent aggregates in 12 well plates and tested for the intracellular antigens nestin, TuJ-1 and α-SMA using the procedure outlined in section 2.2.2.

The rMSC aggregates and DS7 aggregates were analysed using flow cytometry for the intracellular antigens nestin and α-SMA. Free floating aggregates were removed with induction medium and pelleted at 250 X g, while adherent aggregates were washed with PBS. Both types of aggregate were incubated with 3ml of 0.25% trypsin and 0.1% versene at 36°C for five minutes in 35mm dishes (nunc) for free floating aggregates, and three minutes in the 25cm^2 tissue culture flasks for adherent aggregates. After incubation the free floating aggregates were dissociated by trituration, whereas the adherent aggregates were dissociated by slapping the side of the tissue culture flask. Once a single cell suspension was achieved CCM was added to inactivate the trypsin. For comparison with the induced condition rMSCs and DS7 clone were grown to confluency in CCM in 75cm^2 tissue culture flasks and trypsisnised. After collecting the cells a procedure similar to the one used for cell surface antigen expression was followed (section 2.2.4) with the some adaptations.

Firstly, prior to incubation in intracellular primary antibodies, and after fixation in 0.25% PFA, the PFA was removed with a wash of PBS and the cells were permeabilisated at 37°C for 30 minutes in 1ml of 0.2% Triton-X-100 dissolved in PBS at pH 7. 1ml of wash buffer was added to the 0.2% Triton-X-100, the cells were spun at 250 X g, resuspended in wash buffer and 800 000 cells were dispensed in 200µl volumes into 15ml tubes. For intracellular staining the wash buffer consisted of 1% goat serum (Sigma-Aldrich), 0.2% Tween-20 (Sigma-Aldrich) and 0.1% sodium azide dissolved in PBS. The primary and secondary antibodies were used at the same dilution as for immuncytochemistry. Finally thresholds that determined the frequency of positive cells were set using a negative control consisting of cells that had been incubated in the appropriate secondary antibody only, prior to analysing levels of tested cell surface antigens.

2.3.3 Analysis of aggregate frequency and size

To analyse the frequency of rMSC, DS7 and DP9 aggregates the three cell types were induced to form aggregates at three different passage numbers (section 2.3.1). When the aggregates first appeared 20 non-overlapping visual fields at four times magnification were taken for each passage number. The number of aggregates was counted in each visual field and the mean number of aggregates per visual field was calculated for each cell type. To analyse aggregate size 20 randomly selected non-overlapping fields were taken of aggregates at each passage number at 20 times magnification immediately after they began to form. The analysis was repeated for three different passage numbers. The area of the aggregates was measured in micrometers using Image J software, and the mean area was calculated for the aggregates across all three passage numbers.

2.3.4 Generation of conditioned media

Once the aggregates had formed after induction of rMSCs and the dermal clones DS7 and DP9, conditioned media was generated by culturing the aggregates in aggregate induction medium for three days at 37°C, 5% CO_2 and 4.9% O_2. The aggregates were removed from the medium by centrifugation at 250 X g, the medium was filter sterilised into fresh 15ml tubes using 0.2µm filters (VWR) and stored at -20°C.

2.3.5 The effect of conditioned media on neural progenitor cell development

Adult hippocampal progenitor cells (AHPCs) were kindly donated by Fred Gage (Salk Institute). Prior to treatment with conditioned media AHPCs were passaged once at a dilution of 1:3 and expanded in 75cm^2 tissue culture flasks coated overnight with poly-L-ornithine (10µg/ml; Sigma-Aldrich) and mouse laminin (5µg/ml; Sigma-Aldrich). Expansion medium consisted of high glucose DMEM:F12 (Irvine Scientific), 1 x N-2 supplement, 2mM L-glutamine, 20 units/ml Penicillin-Streptomycin and 20ng/ml bFGF. The conditioned media from all three cell types was cultured with the AHPCs using an established procedure with adaptation [125]. Eight well glass culture slides (BD Falcon) were coated with poly-L-ornithine (50µg/ml) and laminin (5µg/ml). AHPCs were seeded onto the coated culture slides at a density of 10 000 cells/cm^2 and allowed to adhere overnight in expansion medium at 5% CO_2 and 37°C. After 24 hours the expansion medium was removed, conditioned media from each cell type was defrosted and added to the wells. Two controls were cultured alongside the conditioned media samples; the first was AHPCs cultured in expansion medium and the second was AHPCs cultured in fresh aggregate induction medium without EGF and bFGF. The medium in all three conditions was changed at three and six days and phase images were taken of the AHPCs at these time points. After seven days culture the cells were fixed using 4% PFA and tested for expression of the intracellular antigens nestin, TuJ-1, and GFAP (at the same dilutions as in section 2.2.2) and GalC (Chemicon; 1:200). The procedure used was very similar to that previously discussed for immuncytochemistry (section 2.4), except here Cy3 anti-mouse and anti-rabbit secondary antibodies (Jackson Immuno Research laboratories) were used instead of FITC. The number of cells positive for each antigen and the total number of cells were then counted. The two counts were used to calculate the percentage of positive cells for each antigen.

2.4 Data analysis

2.4.1 Image analysis

Unless otherwise stated all labelled cells were visualised using a Nikon Diaphot 300 inverted fluorescent microscope, and the images were captured using a Nikon DXM 1200 camera with individual filters for each channel. Corresponding phase contrast images were obtained using the same microscope and other phase images were

gathered using an inverted Nickon 330 bright field microscope. Both colour and phase contrast images were adjusted using Adobe Photoshop software (Adobe systems, Mountain View, CA).

2.4.2 Statistical analysis

Statistical analysis was conducted by entering macros and equations into Microsoft excel. When the samples had homogenous variances and were normally distributed the parametric one-way Analysis of Variance (ANOVA) test was performed to check if differences between the means were significant. If a significant difference between the means was computed using the ANOVA test, then a post hoc Tukey test was performed to determine which means were significantly different from each other and which were not. When the sample variances were not homogeneous or the sample distribution was not normal then the non-parametric Kruskal-Wallis test was used to test if there were significant differences between the medians. If a significant difference was computed between the medians using the Kruskal-Wallis test, more than one Mann-Whitney U-test for unmatched samples was used – with the Bonferroni-Holm multistep correction – to determine which medians were significantly different.

CHAPTER 3: RESULTS

3.1 Characterisation of cells

3.1.1 Morphology and behaviour of rMSCs and the dermal clones

The morphology of all three cell types changed notably during culture. After initially isolating rMSCs (P0) a number of spindle shaped cells (Figure 1A arrows) and tight round cells (Figure 1A arrow heads) were observed. After passage up to P2 much broader and flatter cells predominated in the cultures (Figure 1E,F asterisks). During expansion to confluence it was apparent that rMSC cultures were dynamically changing between smaller rounder cells to large flat cells. Shortly after initially seeding the cells, the culture was dominated by smaller cells (Figure 2A, arrow), and after five days of culture the cells were larger and growing in colonies (Figure 2F, asterisk). Finally, at high confluence large flat cells dominated the culture (Figure 2I, asterisk). The dermal clone DS7 showed considerable changes in morphology during expansion to confluence. At two days culture a large proportion of DS7 cells displayed a long and thin morphology (Figure 3A,B), whereas at high confluence after eleven days in culture the cells displayed a small, tight circular morphology (Figure 3G,H). In contrast, the dermal clone DP9 showed a flattened fibroblast-like morphology at two days culture (Figure 4A,B), and expanded in colony-like clumps (Figure 4C,D), that increased in size to cover all the tissue culture plastic at confluence (Figure 4G,H).

It has been observed that the dermal clones DS7 and DP9 would have required at least 16 population doublings to produce a confluent 35mm culture dish after their isolation, and that the majority of single cells failed to proliferate [18]. The corollary of this is the technique used to isolate both the dermal clones has selected for cells with significant proliferation capacities. This is reflected in the short population doubling times of 2.7 days for the P28 DS7 clone (Figure 5B) and 2.5 days for the P28 DP9 clone (Figure 5C). A much longer doubling time of 5.4 days for the P2 primary rMSCs (Figure 5A) is more indicative of the slow cycling nature of stem cells *in vivo*. Alternatively slow cycling could indicate suboptimal culture conditions for the rMSCs

compared to the two dermal clones. The proliferation graphs are summarised in Table 4.

3.1.2 Chromosome counting and karyotype analysis

Chromosome counting data for each of the cell types rMSCs, DS7 and DP9 is summarised in Table 1. Counting of metaphases in P4 rMSCs revealed they were close to diploid, however 46.66% of cells counted had more than the normal rat diploid chromosome number of 42. The average chromosome number was 42.3, with only 26.66% of rMSCs showing a normal number of chromosomes. Karyotyping of three metaphase cells revealed one normal rat karyotype (Figure 6F), one cell showing 43 chromosomes with a trisomy for chromosome nine (Figure 6G), and one cell with 44 chromosomes with trisomies for chromosomes eight and nine. The metaphase spreads of the P28 DS7 clone showed that these cells were polyploid (Figure 6A,B) and a detailed karyotypic analysis was not possible. The metaphase spread counts for P28 DP9 clone showed 53.33% of the cells analysed had the normal rat diploid chromosomes number of 42 and 33.33% of metaphases had only 41 chromosomes. The rest of the cells counted had one more chromosome (13.33%) than the normal rat diploid number. One of the Karyograms revealed that one of the counts of 41 chromosomes was possibly due to a deletion of chromosome 14 (Figure 6D).

3.1.3 Intracellular antigen analysis

Prior to analysis of the mesenchymal intracellular antigens vimentin, fibronectin and α-SMA, rMSCs and the dermal clones DP9 and DS7 were expanded to confluence in CCM. The three mesenchymal markers were expressed in rMSCs (Figure 7D – F), which was supported by flow cytometry data (Table 2). The dermal clone DS7 also expressed the three mesenchymal markers (Figure 7J – L) although the expression of α-SMA was heterogeneous, with some cells expressing the antigen more strongly then others. However, the differences in levels of expression were not large enough to show up as two distinct populations by flow cytometry (Table 2). Finally immunocytochemistry showed that DP9 was positive for the two mesenchymal markers fibronectin and α-SMA (Figure 7P – R) but only expressed vimentin at levels detectable by flow cytometry (Table 2).

Analysis of neural intracellular antigen expression in rMSCs and dermal clones DS7 and DP9 was examined after expansion to confluence in CCM. Based purely on immunocytochemistry data both primary rMSCs and dermal clone DP9 were negative for the neural stem cell marker nestin, TuJ-1 and GFAP (Figure 7A – C & Figure 7M – O). Seemingly contradictory evidence shown from flow cytometry readings indicated expression of these neural antigens in the dermal clone DP9 (Table 2). However, the mean fluorescence intensity (MFI) was low compared to other antigens that were detected by both immunocytochemistry and flow cytometry. Therefore, it can be concluded that the neural antigens were expressed at very low levels in the DP9 clone, only detectable by flow cytometry. Conversely, nestin was detected by flow cytometry in rMSCs at MFI levels comparable to antigens detected by both techniques; however, only 0.35% of the cells expressed nestin (Table 2). Immunocytochemistry showed that both nestin and TuJ-1 were expressed in a small proportion of DS7 cells, whereas GFAP was not expressed (Figure 7G – I). The dual population of nestin expressing cells was also clearly shown by flow cytometry with 28.60% of cells expressing nestin at a high MFI (377.74). However, a dual population was not demonstrated by flow cytometry for the neuronal antigen TuJ-1; instead 93.46% of cells expressed the antigen at a low MFI (31.39). The correlation between nestin expressing cells in the dermal clone DS7 and morphology was investigated further. These data showed there was no correlation between morphology and nestin expression, because nestin was expressed in a wide variety of cellular morphologies in DS7 cells. Examples included small round cells (Figure 8A,B asterisks), large flat cells (Figure 8C,D and Figure 8G,H arrows), and bipolar cells (Figure 8E,F and Figure 8G,H arrow heads).

The expression of the hair follicle dermal sheath and papilla marker Versican was investigated in all three cell types. Versican was shown to be specific to both components of the follicle dermis (Hoechst 33342 and fluorescence) and not the follicle root sheath (Hoechst 33342 only) of early anagen rat vibrissae follicles (Figure 9A – C). The follicle dermal clones DS7 and DP9 both expressed versican (Figure 9E,F) and the primary rMSCs of bone marrow origin did not (Figure 9D).

3.1.4 Cell surface antigen analysis

Haematopoietic and mesenchymal cell surface markers were used to measure similarity between the two dermal clones DS7 and DP9 and rMSCs. The cells were grown to confluence in CCM and analysed using flow cytometry. Haematopoietic

markers CD45 and CD34 were negative in rMSCs and both dermal clones DS7 and DP9. In contrast, mesenchymal markers CD44 and CD90 were expressed in all three cell types (Figure 10). The more specific mesenchymal marker, CD105, was not expressed in the dermal clones but was expressed in rMSCs (Figure 10). Hence by comparison with rMSCs it can be concluded that the dermal clones DS7 and DP9 show some homologies with the mesenchymal cell surface phenotype (summarised in Table 3). However, it must be noted that these markers do not definitively define MSCs as, for example, CD44 is also expressed in epithelial cells [38].

Closer examination of CD44 expression in the dermal clone DS7 revealed two populations of cells expressing CD44 at different levels, which remain as the cells are proliferated. This is evidenced by flow cytometry histograms showing dual peaks between similar ranges of fluorescence intensities at two different passage numbers (Figure 11A,B). Furthermore, the frequency of the two CD44 positive populations of cells appeared to change as the cells were proliferated, indicating DS7 was constantly changing during expansion in culture. At P30 there is a similar cell count for each population indicated by the peaks being of a similar size (Figure 11A). However, at P41 there is a much higher frequency of cells at the lower fluorescence intensity peak compared to the higher intensity peak (Figure 11B). These data suggest that as DS7 is passaged either the cells expressing CD44 at a higher level are converted into those expressing CD44 at a lower level, or the cells expressing CD44 at a lower level become dominant in the culture, perhaps by a more rapid rate of proliferation. It can be concluded that as DS7 clone is passaged the expression of CD44 declines through the increase in proportion of cells expressing CD44 at a lower level.

3.1.5 Potency of rMSCs and the dermal clones

Unsurprisingly, osteogenic potential was detected in rMSCs by Von Kossa staining after three weeks induction in osteogenic medium (Figure 12A,B). However, it was clear that DS7 and DP9 were unable to form bone nodules over the same time period, as demonstrated by the lack of mineralisaton detected by Von Kossa staining (Figure 12C – F).

Using two different protocols rMSCs and the dermal clone DS7 were adipogenic. However, the dermal clone DP9 was not adipogenic using either protocol (Figure 13G – I). The first protocol (Figure 13 and Figure 14) involved growing the cells to confluence prior to differentiation and differentiating the cells in medium containing

DMEM and 10% FCS. The second protocol (Figure 15) involved seeding the cells at a lower density and differentiating them immediately in medium containing MEM, 15% rabbit serum, a 10 fold lower concentration of dexamethasone and without indomethacin. As expected P4 rMSCs were adipogenic using the first (Figure 13A – C) and second protocols (Figure 15A – C), with slightly different lipid vacuole distributions within the cells. Adipogenic potential was shown in the dermal clone DS7 as widely distributed (Figure 14A), high density oil red-O positive areas of cells (Figure 13D,E and Figure 14E,G) using the first protocol, and intracellular accumulations of lipid vesicles using the second protocol (Figure 15D,E). The differing characteristics of the lipid vacuole accumulation could have been due to the two different protocols used. Using the second protocol, adipogenesis in DS7 declined as passage number was increased. At P20 the amounts of adipogenesis were low, with a small minority of oil red-O positive cells (Figure 15D – F), whereas at P33 no cells displayed adipogenic potential (Figure 15G – I). In summary unlike bone marrow rMSCs the dermal clones showed limited capabilities of mesenchymal differentiation. Neither clone was osteogenic, and only the DS7 clone was adipogenic.

3.2 Aggregates and conditioned media

3.2.1 Aggregate formation

Aggregate formation was possible in rMSCs and the dermal clones DS7 and DP9 following transfer of the cells as a single cell suspension to inductive serum free medium supplemented with EGF (10ng/ml) and bFGF (10ng/ml) in 4.9% O_2. However the seeding density of 100 000 cells/cm^2 – used previously for human MSCs [128] – was found to be suboptimal for aggregate formation in the dermal clones as the aggregates formed slowly over a period of several weeks (data not shown). Limited numbers of aggregates were yielded and the majority of cells remained as an adherent monolayer. When rMSCs were seeded for induction at 100 000 cells/cm^2 in 25cm^2 tissue culture flasks a higher yield of free floating aggregates formed over a period of up to one week (Figure 16A,B).

It was noted that a density of 100 000 cells/cm^2 corresponded to a confluent 75cm^2 tissue culture flask of rMSCs when the cells were grown in CCM prior to induction. Therefore, to optimise the seeding density for aggregate formation in the two dermal clones DS7 and DP9, it was decided that the cells would be allowed to become

confluent in a 75cm^2 tissue culture flask prior to induction. Once confluent the cells were seeded in 25cm^2 flasks at densities corresponding to a confluent 75cm^2 tissue culture flask and a half confluent 75cm^2 tissue culture flask for comparison. This translated to seeding densities that ranged from 160 000 cells/cm^2 (Figure 17A – C) to 320 000 cells/cm^2 (data not shown) for the DS7 clone and 128 000 cells/cm^2 (Figure 18A) to 256 000 cells/cm^2 (Figure 18B – D) for the DP9 clone. Both the higher and lower seeding densities showed an increased efficiency of aggregate formation in both types of dermal clone. The yield of aggregates was increased and the time taken for aggregate formation was decreased at the two seeding densities. Aggregates formed over a similar time period at both seeding densities with the higher of two densities producing a greater yield of aggregates. Hence, it was decided either seeding density could be used to generate aggregates in both the dermal cell types.

At the optimised seeding densities rMSCs and the dermal clone DS7 were able to form aggregates in a similar fashion (Figure 16A,B & Figure 17A – C). Firstly aggregations of cells formed on the tissue culture ware, after 4-7 days these aggregations lifted off and became free floating spheres of variable morphology between cell types. The dermal clone DP9 formed aggregates over a much shorter time period of less than two days. The aggregates did not adhere to the tissue culture plastic, instead forming free floating aggregates after two days from the single cell suspension (Figure 18A – D). If the dermal clones DS7 and DP9 were left for more than one week then the free floating aggregates adhered to each other to form a larger structure of many aggregates. This observation was particularly prevalent in the DP9 clone, although the aggregates were easily dissociated from each other when the medium was changed.

Aggregates were observed in primary rMSCs at passage numbers ranging from passage three to passage 10 (data not shown). However, at passage 10 mainly adherent aggregates were formed with a very few free floating cellular aggregates. Because of the high amount of expansion required in the isolation of the dermal clones DS7 and DP9 it was only possible to induce aggregates at a high passage number. Aggregates of the dermal clones DS7 and DP9 formed optimally at passage 37 and passage 31 respectively.

3.2.2 Aggregate antigen expression profiles

Aggregates for rMSCs and the dermal clones DS7 and DP9 were characterised in terms of their cell surface antigen expression, by both immunocytochemistry and flow cytometry. All three types of aggregates when grown in inductive serum free conditions expressed the neural stem cell marker nestin. Both rMSCs and the dermal clone DP9 showed an increase in nestin expression, after they were transferred from growing as an adherent monolayer in high serum control conditions (Figure 7A,M), to serum free aggregate forming inductive conditions (Figure 16E and Figure 18E). However, the dermal clone DS7 expressed nestin in both control conditions (Figure 7G) and inductive conditions (Figure 17F), which was confirmed by flow cytometry. In contrast to nestin, a significant reduction in α-SMA expression in DS7 was also shown by flow cytometry, which indicated a loss of mesodermal identity under the inductive conditions (Figure 17D,E). The rMSCs showed a similar reduction in α-SMA expression when transferred to inductive conditions; however – unlike DS7 – a concomitant increase in nestin expression was observed (Figure 16C,D). Unlike rMSCs and DS7, α-SMA expression in the dermal clone DP9 remained high after transfer from control conditions (Figure 7R) to inductive conditions (Figure 18F). Finally, rMSC aggregates showed an increase in the neuronal antigen TuJ-1 expression (Figure 16F) compared to the control (Figure 7B), whereas dermal clone aggregates DS7 and DP9 did not. Hence it can be concluded that under inductive conditions aggregates of all three cell types showed variable degrees of change in antigen expression. However, rMSC aggregates showed the most significant changes with upregulation of the neural stem cell marker nestin and the neuronal marker TuJ-1 and downregualation of the mesodermal antigen α-SMA, when compared to control conditions.

3.2.3 Aggregate frequency and size

Aggregates were compared in terms of their frequency and size by counting and measuring (summarised in Table 5). The differences between rMSC and DS7 aggregates mean areas, and the mean areas of rMSC and DP9 aggregates, were statistically significant ($p < 0.05$). However, the difference in DS7 and DP9 aggregate mean areas were not statistically significant ($p < 0.05$). The mean aggregate frequencies of rMSCs and DS7, and DS7 and DP9 were significantly different ($p < 0.025$). However, the difference in mean aggregate frequency between rMSC and DP9 aggregates were not statistically significant ($p < 0.025$). In summary the mean

area data indicated a divide between the aggregates of dermal clones and rMSC aggregates (Figure 19A), whereas the frequency data set aside the aggregates of the dermal clone DS7 from rMSC and DP9 aggregates (Figure 19B). It is likely that different balances between proliferation and cell death of the DS7 and DP9 clone aggregates and rMSC aggregates (Figure 5A – C) explains the different sizes and frequencies of the aggregates formed.

3.2.4 Reversible neural-like differentiation in dermal clone DS7

Individual cells that were still adherent to the tissue culture plastic showed a neural-like morphology (Figure 20A – C), and developed alongside DS7 aggregates (Figure 20D) after induction. The observation that the adherent cells switched from a neuronal-like morphology back to flat fibroblast cells following the addition of fresh induction medium (Figure 20E,F) could be explained in two different ways. It is possible the neuronal-like cells died and the small proportion of remaining fibroblast-like cells proliferated and became dominant. Or the neuronal cells themselves reverted back to the fibroblast-like morphology. The mechanism by which the observations were occurring, could be demonstrated if photomicrographs were taken of the same cells before and after the medium change.

3.2.5 The effect of conditioned media on AHPC development

AHPCs were seeded at a density of 10 000 cells/cm^2, which produced a sub-confluent culture after the cells were allowed to adhere overnight (Figure 21A and Figure 22A). Control conditions consisted of aggregate induction medium without EGF and bFGF and AHPC proliferation medium containing bFGF. After three days culture the AHPCs had clearly proliferated under the control conditions (Figure 21B,C) and at six days the cells were at a high density, maintained a circular morphology but showed very limited process elaboration (Figure 21D,E).

After seven days culture the controls were fixed and analysed for lineage specific antigens (Figure 23A – H). When cultured under control conditions the AHPCs were positive for the neural stem cell marker nestin (Figure 23A,B) and the early neuronal antigen TuJ-1 (Figure 23C – D). With the aggregate induction control 100% of AHPCs were positive for nestin and 97% were positive for TuJ-1, whereas with the AHPC proliferation control 99% of AHPCs were positive for nestin and 97% were positive for TuJ-1 (Figure 25 and Table 6). Neither control condition increased

expression of the astrocyte marker GFAP (Figure 23E – F) and the oligodendrocyte antigen GalC (Figure 23G – H), with 0% of AHPCs expressing the two antigens in each case (Figure 25 and Table 6). In conclusion the expression profile determined in the controls was typical of a neuroblast.

AHPCs were cultured with conditioned media to determine its effect on their development. Conditioned media was generated by growing cellular spheres – from rMSCs and the dermal clones DS7 and DP9 – for three days in serum free medium supplemented with EGF and bFGF. AHPCs were seeded at 10 000 cells/cm^2 prior to the addition of the conditioned media samples. By comparison of the photomicrographs at zero, three and six days treatment with conditioned media it is clear the AHPCs continue to proliferate throughout the time course (Figure 22A – G). However DP9 conditioned medium (DP9-CM) induced less proliferation between day three and day six compared to the DS7 and rMSC conditioned media samples (Figure 22D,G). By comparing the phase images of the conditioned media samples (Figure 22A – G) with the control conditions (Figure 21A – E) it can be concluded that there was more extensive process development in the AHPCs cultured with conditioned media. Using all three conditioned media samples the cells have adopted glial-like morphologies with limited secondary arborisation. The rMSC conditioned medium induced a distinct branching pattern emanating from the soma and astrocyte-like bipolar morphologies (Figure 22B, arrow and arrow head). The bipolar morphologies were also seen in AHPCs cultured with DS7 and DP9 conditioned media (Figure 22C,D arrow heads).

At seven days culture the AHPCs treated with conditioned media were fixed and analysed for the same lineage specific antigens as the controls. This analysis showed a loss of the neuroblast phenotype in AHPCs after treatment with conditioned media samples, evidenced by a dramatic decline in TuJ-1 expression in the conditioned media treatments compared to the control conditions. In the two controls 97% of AHPCs were positive for TuJ-1, whereas after treatment with rMSC and DS7 conditioned media TuJ-1 expression declined to 0% (Figure 24D,E, Figure 25 and Table 6). In contrast to the changes in TuJ-1 expression, nestin expression in AHPCs remained almost identical to the control conditions when AHPCs were treated with rMSC and DS7 conditioned media. 100% of AHPCs treated with rMSC and DS7 conditioned media expressed nestin (Figure 24A,B, Figure 25 and Table 6). AHPCs showed a slightly different response to DP9-CM compared to rMSC and DS7 conditioned media. A less dramatic decline in TuJ-1 expression was evident as 38%

of AHPCs expressed TuJ-1, whereas there was a complete loss of nestin expression with 0% of AHPCs expressing nestin after treatment with DP9-CM (Figure 24F,C, Figure 25 and Table 6).

As TuJ-1 expression declined a concomitant increase in expression of the astrocytic marker GFAP was found in a small proportion of AHPCs treated with rMSC conditioned medium (8% $GFAP^+$), DS7 conditioned medium (DS7-CM; 2% $GFAP^+$) and DP9-CM (12% $GFAP^+$) (Figure 24G – I, Figure 25 and Table 6). However, no cells expressed the oligodendrocyte specific antigen GalC after treatment with conditioned media (Figure 24J – L, Figure 25 and Table 6).

3.3 Figures

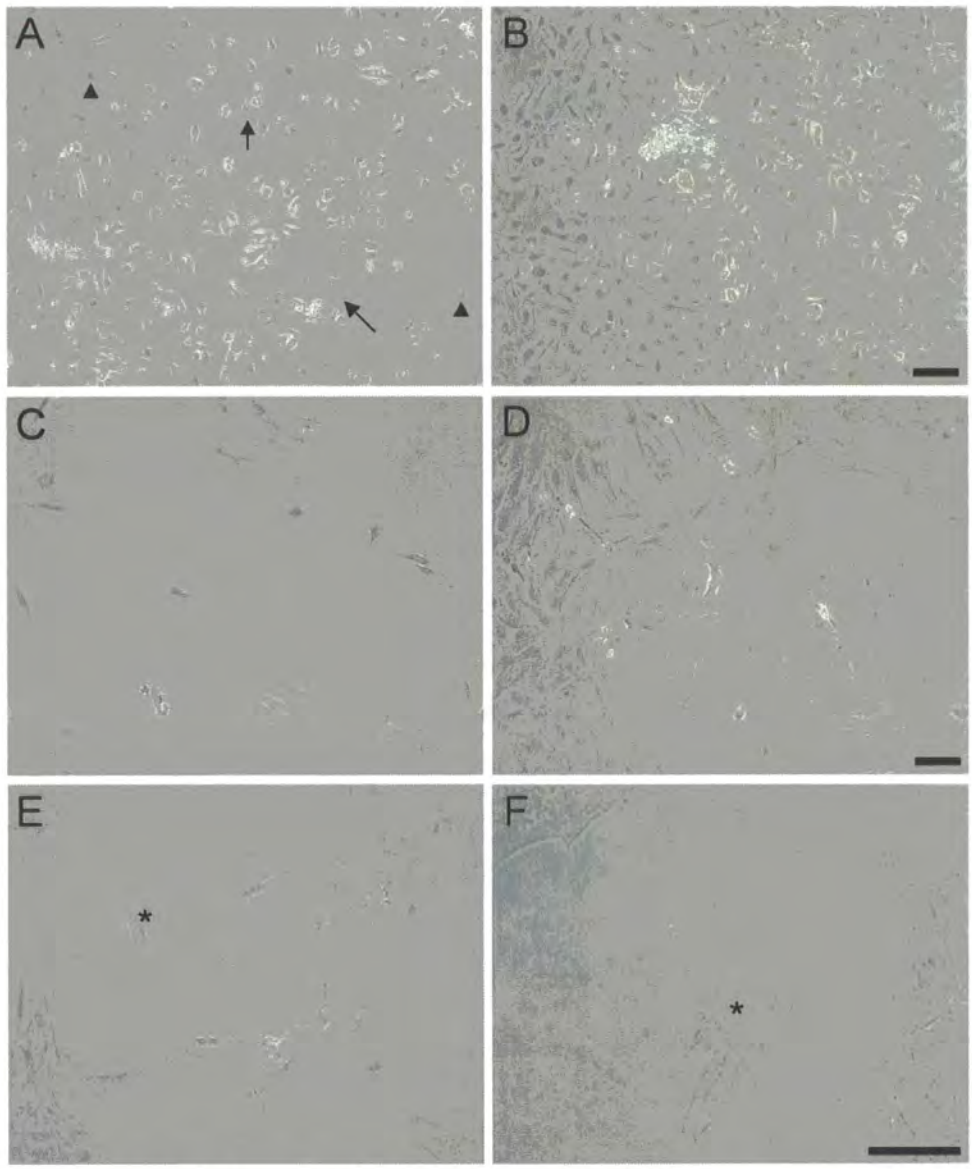

Figure 1: Isolation of rMSCs from the postnatal bone marrow of the femurs and tibias of 6 - 8 month old Wistar rats. Photomicrographs show isolated cells growing at P0 (A & B), P1 (C & D) and P2 (E & F). Five days after the cells were isolated (A) they showed distinct morphologies including ovoid (arrow heads) and bipolar (arrows). After seven days P0 rMSCs became confluent and began to spread out (B). Once passaged rMSCs displayed a more flattened morphology (C) and grow in colonies (D). At P2 rMSCs showed a larger and increasingly flattened morphology (asterisks in E and F). *Scale bars : 100µm.*

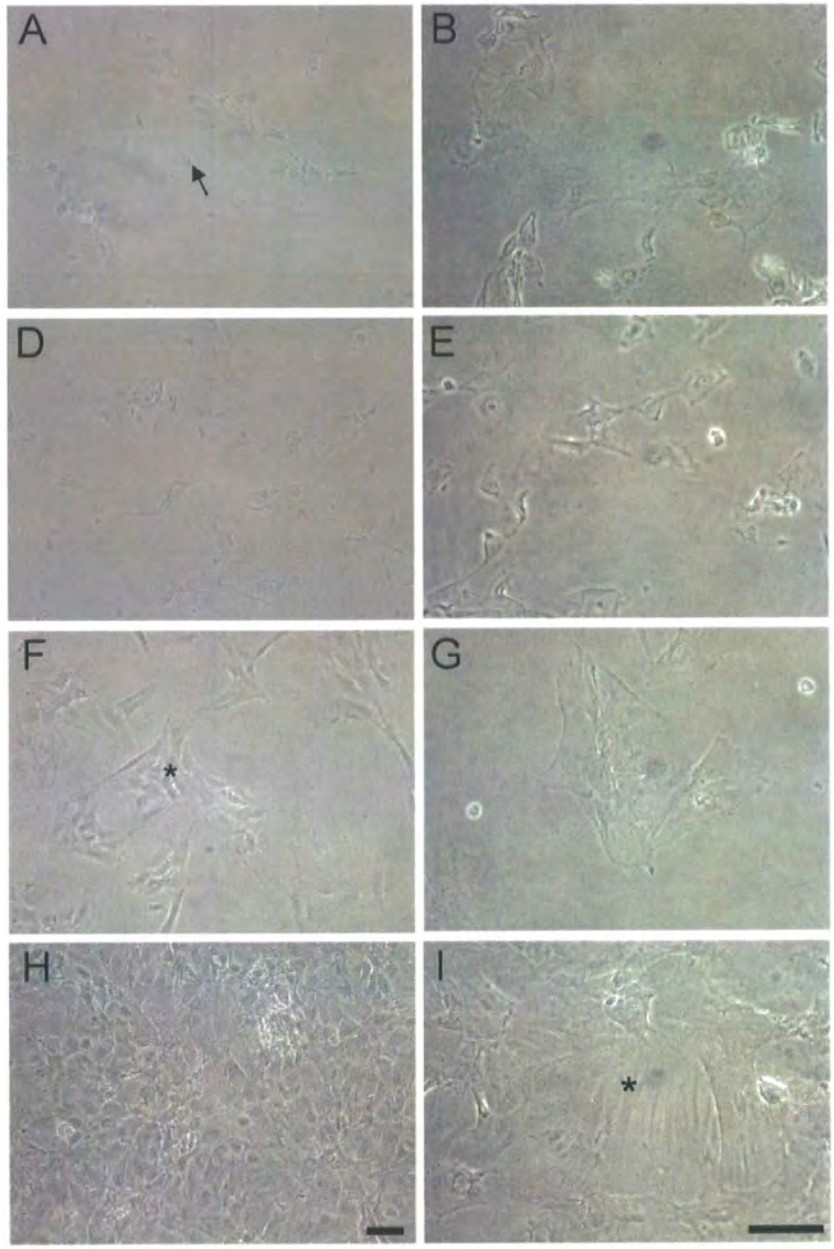

Figure 2: Phase photomicrographs showing the growth of P2 rMSCs over 11 days in CCM. The cells were plated at a density of 30 000 cells per well in 24 well plates and cultured for 11 days. Phase photomicrographs were taken at 10 and 20 times magnification after two days (A & B), three days (C & D), five days (E & F) and 11 days (G & H). After being photographed the cells were then trypsinsed and counted. *Scale bars : 100μm.*

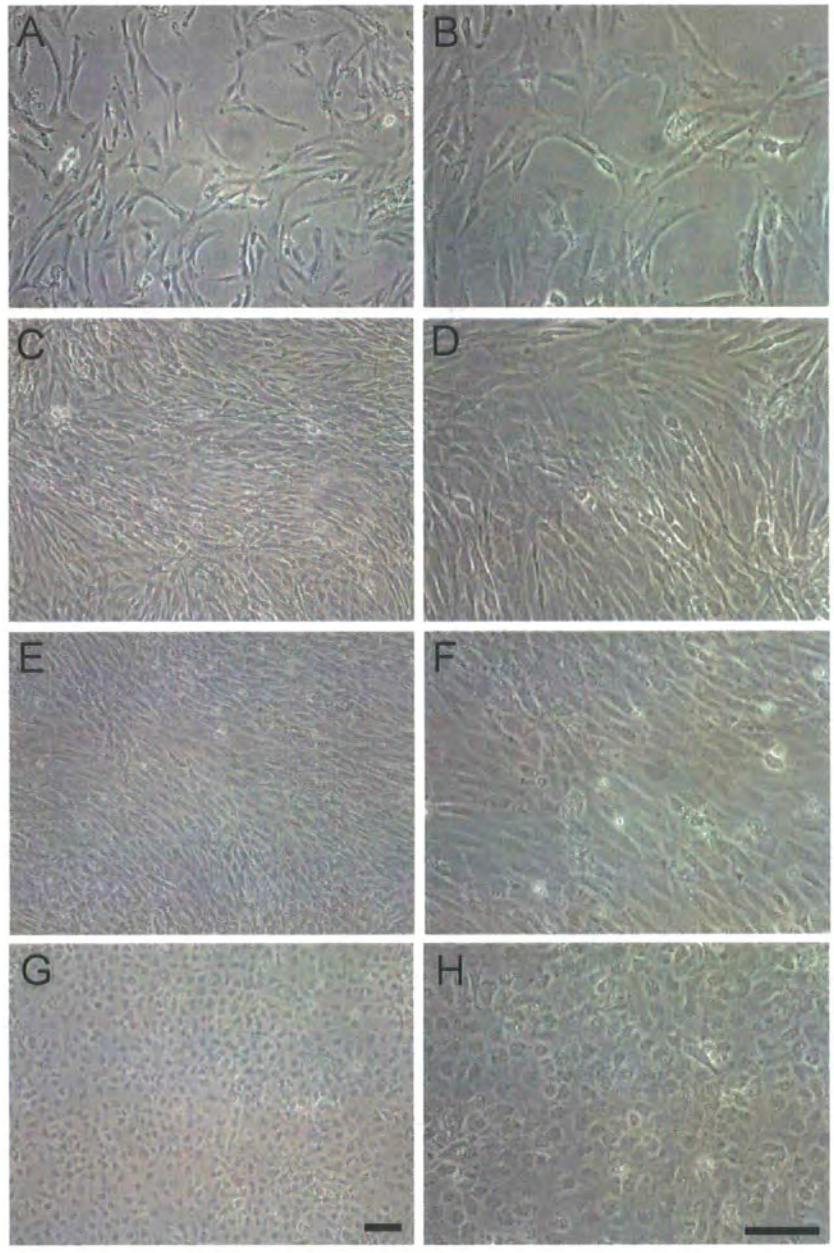

Figure 3: Phase photomicrographs showing the growth of P28 dermal clone DS7 over 11 days in CCM. The cells were plated at a density of 30 000 cells per well in 24 well plates and cultured for 11 days. Phase photomicrographs were taken at 10 and 20 times magnification after two days (A & B), three days (C & D), five days (E & F) and 11 days (G & H). After being photographed the cells were then trypsinsed and counted. *Scale bars : 100μm.*

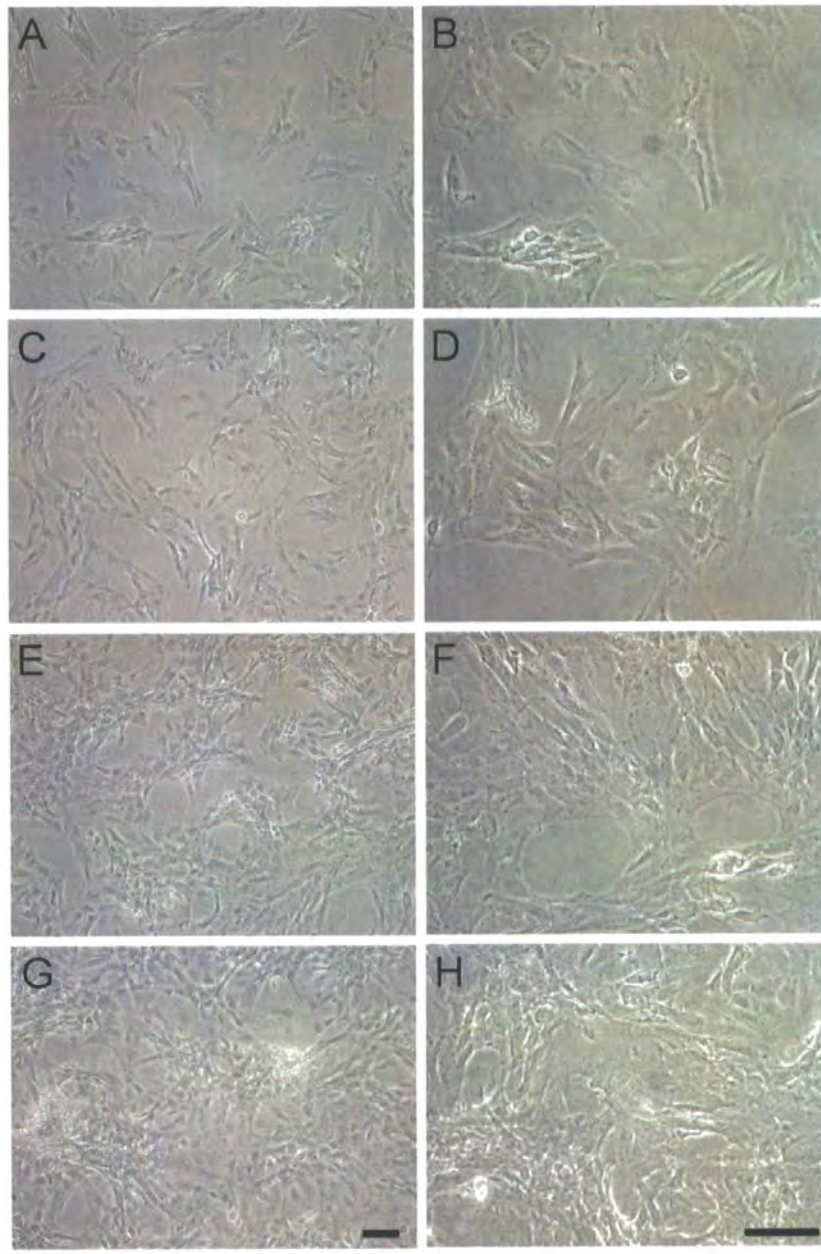

Figure 4: Phase photomicrographs showing the growth of P28 dermal clone DP9 over 11 days in CCM. The cells were plated at a density of 30 000 cells per well in 24 well plates and cultured for 11 days. Phase photomicrographs were taken at 10 and 20 times magnification after two days (A & B), three days (C & D), five days (E & F) and 11 days (G & H). After being photographed the cells were then trypsinsed and counted. *Scale bars : 100µm.*

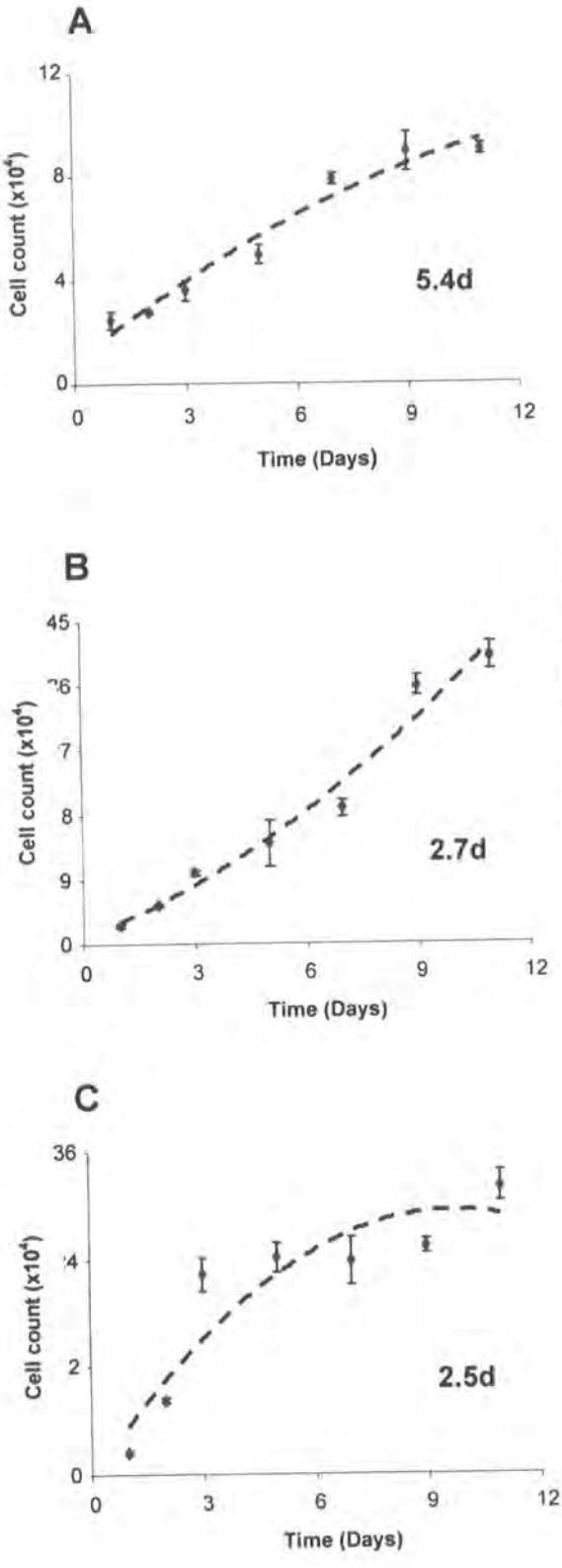

Figure 5: Proliferation graphs showing the slower growth rate of P2 rMSCs compared to the P28 dermal clones DS7 and DP9 over 11 days in CCM. All three cell types were plated at a density of 30 000 cells per well in 24 well plates and counted in triplicate at one, two, three, five, seven, nine and 11 days. The graphs show the growth curves using the mean count ±SEM at each time point of rMSCs (A), and the dermal clones DS7 (B) and DP9 (C). The population doubling time in days is indicated in the bottom right hand corner of each of the graphs.

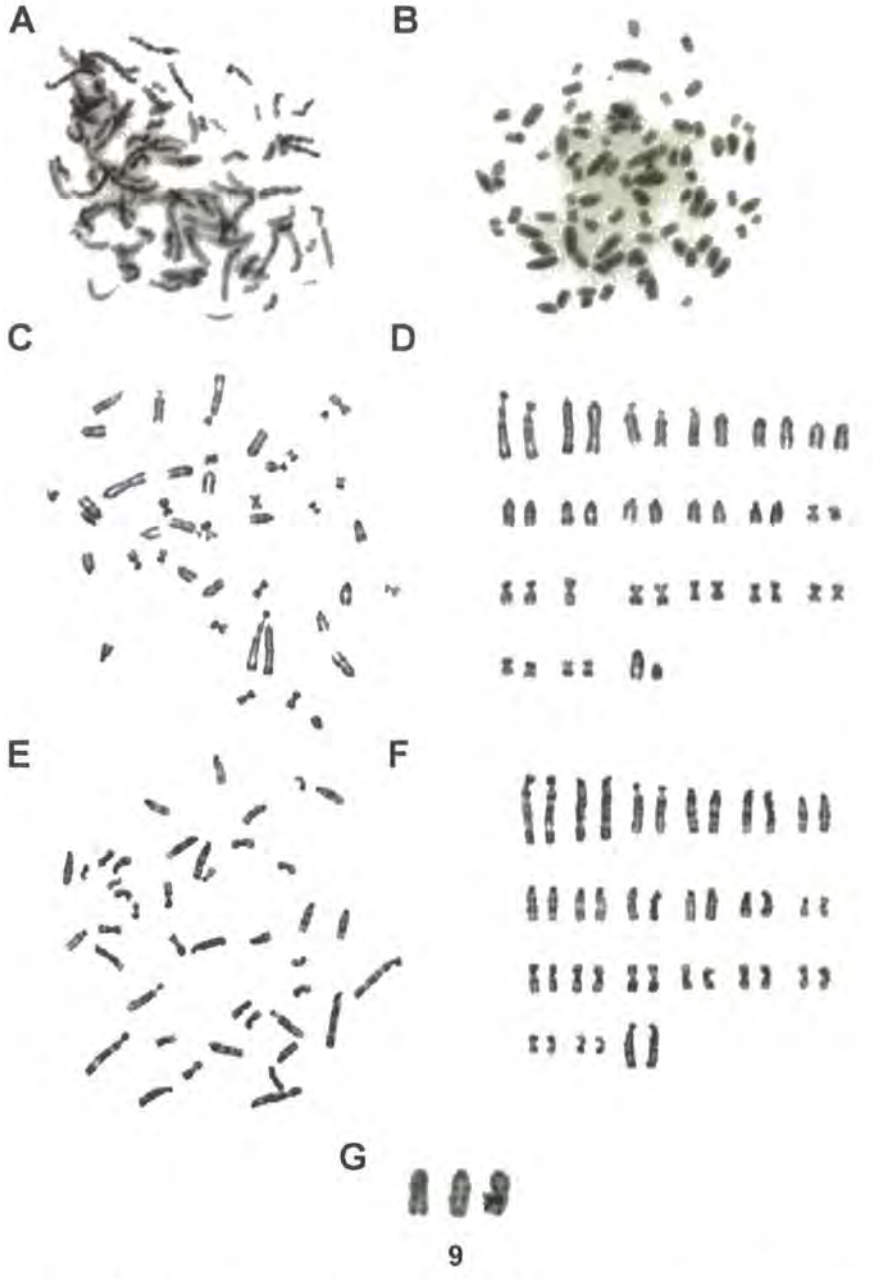

Figure 6: Chromosome counting and detailed karyotype analysis showing abnormalities in the two dermal clones DS7, DP9 and P4 rMSCs. Metaphase chromosomes were karyotyped and counted by Chrombios GmbH. Only polyploid metaphases were observed in DS7 clone (A & B) and therefore a detailed karyogram could not be produced. An example metaphase spread (C) and karyogram (D) are shown for the DP9 clone. The karyogram (D) is an example of a deletion at chromosome 14 that produced a count of 41 chromosomes. Lastly the chromosomes of primary rMSCs were counted and karyotyped. The metaphase spread (E) illustrates how counts of rMSC chromosomes were produced. The karyogram (F) shows rMSCs with no abnormalities. However, abnormalities in rMSC karyotypes were detected and at least partially accounted for by trisomies, which were observed on chromosome 9 of one of the karyograms (G).

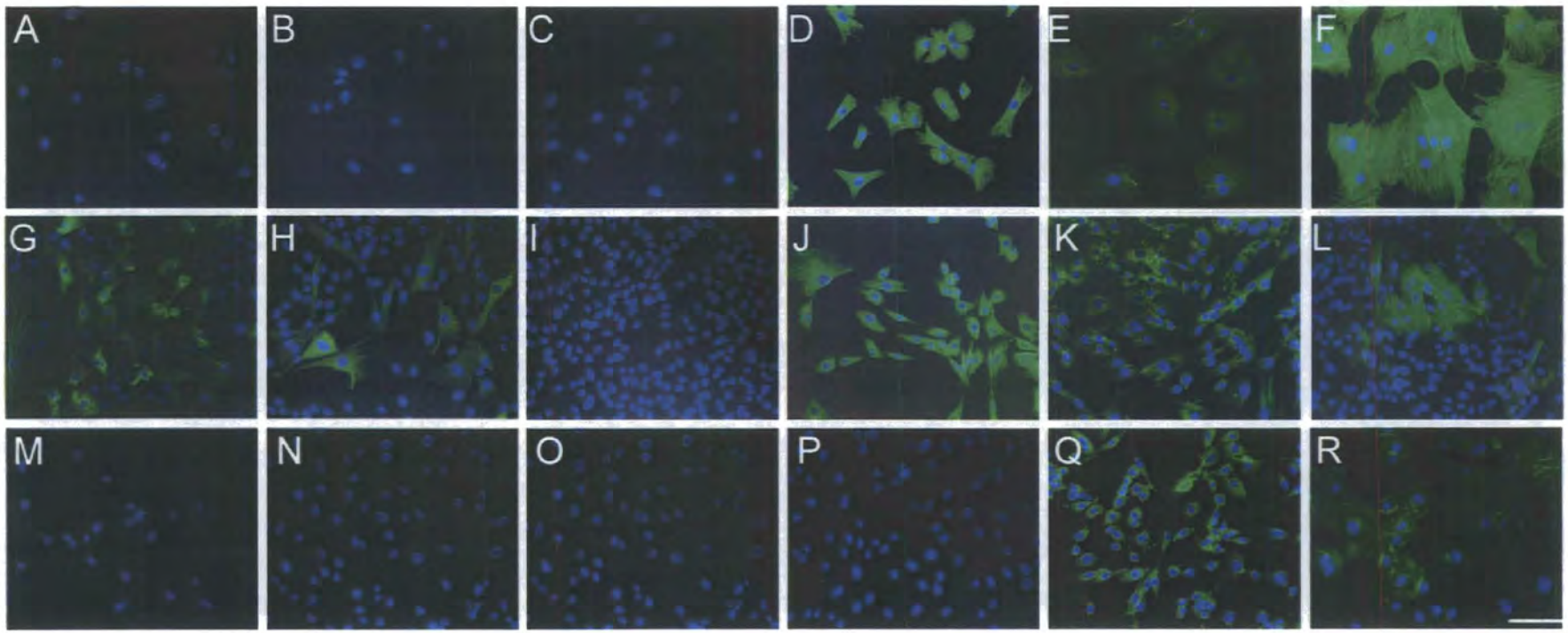

Figure 7: Expression profile of both neural and mesenchymal antigens on primary P3 rMSCs and P25 DS7 and DP9 deraml clones cultured in CCM for 24 hours. The neural stem cell marker nestin the neuronal marker TuJ-1 and the astrocytic marker GFAP were tested on primary rMSCs (A – C), DS7 clone (G – I) and DP9 clone (M – O). The mesenchymal antigens vimentin, fibronectin and α-SMA were tested on primary rMSCs (D – F), DS7 clone (J – L) and DP9 clone (P – R).

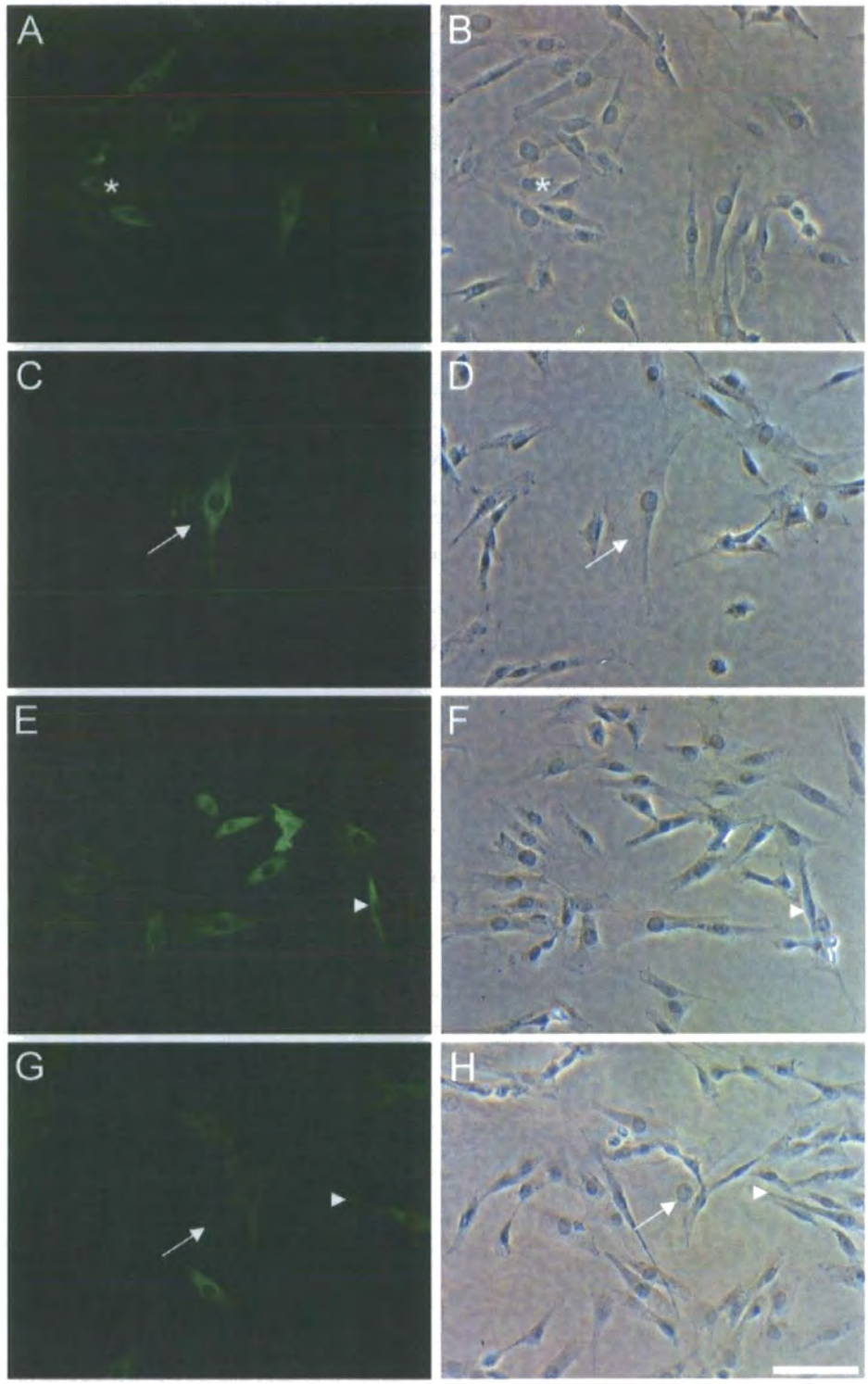

Figure 8: The expression of nestin in the dermal clone DS7 grown in CCM at 20 000 cells/cm^2 does not correlate to cellular morphology. Fluorescent photomicrographs show nestin expression (A, C, E & G) and their corresponding phase photomicrographs (B, D, F & H). *Scale bar : 100µm.*

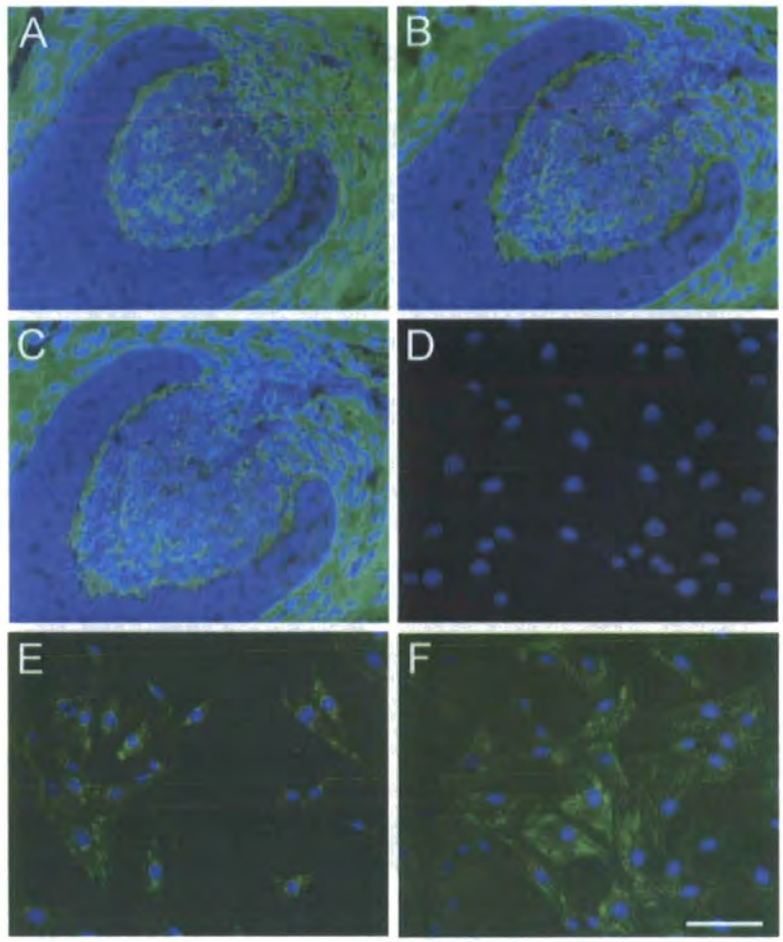

Figure 9: The dermal clones DS7 and DP9 express the dermal papilla specific antigen versican whereas rMSCs do not. Fluorescent photomicrographs A – C are 7µm sections taken from early anagen rat hair follicles embedded in OCT, which were used as positive controls. Fluorescent photomircraphs D – F test expression of versican in rMSCs (D) and the dermal clones DS7 (E) and DP9 (F).
Scale bar : 100µm.

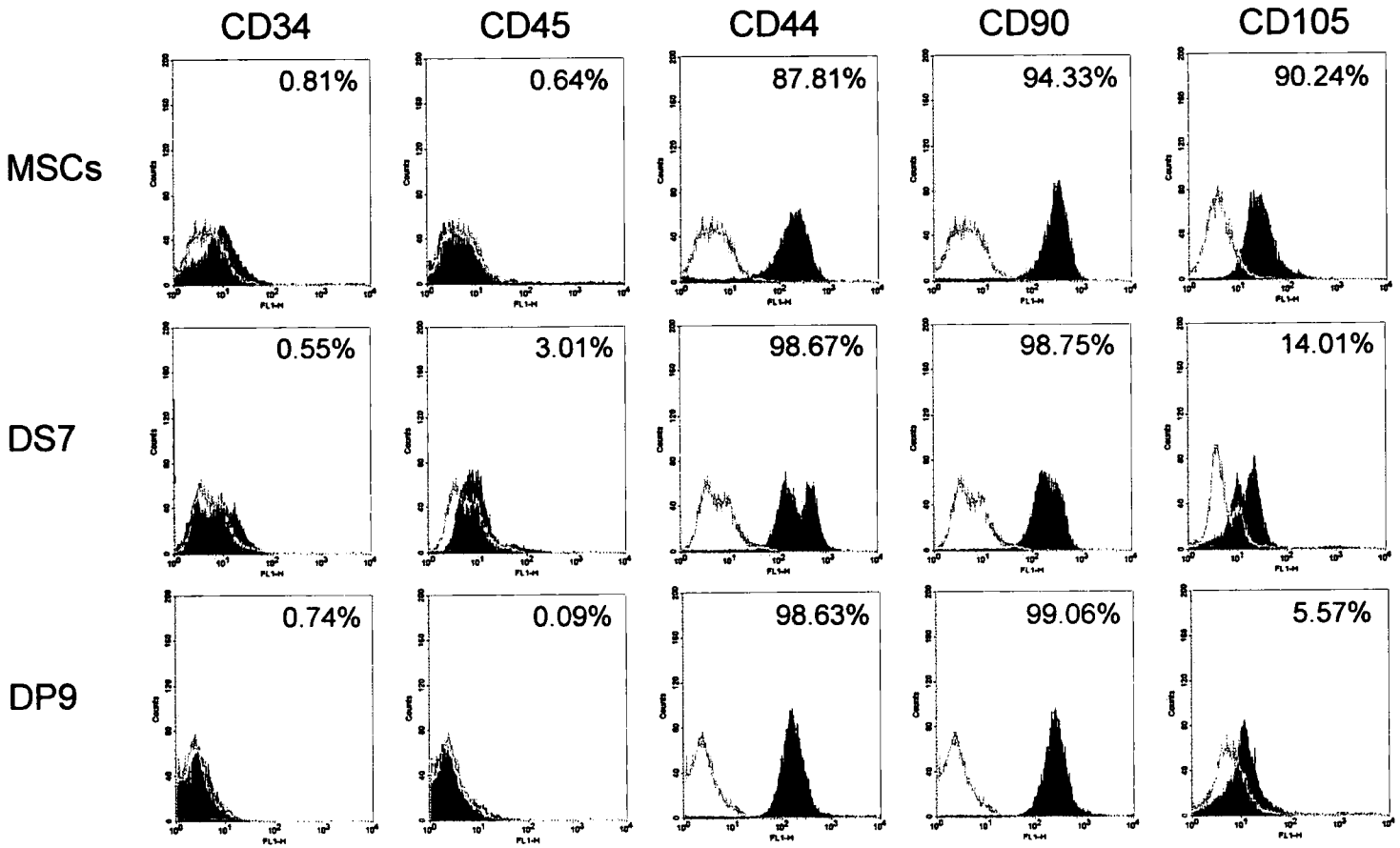

Figure 10: Expression of the cell surface mesenchymal antigens CD44 and CD90, but not haematopoietic cell surfaces antigens CD34 and CD45 by rMSCs and the dermal clones DS7 and DP9. Prior to analysis all cell types were grown in CCM until confluency was reached. For each antigen the black peaks represent detection of primary antibodies by FITC conjugated secondary antibodies and the white peaks are controls that account for non-specific secondary antibody binding to the P3X control. The y-axis represents cell count and the x-axis fluorescence intensity. The percentages of positive cells are shown in the top right of each histogram.

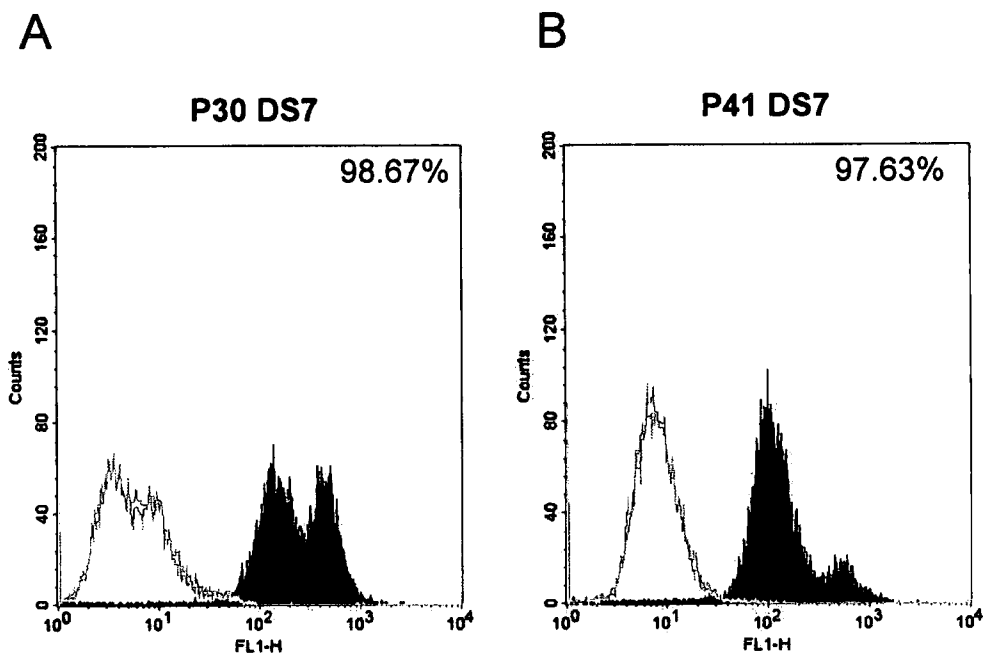

Figure 11: The changing expression of the cell surface antigen CD44 in the dermal clone DS7 at passage 30 and passage 41 in CCM. The two flow cytometry histograms show the pattern of CD44 expression at passage 30 (A) and passage 41 (B). The black peaks represent detection of populations expressing CD44 by FITC conjugated secondary antibodies and the white peaks are controls that account for non-specific secondary antibody binding to the P3X control. The y-axis represents cell count and the x-axis fluorescence intensity. The percentages of positive cells are shown in the top right of each histogram.

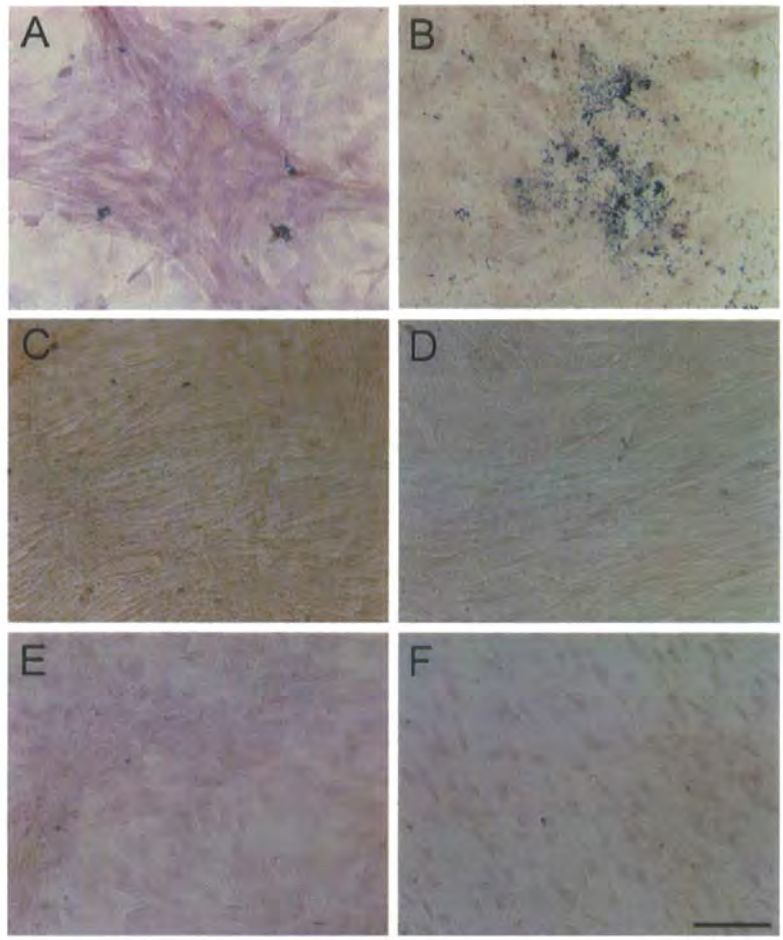

Figure 12: Primary rMSCs show osteogenic potential after three weeks treatment in osteogenic medium whereas dermal clones DS7 and DP9 do not. The extent of osteogenic differentiation was assessed by examining deposition of calcium using the Von Kossa stain with haematoxylin and eosin counter staining, after treatment with osteogenic medium and control CCM. The left photomicrographs (A, C & E) are controls whereas the right photomicrographs (B, D & F) represent cells treated with osteogenic medium. The cell types are represented as follows; rMSCs (A & B), DS7 clone (C & D), and DP9 clone (E & F). (*Scale bar : 100μm*).

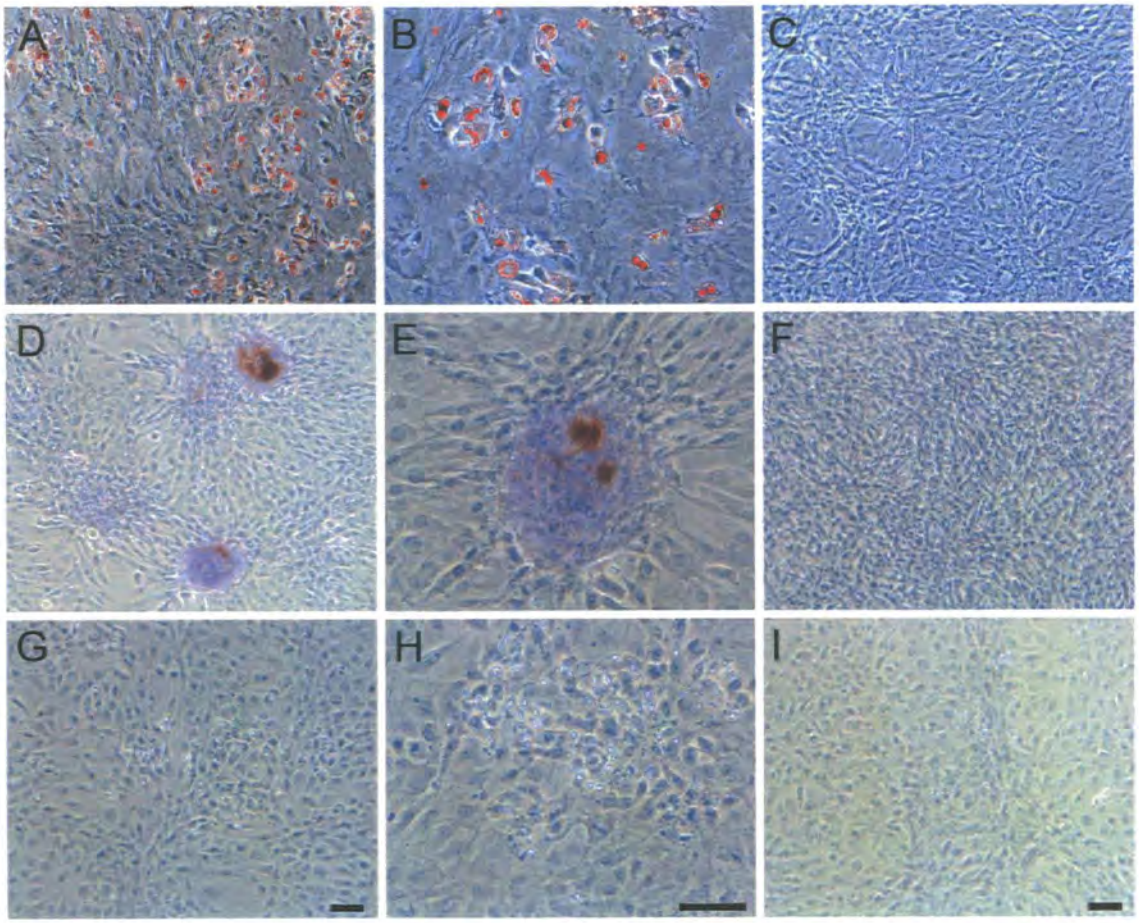

Figure 13: Primary rMSCs and the dermal clone DS7 show adipogenic potential after three weeks treatment in adipogenic medium, whereas the dermal clones DP9 does not. Adipogenic differentiation was assessed by examining intracellular accumulation of lipid droplets using the oil red-O assay on fixed cells, after treatment with adipogenic medium and control CCM. The right photomicrographs (C, F & I) are controls whereas the left photomicrographs represent cells treated with adipogenic medium at 10 times magnification (A, D & G) and 20 times magnification (B, E & H). The cell types are represented as follows; rMSCs (A – C), DS7 clone (D – F), and DP9 clone (G – I). *Scale bars : 100µm.*

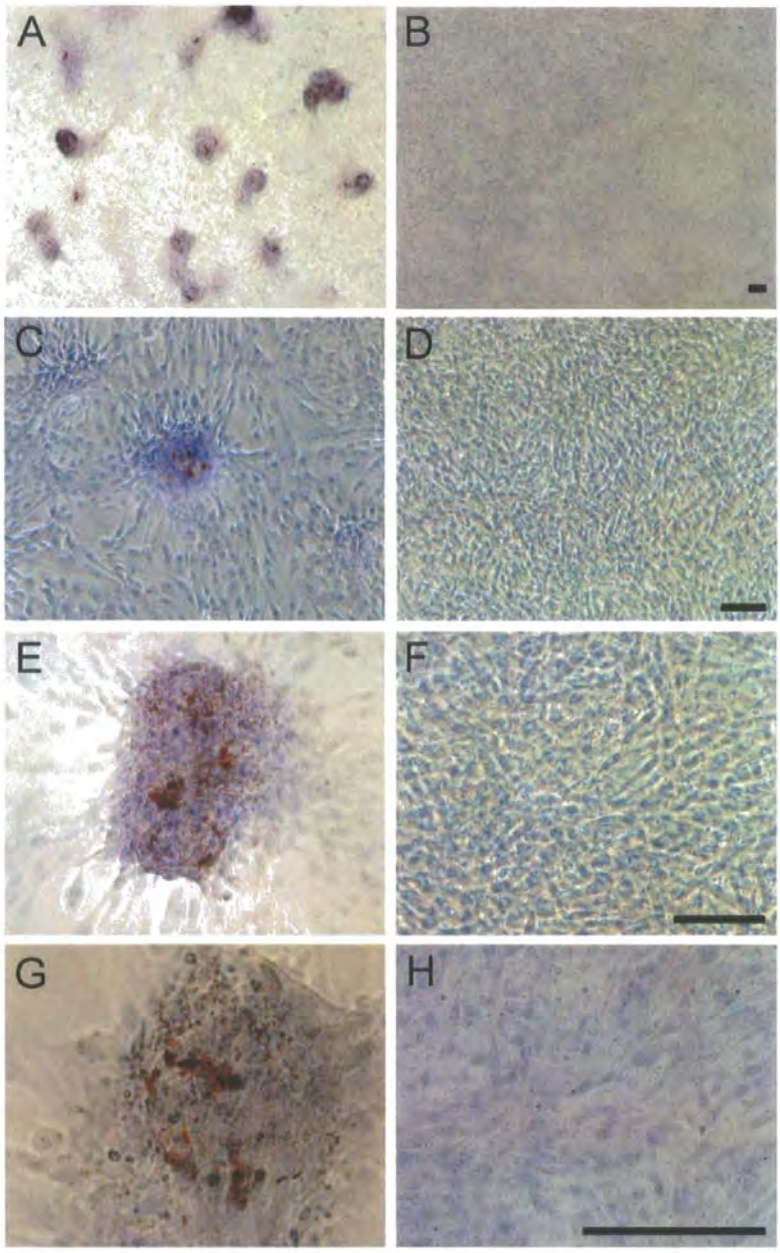

Figure 14: Detailed analysis of the adipogenic potential of the dermal clone DS7 after three weeks induction in adipogenic medium. Adipogenic differentiation was assessed by examining intracellular accumulation of lipid droplets using the oil red-O assay on fixed cells, after treatment with adipogenic medium and control CCM. The left photomicrographs (A, C, E & G) represent cells treated with adipogenic medium at four times (A), 10 times (C), 20 times (E) and 40 times magnification. The right photomicrographs (B, D, F & H) represent controls at four times (B), ten times (D), 20 times (F) and 40 times (H) magnification. *Scale bars : 100µm.*

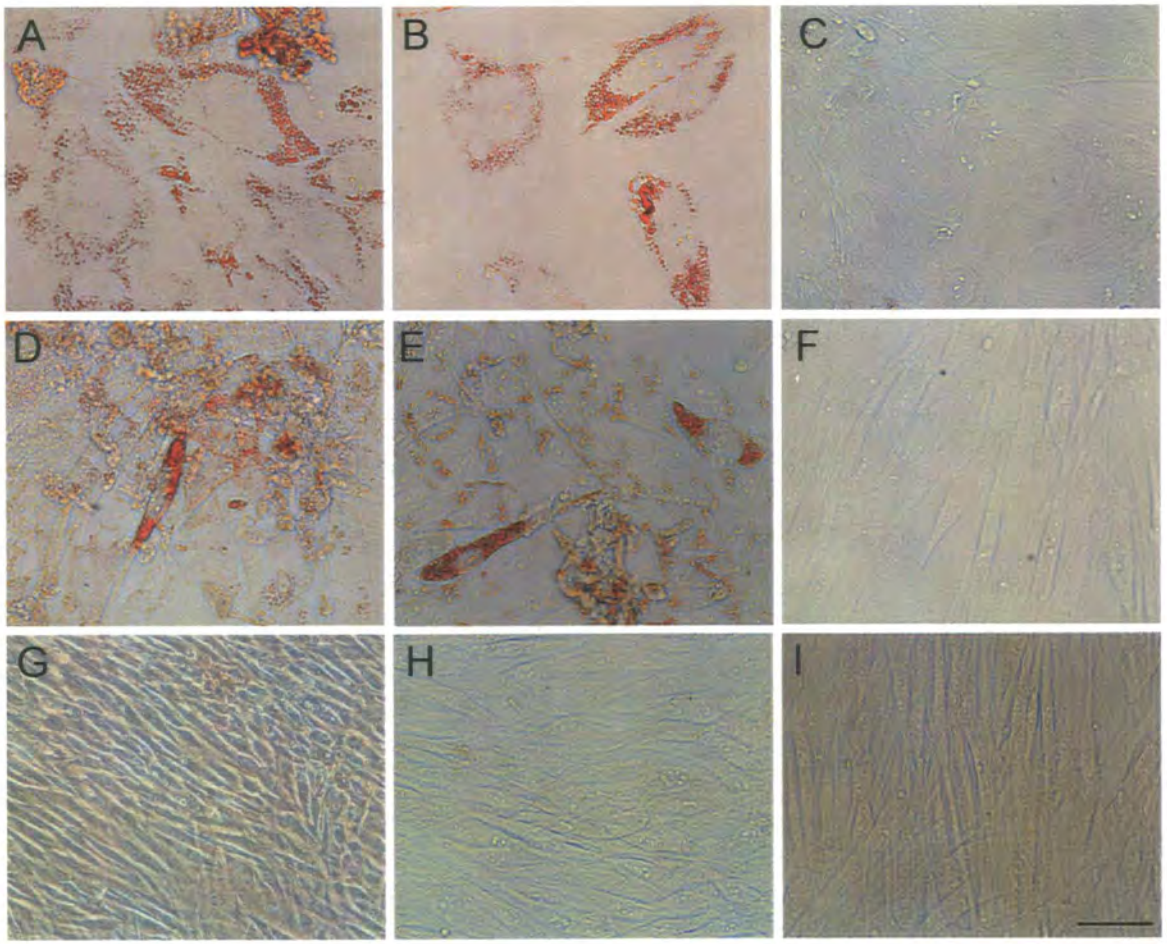

Figure 15: The adipogenic potential of the dermal clone DS7 declines as passage number increases, after one week induction in adipogenic medium previously used for dermal cells. Adipogenic differentiation was assessed by examining intracellular accumulation of lipid droplets using the oil red-O assay on fixed cells, after treatment with adipogenic medium and control medium consisting of 10% FCS in MEM. The left photomicrographs (A, B, D, E, G & H) are cells treated in adipogenic medium, whereas the right photomicrographs (C, F & I) are cells treated under control conditions. Cell types are represented by the following photomicrographs; A – C are P4 rMSCs, D – F are P20 dermal clone DS7 and G – I are P33 dermal clone DS7. *Scale bar : 100μm.*

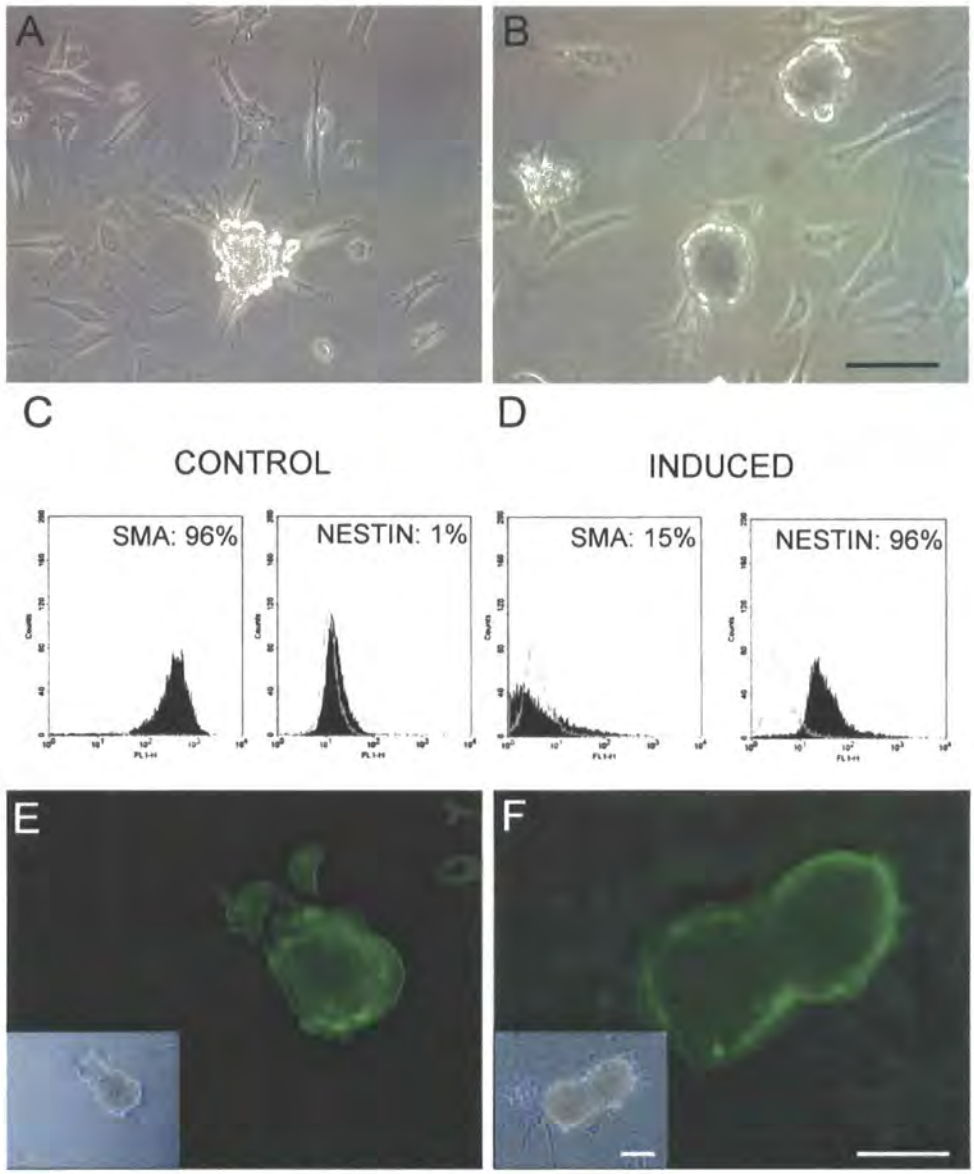

Figure 16: Generation of P3 MSC cellular aggregates positive for neural antigens and negative for the mesodermal antigen α-SMA following transfer to inductive serum free medium supplemented with EGF (10ng/ml) and bFGF (10ng/ml). Photomicrographs show free floating MSC aggregates form after 7 days induction at a density of 100 000 cells/cm^2 (A & B). Small adherent aggregates appeared after two days induction (A). At 7 days some of the adherent aggregates detached and developed into free floating aggregates (B). Flow cytometric analysis of the neural stem cell marker nestin and the mesodermal marker α-SMA (C & D). Cells were cultured under standard (control) conditions until confluent (C) and inductive (induced) conditions (D) for 7 days. After culture the cells were trypsinised to produce a single cell suspension, fixed and labelled with antibodies directed against nestin and α-SMA. The black peaks represent detection of primary antibodies by FITC conjugated secondary antibodies and the white peaks are controls that account for non-specific secondary antibody binding. The y-axis represents cell count and the x-axis fluorescence intensity. The percentage of positive cells for each antigen is indicated on the individual histograms. Immunocytochemistry and corresponding phase images (insets) revealed the aggregate expression pattern of the neural stem cell marker nestin (E) and the neuronal marker TuJ-1 (F). *Scale bars : 100μm.*

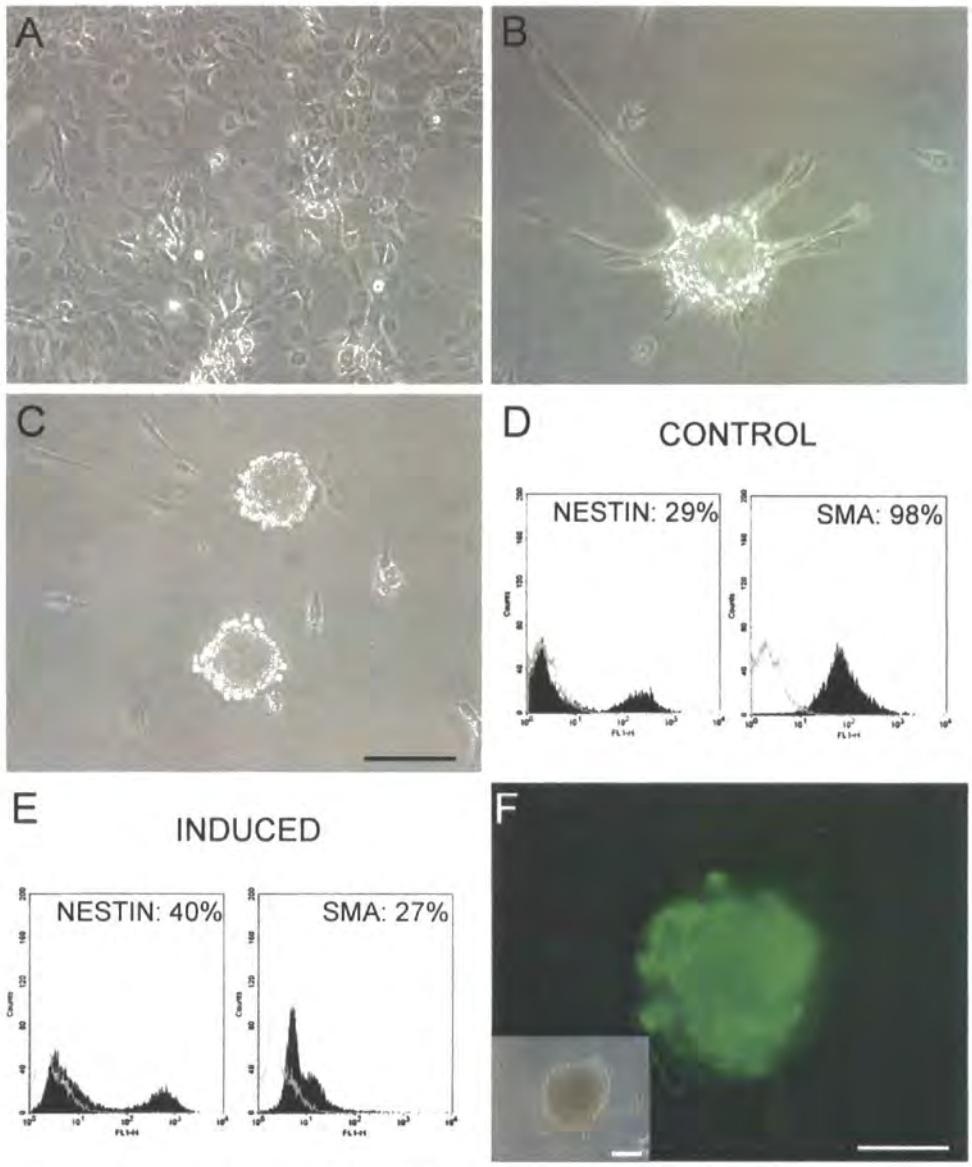

Figure 17: Generation of P37 DS7 clone cellular aggregates positive for the neural stem cell antigen nestin following transfer to inductive serum free medium supplemented with EGF (10ng/ml) and bFGF (10ng/ml). Photomicrographs show free floating DS7 aggregates gradually form over a period of 7 days after induction at a density of 160 000 cells/cm^2 (A – C). After one day induction cells adhered to the tissue culture plastic at a high density and displayed a rounded morphology (A). At 5 days adherent aggregates formed (B), which subsequently became detached and developed into free floating aggregates at 7 days (C). Flow cytometric analysis of the neural stem cell marker nestin and the mesodermal marker α-SMA (D& E). Cells were cultured under standard (control) conditions until confluent (D) and inductive (induced) conditions (E) for 7 days. After culture the cells were trypsinised to produce a single cell suspension, fixed and labelled with antibodies directed against nestin and α-SMA. The black peaks represent detection of primary antibodies by FITC conjugated secondary antibodies and the white peaks are controls that account for non-specific secondary antibody binding. The y-axis represents cell count and the x-axis fluorescence intensity. The percentage of positive cells for each antigen is indicated on the individual histograms. Immunocytochemistry and corresponding phase image (inset) revealed the aggregate expression pattern of the neural stem cell antigen (F). *Scale bars : 100μm.*

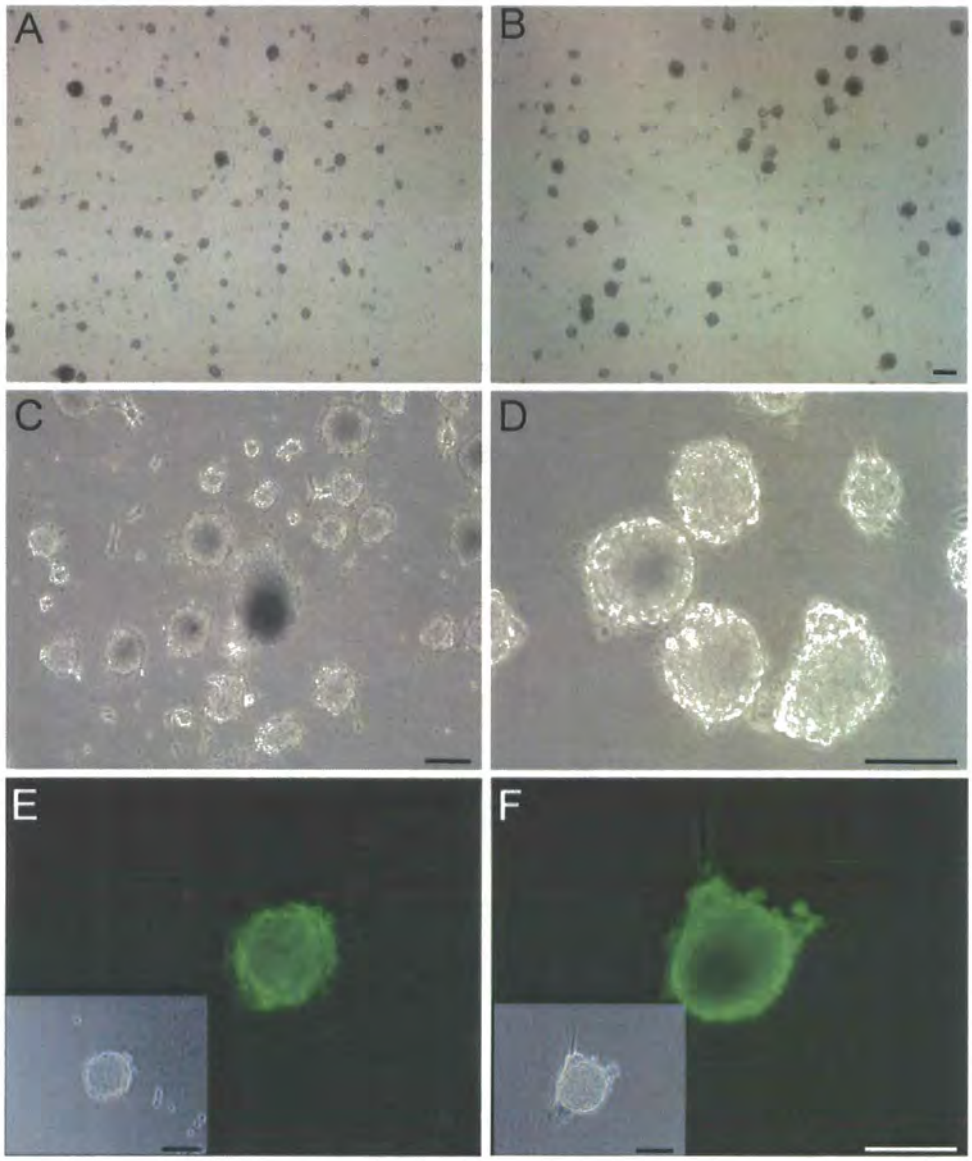

Figure 18: Generation of P31 DP9 clone cellular aggregates positive for the neural stem cell marker nestin and the mesodermal marker α-SMA following transfer to inductive serum free medium supplemented with EGF (10ng/ml) and bFGF (10ng/ml). The low magnification photomicrographs show DP9 is able to form aggregates after induction at densities of both 128 000 cells/cm^2 (A) and 256 000 cells/cm^2 (B). Higher magnification photomicrographs of the clone induced at 256 000 cells/cm^2 (C & D) show the vast majority of aggregates were free floating after one day in induction medium. Immunocytochemistry and corresponding phase images (insets) reveals the aggregate's expression profile for the neural stem cell marker nestin (E) and the mesodermal marker α-SMA (F). *Scale bars : 100μm.*

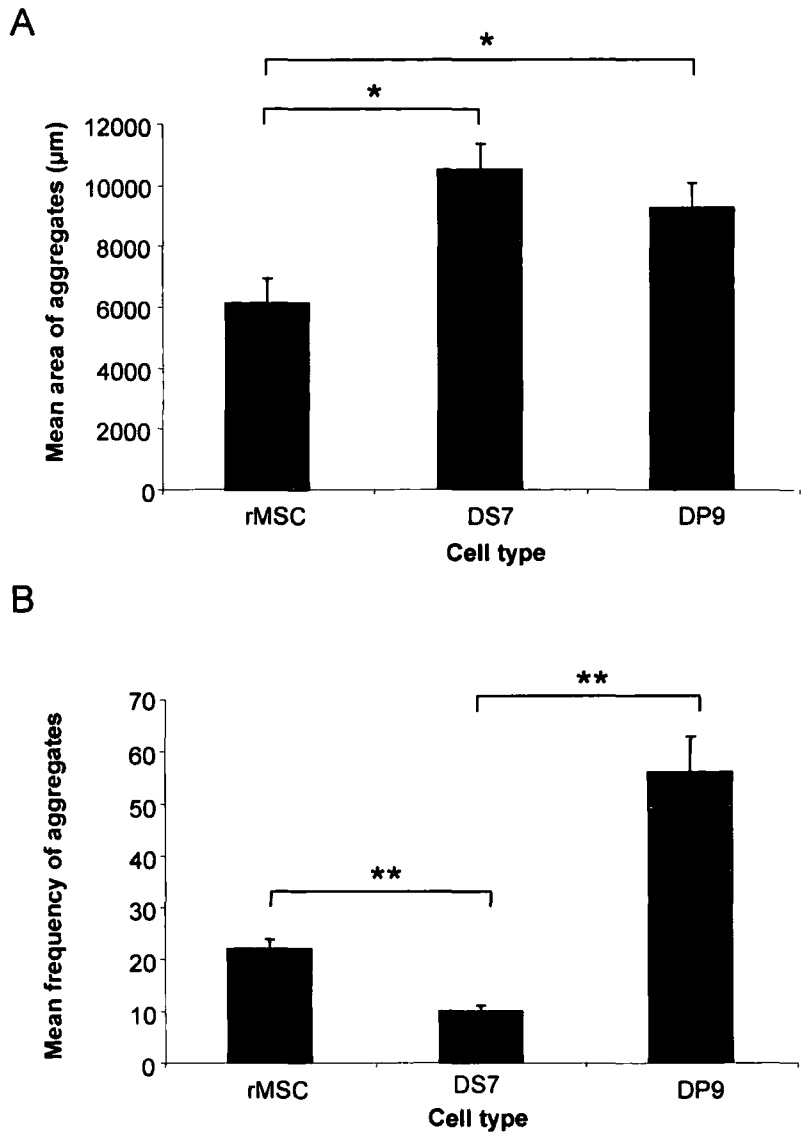

Figure 19: Aggregates formed by rMSCs and dermal clones DS7 and DP9 showed differences in terms of their area and frequency, after induction in serum free medium supplemented with EGF (10ng/ml) and bFGF (10ng/ml). Mean ± SEM aggregate area (A) and frequency (B) were determined. The post hoc Tukey *test* determined that the difference in the mean areas of rMSC and DS7 aggregates, and the mean areas of rMSC and DP9 aggregates, were statistically significant (* = $p < 0.05$). The difference in the areas of DS7 and DP9 aggregates were not statistically significant ($p < 0.05$). Aggregate frequency data was not compatible with the ANOVA test because the variances were not homogeneous even after transforming the data. The non-parametric Kruskal-Wallis *test* was used instead and showed there were statistically significant differences between the median frequencies of aggregates ($p < 0.05$). The Mann-Whitney U-test with the Bonferroni-Holm multi-step correction, showed that the frequency of rMSC and DS7 aggregates, and DS7 and DP9 aggregates were statistically significantly different (** = $p < 0.025$). The difference in mean aggregate frequency between rMSC and DP9 aggregates were not statistically significant ($p < 0.025$).

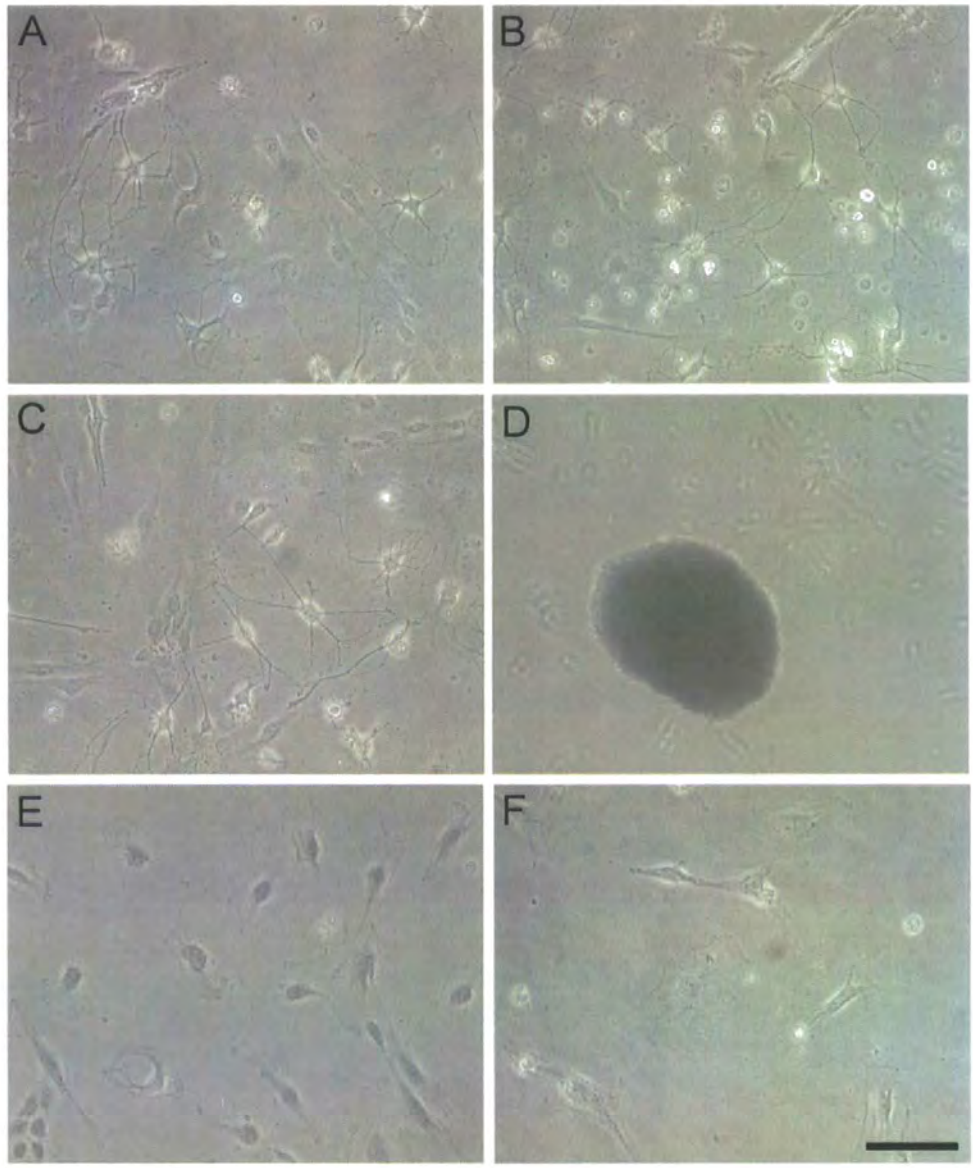

Figure 20: Formation of reversible neural-like structures and aggregates in cultures of P33 DS7 following transfer to inductive serum free medium containing EGF (10ng/ml) and bFGF (10ng/ml). Changes in adherent cell morphology were shown after treatment with induction medium with the majority of cells adopting a neuronal-like morphology (A – C). Free floating aggregate formation (D) was seen alongside changes to adherent cells. The day after a medium change, adherent fibroblast-like cells became dominant once again (E & F). *Scale bar : 100µm.*

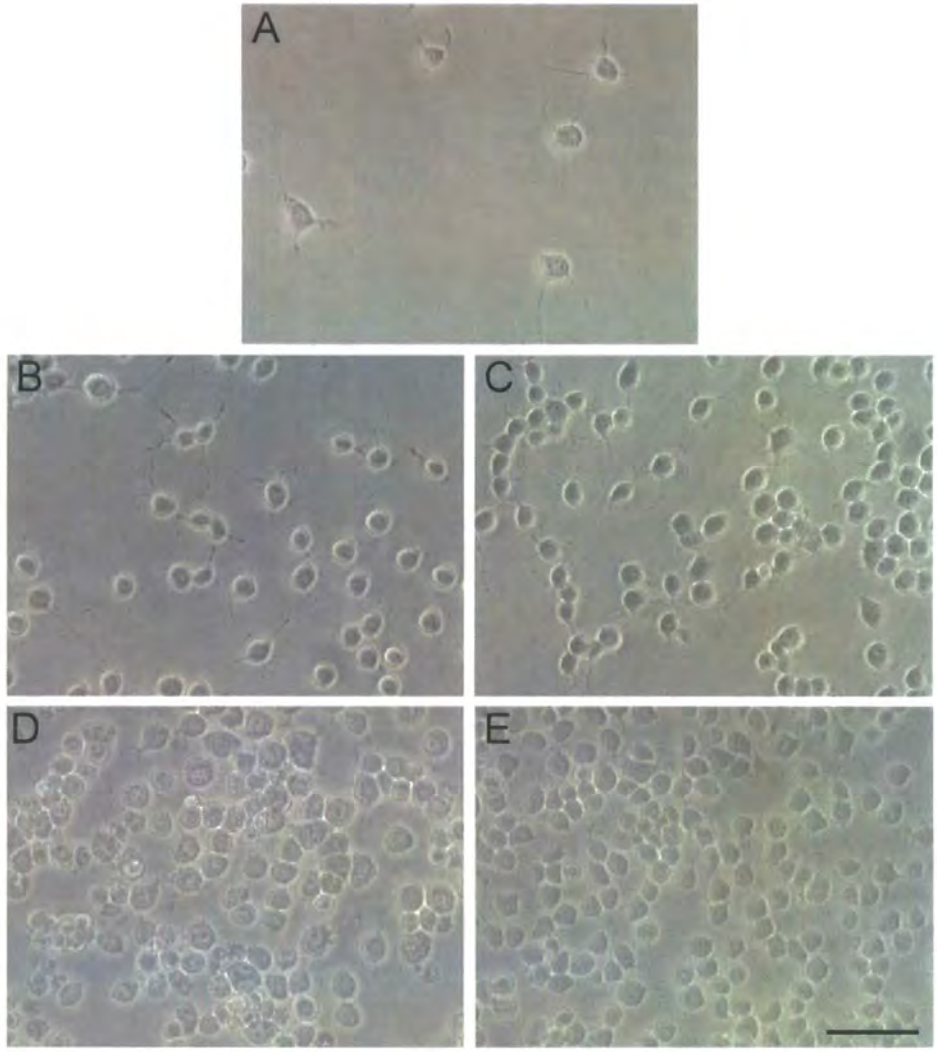

Figure 21: Under the two control conditions AHPCs continued to proliferative and maintained a rounded morphology with minimal process development. AHPCs were seeded at 10 000 cells/cm^2 prior to the addition of the two control media samples (A). The control consisting of aggregate induction medium without EGF (10ng/ml) and bFGF (10ng/ml) is represented by photomicrographs of AHPCs after three (B) and six (D) days' culture. The AHPC proliferation medium control is represented by photomicrographs of AHPCs after three (C) and six (E) days' culture. *Scale bar : 50µm.*

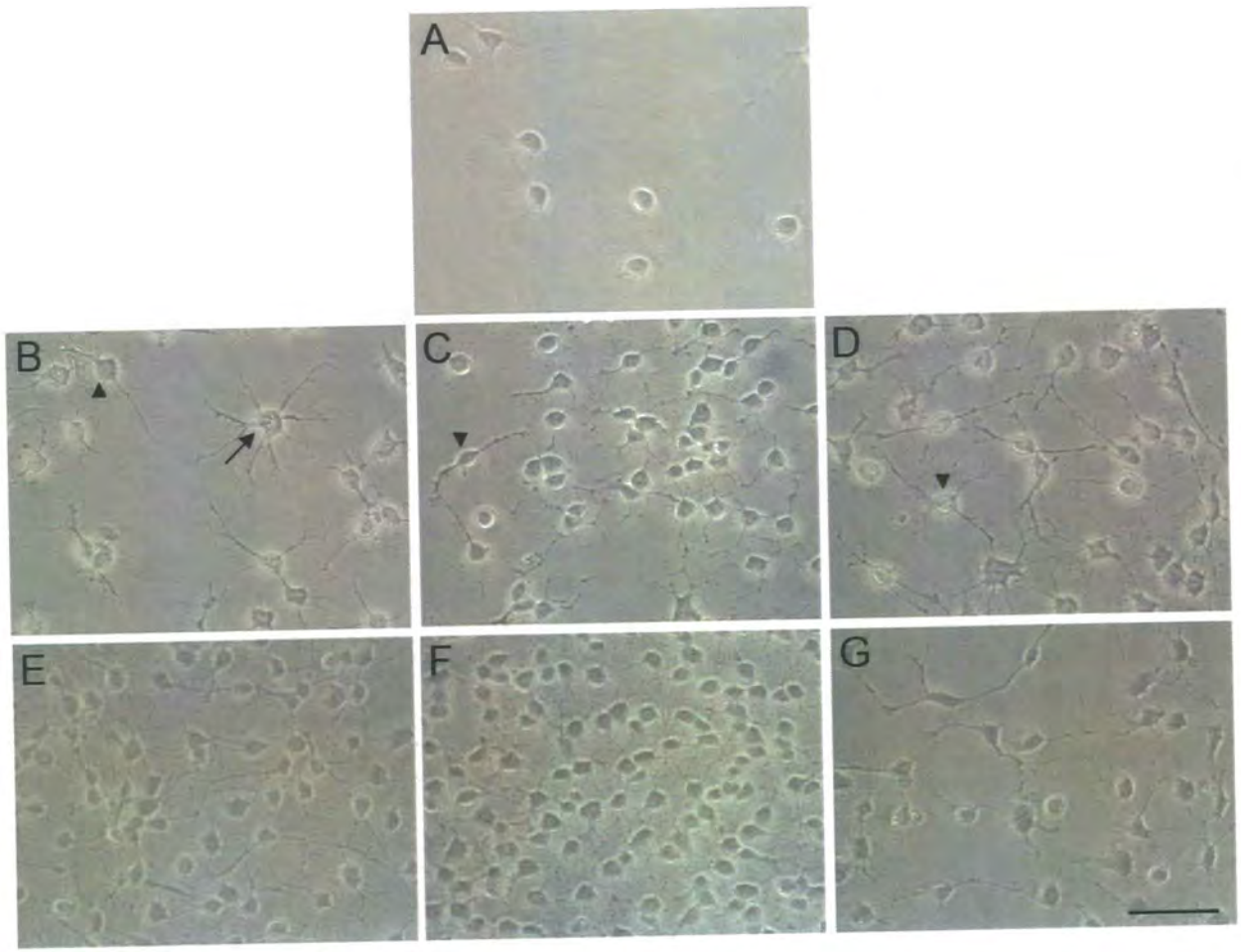

Figure 22: Conditioned media obtained from cellular spheres of rMSCs and dermal clones DS7 and DP9 induced process development in AHPCs. Conditioned media was generated by growing cellular spheres for three days in serum free medium supplemented with EGF (10ng/ml) and bFGF (10ng/ml). AHPCs were seeded at 10 000 cells/cm^2 prior to the addition of the conditioned media samples (A). MSC-CM is represented by photomicrographs of AHPCs after three (B) and six (E) days' culture. DS7-CM is shown in the photomicrographs of AHPCs after three (C) and six (F) days' culture. Finally, the effect of DP9-CM on AHPC development is shown after three (D) and six (G) days' culture. *Scale bar : 50µm.*

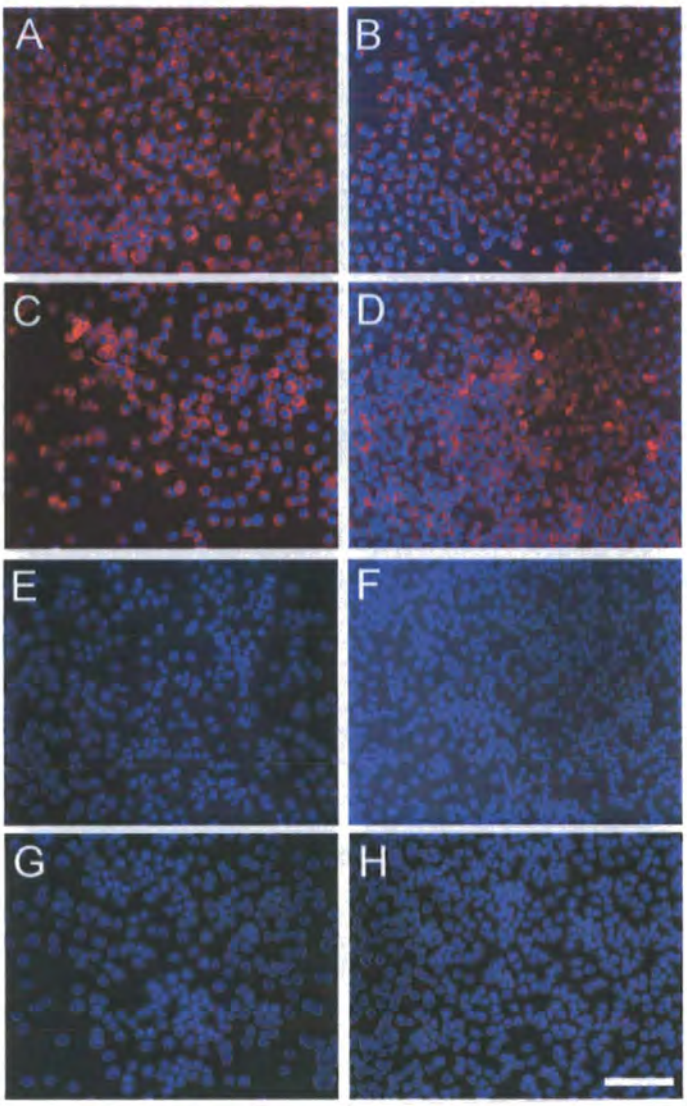

Figure 23: Nestin and TuJ-1 expression are high in AHPCs after culture for seven days in the aggregate induction medium without EGF and bFGF control, and the AHPC proliferation control. The aggregate induction medium without EGF and bFGF control is represented by the fluorescent photomicrographs A, C, E and G. Whereas the AHPC proliferation control is shown in the fluorescent photomicrographs B, D, F and H. AHPCs were tested for nestin (A & B), TuJ-1 (C & D), GFAP (E & F) and GalC (G & H) antigen expression after seven days culture under the two conditions. *Scale bar : 100μm.*

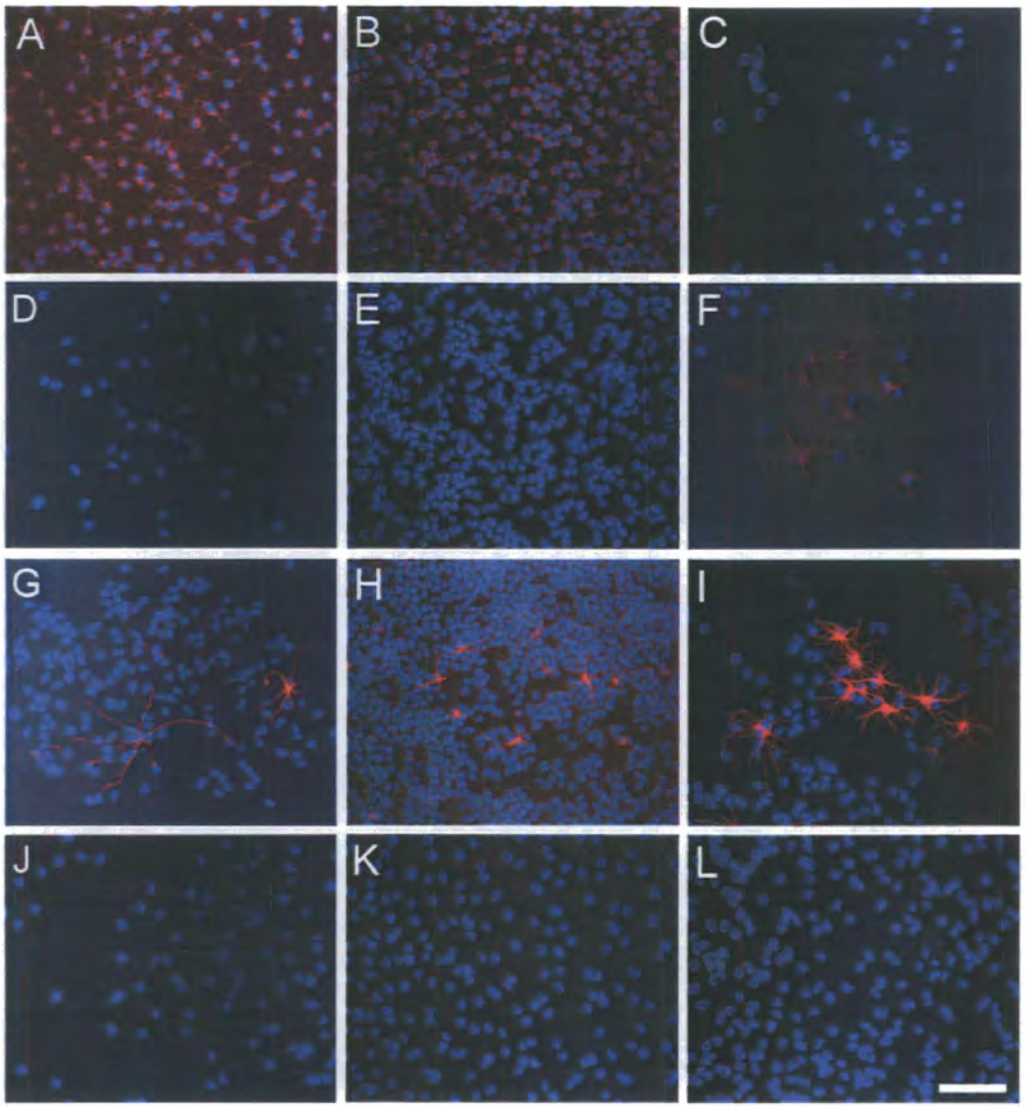

Figure 24: After seven days in MSC-CM and DS7-CM AHPCs express nestin at a high level and GFAP at a low level, whereas in DP9-CM a small proportion of AHPCs express TuJ-1 and GFAP but not nestin. Conditioned media samples are represented as follows; MSC-CM (A, D, G & J), DS7-CM (B, E, H & K) and DP9-CM (C, F, I & L). AHPCs were tested for nestin (A, B & C), TuJ-1 (D, E & F), GFAP (G, H & I) and GalC (J, K & L) antigen expression after seven days culture with the conditioned media samples. *Scale bar : 100µm.*

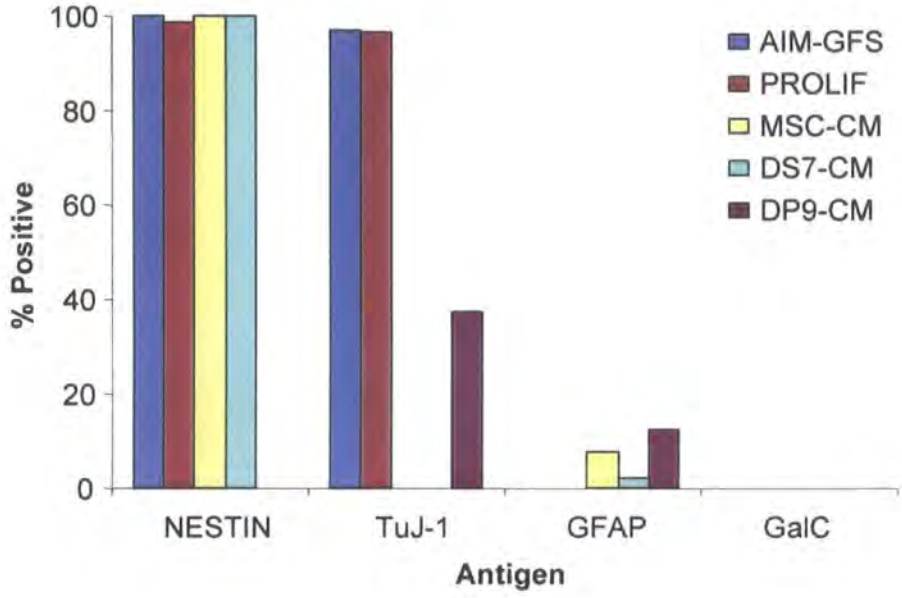

Figure 25: Cell counts reveal that after seven days in MSC-CM, DS7-CM and DP9-CM nestin, TuJ-1 and GFAP expression in AHPCs changes compared to the two controls. The bars represent the percentage of positive cells per field of view for the two controls (AIM-GF and PROIF) and the three conditioned media samples (MSC-CM, DS7-CM and DP9-CM). Therefore, there were potentially five bars for each of the antigens nestin, TuJ-1, GFAP and GalC. However, bars did not show on several occasions, where no AHPCs were positive for the antigen. No statistical tests were performed to determine whether conditions were significantly different as the experiment was not repeated. *Abbreviations; AIM-GFS: the control aggregate induction* medium *without EGF and bFGF, PROLIF: the control AHPC expansion* medium,

3.4 Summary tables

Cell type	rMSCs	DS7	DP9
Chromosome count	**%**	**%**	**%**
41	26.66		33.33
42	26.66		53.33
43	33.33		13.33
44	13.33		
Polyploid		100	

Table 1: Summary of chromosome counting data showing an abnormal chromosome number in at least a proportion of each cell type. A total of 15 metaphase chromosomes were counted for rMSCs and the dermal clones DS7 and DP9 by Chrombios GmbH.

Cell type	rMSCs		DS7		DP9	
Antigen	**% Positive**	**MFI**	**% Positive**	**MFI**	**% Positive**	**MFI**
Nestin	0.35	212.82	28.60	377.74	7.07	17.99
TuJ-1	4.83	47.54	93.46	31.39	97.99	30.99
GFAP	11.08	16.36	0.44	29.47	96.47	48.07
Vimentin	98.06	453.93	99.25	211.62	98.47	20.94
Fibronectin	97.14	267.03	99.42	255.20	96.46	169.16
α-SMA	96.26	380.46	96.93	73.94	98.73	339.76

Table 2: Flow cytometry data showing percentage of positive cells alongside the mean fluorescence intensity (MFI), which when considered together agree with immunocytochemistry data. rMSCs and the dermal clones DS7 and DP9 were grown to confluency in CCM, fixed in PFA, permiabalised and tested for the following antigens; nestin, TuJ-1, GFAP, vimentin, fibronectin and α-SMA.

Cell type	rMSCs		DS7		DP9	
Antigen	**% Positive**	**MFI**	**% Positive**	**MFI**	**% Positive**	**MFI**
CD34	1.32±0.67	30.91	2.42±1.57	14.46	0.95±0.95	12.38
CD45	1.80±1.49	46.90	1.28±0.65	15.51	0.52±0.63	15.51
CD44	92.97±3.12	151.43	93.62±3.66	228.10	91.52±4.29	164.32
CD90	94.83±1.99	107.06	96.46±0.79	198.22	95.56±0.82	273.11
CD105	87.62±1.29	107.22	28.83±1.23	55.85	1.40±1.08	130.56

Table 3: Summary of cell surface antigen expression showing that like rMSCs dermal clones DS7 and DP9 express mesenchymal antigens but not haematopoietic antigens. The mean percentage of positive cells is shown for each antigen ± SEM alongside a typical MFI reading for the positive cells. rMSCs and the dermal clones DS7 and DP9 were grown to confluency in CCM, fixed in PFA and tested for the following cell surface antigens; CD34, CD45, CD44 , CD90 and CD105.

Cell type	rMSCs	DS7	DP9
Days	**Cell count ($x10^3$)**	**Cell count ($x10^3$)**	**Cell count ($x10^3$)**
1	24.7±3.2	24.8±2.1	25.0±2.5
2	27.5±0.7	82.2±3.3	52.7±2.4
3	36.0±4.1	223.7±18.3	99.3±4.2
5	49.7±3.7	241.0±16.9	140.0±32.5
7	78.8±2.1	237.2±26.9	188.2±10.5
9	89.2±7.4	253.3±8.6	358.7±14.1
11	90.0±2.0	319.2±17.4	400.0±19.4

Table 4: The slower growth rate of rMSCs compared to the dermal clones DS7 and DP9 over 11 days in CCM. All three cell types were plated at a density of 30 000 cells per well and counted at one, two, three, five, seven, nine and 11 days. The mean count ±SEM at each time point of rMSCs and the dermal clones DS7 and DP9 is represented.

Cell type	rMSCs	DS7	DP9
Aggregate area (µm)	6132±806	10516±854	9255±822
Aggregate frequency	22.00±1.75	10.17±0.83	55.60±6.52

Table 5: Aggregates formed by rMSCs and dermal clones DS7 and DP9 showed differences in their area and frequency after induction. Mean aggregate area ±SEM and frequency ±SEM are summarised.

Condition	AIM-GF	PROLIF.	MSC-CM	DS7-CM	DP9-CM
Anitgen	**% Positive**	**% Positive**	**% Positive**	**% Positive**	**% Positive**
Nestin	100	99	100	100	0
TuJ-1	97	97	0	0	38
GFAP	0	0	8	2	12
GalC	0	0	0	0	0

Table 6: Cell counts reveal that after seven days in MSC-CM, DS7-CM and DP9-CM nestin, TuJ-1 and GFAP expression in AHPCs changes compared to the two controls. These data represent the two controls (AIM-GF and PROIF) and the three conditioned media samples (MSC-CM, DS7-CM and DP9-CM).

CHAPTER 4: DISCUSSION

4.1 The relationship of HFSC clones to bone marrow MSCs

The isolation of MSCs from a wide variety of tissues has been has been previously demonstrated. The first part of this study has determined the relationship of two hair follicle clones termed DS7 and DP9 to primary bone marrow derived MSCs. The two cell types were characterised in terms of their morphology, proliferation, expression of intracellular and cell surface antigens and differentiation potential into bone and fat.

After isolation and *ex vivo* expansion, morphologies of MSCs from bone marrow have been described as heterogeneous, ranging from spindle shaped cells to large broad flat fibroblast-like cells [130]. These observations have also been documented in the bone marrow MSCs used in this study. At sub-confluence the DS7 clone resembled spindle shaped MSCs, whereas the DP9 clone was more like the large broad flat MSCs. Therefore the dermal clones represented the two contrasting subpopulations existing within bone marrow MSCs. The morphological change observed in both clones at confluence was probably due constraints put on the cells after reductions in the space available. Neither DS7 nor DP9 proliferation was similar to MSC proliferation; this was almost certainly due to the selective pressure for rapidly dividing cells put on the dermal cells during their isolation. Expression of the intracellular mesenchymal antigens vimentin, fibronectin and α-SMA has been used to define many populations of MSCs isolated from a variety of tissues. However, all three of these markers have rarely been used simultaneously; instead just one is usually tested [85]. Here all three intracellular antigens were tested and expressed by the two clones with the exception of vimentin in DP9. Versican is a proteoglycan that is strongly expressed in rodent and human anagen hair follicle dermal papillae [131]. Its expression in the hair follicle dermal clones DS7 and DP9 and absence from bone marrow rMSCs confirmed the respective origins of these three cell types.

This study has defined the surface protein expression profile of hair follicle dermal clones DS7 and DP9. It has been demonstrated that the phenotype of hair follicle dermal clones is homologous to that of primary rMSCs derived from bone marrow, which suggests they may be related to MSCs. The hair follicle is vascularised,

therefore there is a possibility the dermal clones were derived from circulating haematopoietic progenitors. Further it is feasible the clones are related to endogenous hair follicle dermal cells capable of repopulating the mouse haematopoietic system [26]. Both dermal clones were negative for the haematopoietic cell surface antigen CD34. However, the reliability of CD34 in demonstrating the absence of haematopoietic progenitors is questionable, as bone marrow MSCs have been identified as positive [132] and negative [17] for CD34. Further, CD34 has been used as a pluripotency indicator in studies of stem cells from the hair follicle bulge [29]. Therefore a second haematopoietic antigen CD45 was tested alongside CD34 to provide confirmation of their phenotype. The absence of CD45 and CD34 expression provided strong evidence against a relationship with the haematopoietic populations associated with the hair follicle dermis and instead suggested a possible relationship to bone marrow MSCs. This relationship was reinforced by the DS7 and DP9 being positive for the mesenchymal antigens CD44 and CD90. Expression of CD44 indicates a relationship to bone marrow MSCs because it is known to interfere with the development of haematopoietic stem cells [133]. However, the expression of CD44 and CD90 must be reinforced by the expression of many other cell surface antigens and an ability support haematopoiesis, for DS7 and DP9 to be undeniably classified as bone marrow derived MSCs [70]. This is especially important since CD44 has also been reported as a marker of epithelial and neuronal precursors [38]. Further classification was attempted with the CD105 antigen, which is more specific to bone marrow derived MSCs [17]. However, DS7 and DP9 clones did not express the antigen CD105. The absence of CD105 expression therefore suggests that the DS7 and DP9 clones were not derived from circulating MSCs, which originally resided in the bone marrow.

All previous attempts to determine mesenchymal potential of adult stem cell populations have demonstrated differentiation towards at least two mesodermal lineages. The use of antigens to characterise stem cell populations have their limitations, such as the promiscuous specificity some markers have to the mesenchymal cell types previously outlined. Differentiation towards fat and bone mesenchymal lineages was therefore attempted here in DS7, DP9 and rMSCs. The rMSCs were able to differentiate into bone and fat using all protocols. Neither of the dermal clones was able to differentiate towards bone, whereas DS7 but not DP9 was able to differentiate into fat. The lack of bone differentiation potential in both dermal clones is not in line with a previous study on the mesenchymal potential of clonally derive bone marrow MSCs. In this previous study all but one of the 185 clones were

able to differentiate into at least the bone lineage, which suggests, unlike the follicle dermis cells, this was the basic capability of the vast majority of bone marrow derived MSCs [89]. In contrast, a second study showed an inability of bone differentiation in the majority of clones isolated from bone marrow MSCs, however, this could have been induced by genetic manipulations undertaken to immortalise the clones [90]. A large variation in fat differentiation protocols exists in the literature; therefore two fat protocols were attempted in this study, which showed fat differentiation was still restricted to DS7 and bone marrow MSCs. Fat differentiation was shown to decline in DS7 as passage number increased, which has been shown in studies involving cloned bone marrow MSCs [89] and MSCs from the pancreas [78].

4.2 The ability of adult stem cells to form aggregates

The ability of bone marrow derived MSCs and dermal papilla derived progenitors to form neruosphere-like structures *in vitro* after treatment with EGF and bFGF supplemented serum free medium has already been well established [53, 128]. Therefore the aim of this study was initially to demonstrate the development of neural antigen positive aggregates from the two hair follicle stem cell clones DS7 and DP9. This was attempted using an induction protocol previously described for MSCs [128], and rMSCs derived from bone marrow were used as a positive control. Preliminary findings were encouraging because all three cell types were able to form aggregates. However some differences were observed in the manor by which the aggregates formed. The dermal clone DS7 was most similar to rMSCs because adherent aggregates formed first, which eventually lifted off the tissue culture plastic. By contrast – unlike rMSCs and DS7 – the dermal clone DP9 aggregates did not adhere, instead they formed in suspension similar to aggregates derived from the hair follicle dermis [57, 58]. However, DP9 aggregates were more similar to aggregates from rMSC compared to DS7 aggregates in terms of their frequency.

The expression of nestin was found in aggregates from all three cell types, which is similar to previous findings for neural crest related stem cell populations derived from the skin dermis and MSCs from bone marrow [53, 58, 128]. A loss in mesenchymal identity, previously demonstrated in bone marrow derived cells induced to form aggregates [128], was shown in the dermal clone DS7 and rMSCs by a reduction in α-SMA expression. Expression of α-SMA was maintained in the dermal clone DP9, indicating less progression towards the neural lineage. Flow cytometry data indicated

that the formation of aggregates in DS7 did not increase nestin expression, because it stayed at similar levels after induction. In conclusion aggregates of the two dermal clones do not follow the same changes in gene expression as rMSC aggregates.

The maintenance of nestin expression in DS7 and α-SMA in DP9 suggests aggregate formation in the dermal clones is not driving changes in gene expression. However, the apparent increase in nestin expression in DP9 and decrease in α-SMA expression in DS7 would suggest some differentiation, and that the maintenance of marker expression in the aggregates represents a more primitive phenotype compared to the aggregates of rMSCs. Evidence has been presented that shows induction of nestin expression in aggregates as a result of growing MSCs at very high densities in high serum conditions that does not usually induce nestin expression [134]. This demonstrates that neural markers can be induced solely as a result of high density culture, which could provide an explanation not only for the increase nestin expression in DP9 but also rMSCs. However, the absence of increased nestin expression in DS7 aggregates suggests high density culture is not the only factor important in inducing nestin expression. Neuronal differentiation was demonstrated in aggregates from the high density cultures [134]. Differentiation of these neural antigen positive aggregates was not as rigorously characterised as neural differentiation in aggregates derived from skin and bone marrow MSCs [28, 57, 128]. Despite this the study still demonstrates that high density culture can induce the formation of primitive neural progenitors. Neural differentiation was not attempted here after the high density induction of the dermal clones to form aggregates, therefore these aggregates may not represent neural progenitors, and their formation could be largely due to an artefact created by high density cell culture. Furthermore, the use of nestin as a marker of neural stem cell-like aggregates is unreliable as nestin is known to be expressed in other non-neural stem cell tissues such as skeletal muscle [104]. Therefore in the case of DP9 and rMSC aggregates nestin expression indicates *in vitro* differentiation that is not necessarily indicative of NSCs. A large number of neural markers would be needed to examine if these aggregates have true similarities to NSCs. This study indcates that MSC aggregates more closely represent NSCs as they express the neuronal marker TuJ-1, whereas the DS7 and DP9 dermal clone aggregates do not. Another piece of evidence that suggested neural development was an artefact of the culture conditions was the reversibility of neural morphologies in the adherent DS7 population after induction. The neural-like phenotypes in DS7 could be the result of similar cytoskeletal collapse mechanisms involved in the development of neural-like cells after chemical induction of MSCs.

4.3 The effect of conditioned media on AHPC development

Aggregate conditioned medium from rMSCs and the dermal clones DS7 and DP9 induced process elaboration and maintenance of proliferation in AHPCs. Conditioned media samples from rMSC and DS7 aggregates induced a large decline in TuJ-1 expression but not nestin in AHPCs. In contrast DP9 aggregate conditioned medium induced a smaller decline in TuJ-1 expression and a large decline in nestin expression in AHPCs. Finally all three types of conditioned media induced a small proportion of AHPCs to acquire a $GFAP^+$ astrocyte phenotype but not a $GalC^+$ oligodendrocyte phenotype.

These data provide further evidence that soluble factors produced by adult stem cells induced to form aggregates expressing nestin are able to alter the development of neural progenitor cell populations *in vitro*. In a previous study the effect of conditioned medium from MSCs induced to express nestin resulted in selective attenuation of apoptosis in astrocytic progenitors [126]. In the present study differentiation of AHPCs was probably produced by an instructive effect of the conditioned media on a subpopulation of the AHPCs positive for TuJ-1 and nestin. This resulted in a decline in expression of TuJ-1 in MSC-CM and DS7-CM and a decline in both nestin and TuJ-1 expression in DP9-CM. The absence of GFAP positive cells in control conditions suggests the astrocytic phenotype was not produced by selective survival or proliferation of this subpopulation after treatment with conditioned media. Dual labelling of the TuJ-1 and nestin positive AHPCs with PI would determine if the conditioned media was producing significant levels of cell death in the AHPCs. If significant levels of cell death were observed, then astrocytic differentiation could have been induced by the conditioned media enabling survival and instruction of a small subpopulation of AHPCs capable of astrocytic differentiation. Without selective mechanisms, the phenotypes produced in AHPCs by the conditioned media were likely to be at a transitional stage between undifferentiated AHPC progenitors and more differentiated derivatives.

4.4 The limitations of *in vitro* cell culture

Transformation of cell types *in vitro* is of considerable concern to stem cell biologist as transformed cells are no longer an accurate representation of their *in vivo* counterparts. To use adult stem cells for autologous treatment of degenerative diseases they need to be expanded *in vitro* to create a large enough number of cells. If adult stem cells undergo transformation *in vitro* then they cannot be safely returned the body in a cell replacement context. Transformation has been illustrated in this study by an abnormal karyotype in the dermal clones DS7 and DP9 and rMSCs. DS7 showed a high degree of polyploidy whereas DP9 and rMSCs had fewer but nonetheless significant karyotypic irregularities. A number of phenotypic abnormalities suggestive of transformed cells were observed in DS7. For example differential expression intracellular antigens TuJ-1, nestin and α-SMA suggested the DS7 culture consisted of two distinct populations of cells. Furthermore changes to the expression of the cell surface antigen CD44 and loss of adipogenic potential at high passage numbers indicated DS7 was dynamically changing and adapting to the culture conditions.

Senescence is a phenomenon which is common in adult stem cells and can be speeded up after *in vitro* expansion of MSCs [135, 136]. However, both the dermal clones showed no evidence of senescence, as the DS7 clone continued to proliferate at P41 and the DP9 clone at P32. Indeed the indefinite proliferation of human ES cells *in vitro* is thought to be the result of genetic abnormalities acquired in culture [137]. Hence, it is possible the karyotypic abnormalities in DS7 and DP9 have lead to their continued proliferation *in vitro*. *De novo* mutations can be established *in vitro* by enzymatic dissociation during passage, and variations in oxygen tension [138]. Extra copies of genes evident in the polyploid DS7 could have enhanced proliferation due to expression of duplicated growth stimulating genes. Also karyotypic instability could cause aberrant expression of genes such as telomerase, which maintains telomere length and therefore allows cells to continue dividing [139].

4.5 Concluding remarks

This study has found homologies between clonally derived populations of HFSCs and bone marrow MSCs in terms of their mesenchymal capabilities. It has also demonstrated clonally derived HFSCs can form aggregates similar to those produced by MSCs, which produce soluble factors that induce an astrocytic phenotype in a small proportion of neural progenitor cells. Finally this study has underlined the limitations of expanding adult stem cells *ex vivo*, and highlighted that we must review the techniques used to expand adult stem cells if they are to be used for tissue replacement therapies.

References

1. Thomson, J.A., et al., *Embryonic stem cell lines derived from human blastocysts.* Science, 1998. **282**(5391): p. 1145-7.
2. Amit, M., et al., *Clonally derived human embryonic stem cell lines maintain pluripotency and proliferative potential for prolonged periods of culture.* Dev Biol, 2000. **227**(2): p. 271-8.
3. Potten, C.S. and M. Loeffler, *Stem cells: attributes, cycles, spirals, pitfalls and uncertainties. Lessons for and from the crypt.* Development, 1990. **110**(4): p. 1001-20.
4. Slack, J.M.W., *Essential developmental biology.* 2nd ed. 2006, Malden, MA: Blackwell Pub. 365 p.
5. Slack, J.M., *Stem cells in epithelial tissues.* Science, 2000. **287**(5457): p. 1431-3.
6. Jones, P.H., B.D. Simons, and F.M. Watt, *Sic transit gloria: farewell to the epidermal transit amplifying cell?* Cell Stem Cell, 2007. **1**(4): p. 371-81.
7. Gage, F.H., *Mammalian neural stem cells.* Science, 2000. **287**(5457): p. 1433-8.
8. Lindwall, G., et al., *Heavy water labeling of keratin as a non-invasive biomarker of skin turnover in vivo in rodents and humans.* J Invest Dermatol, 2006. **126**(4): p. 841-8.
9. Anderson, D.J., F.H. Gage, and I.L. Weissman, *Can stem cells cross lineage boundaries?* Nat Med, 2001. **7**(4): p. 393-5.
10. Morrison, S.J., *Stem cell potential: can anything make anything?* Curr Biol, 2001. **11**(1): p. R7-9.
11. Sieber-Blum, M., et al., *Pluripotent neural crest stem cells in the adult hair follicle.* Dev Dyn, 2004. **231**(2): p. 258-69.
12. Jiang, Y., et al., *Pluripotency of mesenchymal stem cells derived from adult marrow.* Nature, 2002. **418**(6893): p. 41-9.
13. Wilmut, I., et al., *Viable offspring derived from fetal and adult mammalian cells.* Nature, 1997. **385**(6619): p. 810-3.
14. Gurdon, J.B., T.R. Elsdale, and M. Fischberg, *Sexually mature individuals of Xenopus laevis from the transplantation of single somatic nuclei.* Nature, 1958. **182**(4627): p. 64-5.
15. Cotsarelis, G., T.T. Sun, and R.M. Lavker, *Label-retaining cells reside in the bulge area of pilosebaceous unit: implications for follicular stem cells, hair cycle, and skin carcinogenesis.* Cell, 1990. **61**(7): p. 1329-37.
16. Reynolds, A.J. and C.A. Jahoda, *Cultured dermal papilla cells induce follicle formation and hair growth by transdifferentiation of an adult epidermis.* Development, 1992. **115**(2): p. 587-93.
17. Pittenger, M.F., et al., *Multilineage potential of adult human mesenchymal stem cells.* Science, 1999. **284**(5411): p. 143-7.
18. Jahoda, C.A., et al., *Hair follicle dermal cells differentiate into adipogenic and osteogenic lineages.* Exp Dermatol, 2003. **12**(6): p. 849-59.
19. Hoogduijn, M.J., E. Gorjup, and P.G. Genever, *Comparative characterization of hair follicle dermal stem cells and bone marrow mesenchymal stem cells.* Stem Cells Dev, 2006. **15**(1): p. 49-60.
20. Sato, Y., et al., *Human mesenchymal stem cells xenografted directly to rat liver are differentiated into human hepatocytes without fusion.* Blood, 2005. **106**(2): p. 756-63.
21. Woodbury, D., et al., *Adult rat and human bone marrow stromal cells differentiate into neurons.* J Neurosci Res, 2000. **61**(4): p. 364-70.
22. Sanchez-Ramos, J., et al., *Adult bone marrow stromal cells differentiate into neural cells in vitro.* Exp Neurol, 2000. **164**(2): p. 247-56.

23. Deng, W., et al., *In vitro differentiation of human marrow stromal cells into early progenitors of neural cells by conditions that increase intracellular cyclic AMP.* Biochem Biophys Res Commun, 2001. **282**(1): p. 148-52.
24. Krause, D.S., et al., *Multi-organ, multi-lineage engraftment by a single bone marrow-derived stem cell.* Cell, 2001. **105**(3): p. 369-77.
25. Taylor, G., et al., *Involvement of follicular stem cells in forming not only the follicle but also the epidermis.* Cell, 2000. **102**(4): p. 451-61.
26. Lako, M., et al., *Hair follicle dermal cells repopulate the mouse haematopoietic system.* J Cell Sci, 2002. **115**(Pt 20): p. 3967-74.
27. Gharzi, A., A.J. Reynolds, and C.A. Jahoda, *Plasticity of hair follicle dermal cells in wound healing and induction.* Exp Dermatol, 2003. **12**(2): p. 126-36.
28. Fernandes, K.J., et al., *A dermal niche for multipotent adult skin-derived precursor cells.* Nat Cell Biol, 2004. **6**(11): p. 1082-93.
29. Amoh, Y., et al., *Multipotent nestin-positive, keratin-negative hair-follicle bulge stem cells can form neurons.* Proc Natl Acad Sci U S A, 2005. **102**(15): p. 5530-4.
30. D'Amour, K.A. and F.H. Gage, *Are somatic stem cells pluripotent or lineage-restricted?* Nat Med, 2002. **8**(3): p. 213-4.
31. Fuchs, E., et al., *At the roots of a never-ending cycle.* Dev Cell, 2001. **1**(1): p. 13-25.
32. Oshima, H., et al., *Morphogenesis and renewal of hair follicles from adult multipotent stem cells.* Cell, 2001. **104**(2): p. 233-45.
33. Tumbar, T., et al., *Defining the epithelial stem cell niche in skin.* Science, 2004. **303**(5656): p. 359-63.
34. Li, L., et al., *Nestin expression in hair follicle sheath progenitor cells.* Proc Natl Acad Sci U S A, 2003. **100**(17): p. 9958-61.
35. Amoh, Y., et al., *Nascent blood vessels in the skin arise from nestin-expressing hair-follicle cells.* Proc Natl Acad Sci U S A, 2004. **101**(36): p. 13291-5.
36. Lavker, R.M., et al., *Hair follicle stem cells: their location, role in hair cycle, and involvement in skin tumor formation.* J Invest Dermatol, 1993. **101**(1 Suppl): p. 16S-26S.
37. Wang, Y., et al., *Patterns of nestin expression in human skin.* Cell Biol Int, 2006. **30**(2): p. 144-8.
38. Kruse, C., et al., *Towards the development of a pragmatic technique for isolating and differentiating nestin-positive cells from human scalp skin into neuronal and glial cell populations: generating neurons from human skin?* Exp Dermatol, 2006. **15**(10): p. 794-800.
39. Hardy, M.H., *The secret life of the hair follicle.* Trends Genet, 1992. **8**(2): p. 55-61.
40. Millar, S.E., *Molecular mechanisms regulating hair follicle development.* J Invest Dermatol, 2002. **118**(2): p. 216-25.
41. Andl, T., et al., *WNT signals are required for the initiation of hair follicle development.* Dev Cell, 2002. **2**(5): p. 643-53.
42. Alonso, L. and E. Fuchs, *Stem cells in the skin: waste not, Wnt not.* Genes Dev, 2003. **17**(10): p. 1189-200.
43. DasGupta, R. and E. Fuchs, *Multiple roles for activated LEF/TCF transcription complexes during hair follicle development and differentiation.* Development, 1999. **126**(20): p. 4557-68.
44. Gat, U., et al., *De Novo hair follicle morphogenesis and hair tumors in mice expressing a truncated beta-catenin in skin.* Cell, 1998. **95**(5): p. 605-14.
45. Widelitz, R.B., et al., *FGF induces new feather buds from developing avian skin.* J Invest Dermatol, 1996. **107**(6): p. 797-803.
46. Barsh, G., *Of ancient tales and hairless tails.* Nat Genet, 1999. **22**(4): p. 315-6.

47. Oliver, R.F. and C.A. Jahoda, *Dermal-epidermal interactions.* Clin Dermatol, 1988. **6**(4): p. 74-82.
48. Reddy, S., et al., *Characterization of Wnt gene expression in developing and postnatal hair follicles and identification of Wnt5a as a target of Sonic hedgehog in hair follicle morphogenesis.* Mech Dev, 2001. **107**(1-2): p. 69-82.
49. Kishimoto, J., R.E. Burgeson, and B.A. Morgan, *Wnt signaling maintains the hair-inducing activity of the dermal papilla.* Genes Dev, 2000. **14**(10): p. 1181-5.
50. Zhang, J., et al., *Bone morphogenetic protein signaling inhibits hair follicle anagen induction by restricting epithelial stem/progenitor cell activation and expansion.* Stem Cells, 2006. **24**(12): p. 2826-39.
51. Sieber-Blum, M., et al., *Characterization of epidermal neural crest stem cell (EPI-NCSC) grafts in the lesioned spinal cord.* Mol Cell Neurosci, 2006. **32**(1-2): p. 67-81.
52. Jahoda, C.A. and A.J. Reynolds, *Dermal-epidermal interactions. Adult follicle-derived cell populations and hair growth.* Dermatol Clin, 1996. **14**(4): p. 573-83.
53. Hunt, D.P., et al., *A highly enriched niche of precursor cells with neuronal and glial potential within the hair follicle dermal papilla of adult skin.* Stem Cells, 2008. **26**(1): p. 163-72.
54. Lechner, A., et al., *Nestin-positive progenitor cells derived from adult human pancreatic islets of Langerhans contain side population (SP) cells defined by expression of the ABCG2 (BCRP1) ATP-binding cassette transporter.* Biochem Biophys Res Commun, 2002. **293**(2): p. 670-4.
55. Jahoda, C.A., et al., *Smooth muscle alpha-actin is a marker for hair follicle dermis in vivo and in vitro.* J Cell Sci, 1991. **99 (Pt 3)**: p. 627-36.
56. Shih, D.T., et al., *Isolation and characterization of neurogenic mesenchymal stem cells in human scalp tissue.* Stem Cells, 2005. **23**(7): p. 1012-20.
57. Toma, J.G., et al., *Isolation of multipotent adult stem cells from the dermis of mammalian skin.* Nat Cell Biol, 2001. **3**(9): p. 778-84.
58. Toma, J.G., et al., *Isolation and characterization of multipotent skin-derived precursors from human skin.* Stem Cells, 2005. **23**(6): p. 727-37.
59. Fernandes, K.J., et al., *Analysis of the neurogenic potential of multipotent skin-derived precursors.* Exp Neurol, 2006. **201**(1): p. 32-48.
60. Joannides, A., et al., *Efficient generation of neural precursors from adult human skin: astrocytes promote neurogenesis from skin-derived stem cells.* Lancet, 2004. **364**(9429): p. 172-8.
61. Hu, Y.F., Z.J. Zhang, and M. Sieber-Blum, *An epidermal neural crest stem cell (EPI-NCSC) molecular signature.* Stem Cells, 2006. **24**(12): p. 2692-702.
62. Mignone, J.L., et al., *Neural potential of a stem cell population in the hair follicle.* Cell Cycle, 2007. **6**(17): p. 2161-70.
63. McKenzie, I.A., et al., *Skin-derived precursors generate myelinating Schwann cells for the injured and dysmyelinated nervous system.* J Neurosci, 2006. **26**(24): p. 6651-60.
64. Amoh, Y., et al., *Implanted hair follicle stem cells form Schwann cells that support repair of severed peripheral nerves.* Proc Natl Acad Sci U S A, 2005. **102**(49): p. 17734-8.
65. Friedenstein, A.J., et al., *Precursors for fibroblasts in different populations of hematopoietic cells as detected by the in vitro colony assay method.* Exp Hematol, 1974. **2**(2): p. 83-92.
66. Friedenstein, A.J., J.F. Gorskaja, and N.N. Kulagina, *Fibroblast precursors in normal and irradiated mouse hematopoietic organs.* Exp Hematol, 1976. **4**(5): p. 267-74.
67. Tavassoli, M. and A. Friedenstein, *Hemopoietic stromal microenvironment.* Am J Hematol, 1983. **15**(2): p. 195-203.

68. Sekiya, I., et al., *Expansion of human adult stem cells from bone marrow stroma: conditions that maximize the yields of early progenitors and evaluate their quality.* Stem Cells, 2002. **20**(6): p. 530-41.
69. Romanov, Y.A., et al., *Mesenchymal stem cells from human bone marrow and adipose tissue: isolation, characterization, and differentiation potentialities.* Bull Exp Biol Med, 2005. **140**(1): p. 138-43.
70. Gronthos, S., et al., *Surface protein characterization of human adipose tissue-derived stromal cells.* J Cell Physiol, 2001. **189**(1): p. 54-63.
71. Conget, P.A. and J.J. Minguell, *Phenotypical and functional properties of human bone marrow mesenchymal progenitor cells.* J Cell Physiol, 1999. **181**(1): p. 67-73.
72. Kaiser, S., et al., *BM cells giving rise to MSC in culture have a heterogeneous CD34 and CD45 phenotype.* Cytotherapy, 2007. **9**(5): p. 439-50.
73. Gronthos, S., et al., *The STRO-1+ fraction of adult human bone marrow contains the osteogenic precursors.* Blood, 1994. **84**(12): p. 4164-73.
74. Baddoo, M., et al., *Characterization of mesenchymal stem cells isolated from murine bone marrow by negative selection.* J Cell Biochem, 2003. **89**(6): p. 1235-49.
75. Bruder, S.P., et al., *Bone regeneration by implantation of purified, culture-expanded human mesenchymal stem cells.* J Orthop Res, 1998. **16**(2): p. 155-62.
76. Kuznetsov, S.A., et al., *Circulating skeletal stem cells.* J Cell Biol, 2001. **153**(5): p. 1133-40.
77. De Bari, C., et al., *Multipotent mesenchymal stem cells from adult human synovial membrane.* Arthritis Rheum, 2001. **44**(8): p. 1928-42.
78. Seeberger, K.L., et al., *Expansion of mesenchymal stem cells from human pancreatic ductal epithelium.* Lab Invest, 2006. **86**(2): p. 141-53.
79. Miura, M., et al., *SHED: stem cells from human exfoliated deciduous teeth.* Proc Natl Acad Sci U S A, 2003. **100**(10): p. 5807-12.
80. Fukuchi, Y., et al., *Human placenta-derived cells have mesenchymal stem/progenitor cell potential.* Stem Cells, 2004. **22**(5): p. 649-58.
81. Erices, A., P. Conget, and J.J. Minguell, *Mesenchymal progenitor cells in human umbilical cord blood.* Br J Haematol, 2000. **109**(1): p. 235-42.
82. Goodwin, H.S., et al., *Multilineage differentiation activity by cells isolated from umbilical cord blood: expression of bone, fat, and neural markers.* Biol Blood Marrow Transplant, 2001. **7**(11): p. 581-8.
83. Tsai, M.S., et al., *Isolation of human multipotent mesenchymal stem cells from second-trimester amniotic fluid using a novel two-stage culture protocol.* Hum Reprod, 2004. **19**(6): p. 1450-6.
84. in 't Anker, P.S., et al., *Mesenchymal stem cells in human second-trimester bone marrow, liver, lung, and spleen exhibit a similar immunophenotype but a heterogeneous multilineage differentiation potential.* Haematologica, 2003. **88**(8): p. 845-52.
85. da Silva Meirelles, L., P.C. Chagastelles, and N.B. Nardi, *Mesenchymal stem cells reside in virtually all post-natal organs and tissues.* J Cell Sci, 2006. **119**(Pt 11): p. 2204-13.
86. Sabatini, F., et al., *Human bronchial fibroblasts exhibit a mesenchymal stem cell phenotype and multilineage differentiating potentialities.* Lab Invest, 2005. **85**(8): p. 962-71.
87. Shi, S. and S. Gronthos, *Perivascular niche of postnatal mesenchymal stem cells in human bone marrow and dental pulp.* J Bone Miner Res, 2003. **18**(4): p. 696-704.
88. Anjos-Afonso, F., E.K. Siapati, and D. Bonnet, *In vivo contribution of murine mesenchymal stem cells into multiple cell-types under minimal damage conditions.* J Cell Sci, 2004. **117**(Pt 23): p. 5655-64.

89. Muraglia, A., R. Cancedda, and R. Quarto, *Clonal mesenchymal progenitors from human bone marrow differentiate in vitro according to a hierarchical model.* J Cell Sci, 2000. **113 (Pt 7)**: p. 1161-6.
90. Okamoto, T., et al., *Clonal heterogeneity in differentiation potential of immortalized human mesenchymal stem cells.* Biochem Biophys Res Commun, 2002. **295**(2): p. 354-61.
91. Lescaudron, L., D. Unni, and G.L. Dunbar, *Autologous adult bone marrow stem cell transplantation in an animal model of huntington's disease: behavioral and morphological outcomes.* Int J Neurosci, 2003. **113**(7): p. 945-56.
92. Li, Y., et al., *Intracerebral transplantation of bone marrow stromal cells in a 1-methyl-4-phenyl-1,2,3,6-tetrahydropyridine mouse model of Parkinson's disease.* Neurosci Lett, 2001. **316**(2): p. 67-70.
93. Chopp, M., et al., *Spinal cord injury in rat: treatment with bone marrow stromal cell transplantation.* Neuroreport, 2000. **11**(13): p. 3001-5.
94. Zhang, J., et al., *Human bone marrow stromal cell treatment improves neurological functional recovery in EAE mice.* Exp Neurol, 2005. **195**(1): p. 16-26.
95. Hardy, S.A., D.J. Maltman, and S.A. Przyborski, *Mesenchymal stem cells as mediators of neural differentiation.* Curr Stem Cell Res Ther, 2008. **3**(1): p. 43-52.
96. Croft, A.P. and S.A. Przyborski, *Generation of neuroprogenitor-like cells from adult mammalian bone marrow stromal cells in vitro.* Stem Cells Dev, 2004. **13**(4): p. 409-20.
97. Kohyama, J., et al., *Brain from bone: efficient "meta-differentiation" of marrow stroma-derived mature osteoblasts to neurons with Noggin or a demethylating agent.* Differentiation, 2001. **68**(4-5): p. 235-44.
98. Dezawa, M., et al., *Specific induction of neuronal cells from bone marrow stromal cells and application for autologous transplantation.* J Clin Invest, 2004. **113**(12): p. 1701-10.
99. Song, H.J., C.F. Stevens, and F.H. Gage, *Neural stem cells from adult hippocampus develop essential properties of functional CNS neurons.* Nat Neurosci, 2002. **5**(5): p. 438-45.
100. Bertani, N., et al., *Neurogenic potential of human mesenchymal stem cells revisited: analysis by immunostaining, time-lapse video and microarray.* J Cell Sci, 2005. **118**(Pt 17): p. 3925-36.
101. Croft, A.P. and S.A. Przyborski, *Formation of neurons by non-neural adult stem cells: potential mechanism implicates an artifact of growth in culture.* Stem Cells, 2006. **24**(8): p. 1841-51.
102. Neuhuber, B., et al., *Reevaluation of in vitro differentiation protocols for bone marrow stromal cells: disruption of actin cytoskeleton induces rapid morphological changes and mimics neuronal phenotype.* J Neurosci Res, 2004. **77**(2): p. 192-204.
103. Lu, P., A. Blesch, and M.H. Tuszynski, *Induction of bone marrow stromal cells to neurons: differentiation, transdifferentiation, or artifact?* J Neurosci Res, 2004. **77**(2): p. 174-91.
104. Sjoberg, G., et al., *Colocalization of nestin and vimentin/desmin in skeletal muscle cells demonstrated by three-dimensional fluorescence digital imaging microscopy.* Exp Cell Res, 1994. **214**(2): p. 447-58.
105. Wislet-Gendebien, S., et al., *Plasticity of cultured mesenchymal stem cells: switch from nestin-positive to excitable neuron-like phenotype.* Stem Cells, 2005. **23**(3): p. 392-402.
106. Reyes, M., et al., *Origin of endothelial progenitors in human postnatal bone marrow.* J Clin Invest, 2002. **109**(3): p. 337-46.

107. Azizi, S.A., et al., *Engraftment and migration of human bone marrow stromal cells implanted in the brains of albino rats--similarities to astrocyte grafts.* Proc Natl Acad Sci U S A, 1998. **95**(7): p. 3908-13.
108. Lee, J., et al., *Migration and differentiation of nuclear fluorescence-labeled bone marrow stromal cells after transplantation into cerebral infarct and spinal cord injury in mice.* Neuropathology, 2003. **23**(3): p. 169-80.
109. Kopen, G.C., D.J. Prockop, and D.G. Phinney, *Marrow stromal cells migrate throughout forebrain and cerebellum, and they differentiate into astrocytes after injection into neonatal mouse brains.* Proc Natl Acad Sci U S A, 1999. **96**(19): p. 10711-6.
110. Brazelton, T.R., et al., *From marrow to brain: expression of neuronal phenotypes in adult mice.* Science, 2000. **290**(5497): p. 1775-9.
111. Shichinohe, H., et al., *In vivo tracking of bone marrow stromal cells transplanted into mice cerebral infarct by fluorescence optical imaging.* Brain Res Brain Res Protoc, 2004. **13**(3): p. 166-75.
112. Mezey, E., et al., *Turning blood into brain: cells bearing neuronal antigens generated in vivo from bone marrow.* Science, 2000. **290**(5497): p. 1779-82.
113. Terada, N., et al., *Bone marrow cells adopt the phenotype of other cells by spontaneous cell fusion.* Nature, 2002. **416**(6880): p. 542-5.
114. Ying, Q.L., et al., *Changing potency by spontaneous fusion.* Nature, 2002. **416**(6880): p. 545-8.
115. Alvarez-Dolado, M., et al., *Fusion of bone-marrow-derived cells with Purkinje neurons, cardiomyocytes and hepatocytes.* Nature, 2003. **425**(6961): p. 968-73.
116. Weimann, J.M., et al., *Stable reprogrammed heterokaryons form spontaneously in Purkinje neurons after bone marrow transplant.* Nat Cell Biol, 2003. **5**(11): p. 959-66.
117. Weimann, J.M., et al., *Contribution of transplanted bone marrow cells to Purkinje neurons in human adult brains.* Proc Natl Acad Sci U S A, 2003. **100**(4): p. 2088-93.
118. Heubach, J.F., et al., *Electrophysiological properties of human mesenchymal stem cells.* J Physiol, 2004. **554**(Pt 3): p. 659-72.
119. Chopp, M. and Y. Li, *Treatment of neural injury with marrow stromal cells.* Lancet Neurol, 2002. **1**(2): p. 92-100.
120. Li, Y., et al., *Human marrow stromal cell therapy for stroke in rat: neurotrophins and functional recovery.* Neurology, 2002. **59**(4): p. 514-23.
121. Gao, Q., Y. Li, and M. Chopp, *Bone marrow stromal cells increase astrocyte survival via upregulation of phosphoinositide 3-kinase/threonine protein kinase and mitogen-activated protein kinase kinase/extracellular signal-regulated kinase pathways and stimulate astrocyte trophic factor gene expression after anaerobic insult.* Neuroscience, 2005. **136**(1): p. 123-34.
122. Shen, L.H., et al., *Intracarotid transplantation of bone marrow stromal cells increases axon-myelin remodeling after stroke.* Neuroscience, 2006. **137**(2): p. 393-9.
123. Shintani, A., et al., *Protection of dopamine neurons by bone marrow stromal cells.* Brain Res, 2007. **1186**: p. 48-55.
124. Isele, N.B., et al., *Bone marrow stromal cells mediate protection through stimulation of PI3-K/Akt and MAPK signaling in neurons.* Neurochem Int, 2007. **50**(1): p. 243-50.
125. Rivera, F.J., et al., *Mesenchymal stem cells instruct oligodendrogenic fate decision on adult neural stem cells.* Stem Cells, 2006. **24**(10): p. 2209-19.
126. Wislet-Gendebien, S., et al., *Nestin-positive mesenchymal stem cells favour the astroglial lineage in neural progenitors and stem cells by releasing active BMP4.* BMC Neurosci, 2004. **5**: p. 33.

127. Chen, J., et al., *Therapeutic benefit of intravenous administration of bone marrow stromal cells after cerebral ischemia in rats.* Stroke, 2001. **32**(4): p. 1005-11.
128. Hermann, A., et al., *Efficient generation of neural stem cell-like cells from adult human bone marrow stromal cells.* J Cell Sci, 2004. **117**(Pt 19): p. 4411-22.
129. Javazon, E.H., et al., *Rat marrow stromal cells are more sensitive to plating density and expand more rapidly from single-cell-derived colonies than human marrow stromal cells.* Stem Cells, 2001. **19**(3): p. 219-25.
130. Digirolamo, C.M., et al., *Propagation and senescence of human marrow stromal cells in culture: a simple colony-forming assay identifies samples with the greatest potential to propagate and differentiate.* Br J Haematol, 1999. **107**(2): p. 275-81.
131. Soma, T., M. Tajima, and J. Kishimoto, *Hair cycle-specific expression of versican in human hair follicles.* J Dermatol Sci, 2005. **39**(3): p. 147-54.
132. Simmons, P.J. and B. Torok-Storb, *CD34 expression by stromal precursors in normal human adult bone marrow.* Blood, 1991. **78**(11): p. 2848-53.
133. Miyake, K., et al., *A VCAM-like adhesion molecule on murine bone marrow stromal cells mediates binding of lymphocyte precursors in culture.* J Cell Biol, 1991. **114**(3): p. 557-65.
134. Tseng, P.Y., et al., *Spontaneous differentiation of adult rat marrow stromal cells in a long-term culture.* J Vet Med Sci, 2007. **69**(2): p. 95-102.
135. Baxter, M.A., et al., *Study of telomere length reveals rapid aging of human marrow stromal cells following in vitro expansion.* Stem Cells, 2004. **22**(5): p. 675-82.
136. Bonab, M.M., et al., *Aging of mesenchymal stem cell in vitro.* BMC Cell Biol, 2006. **7**: p. 14.
137. Enver, T., et al., *Cellular differentiation hierarchies in normal and culture-adapted human embryonic stem cells.* Hum Mol Genet, 2005. **14**(21): p. 3129-40.
138. Hanson, C. and G. Caisander, *Human embryonic stem cells and chromosome stability.* Apmis, 2005. **113**(11-12): p. 751-5.
139. Simonsen, J.L., et al., *Telomerase expression extends the proliferative life-span and maintains the osteogenic potential of human bone marrow stromal cells.* Nat Biotechnol, 2002. **20**(6): p. 592-6.